EUROPEAN COMMISSION
DIRECTORATE-GENERAL
Joint Research Centre

NUMERICAL SIMULATIONS OF BLACK SEA AND ADJOINED AZOV SEA, FORCED WITH CLIMATOLOGICAL AND METEOROLOGICAL REANALYSIS DATA

E. L. Peneva and A. K. Stips

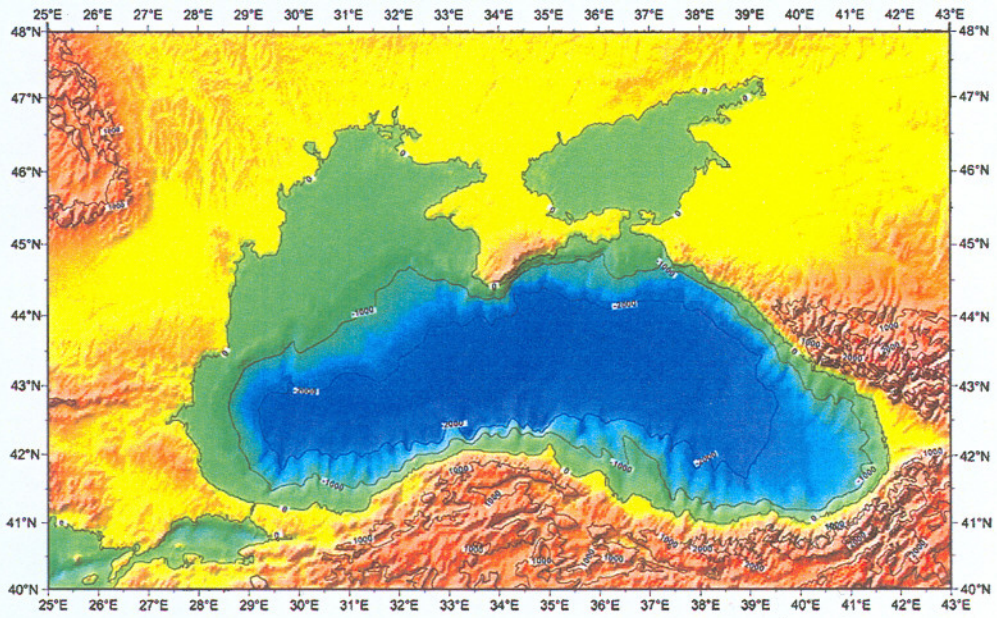

2005

EUR 21504 EN

EUROPEAN COMMISSION
DIRECTORATE-GENERAL
Joint Research Centre

NUMERICAL SIMULATIONS OF BLACK SEA AND ADJOINED AZOV SEA, FORCED WITH CLIMATOLOGICAL AND METEOROLOGICAL REANALYSIS DATA

E. L. Peneva and A. K. Stips

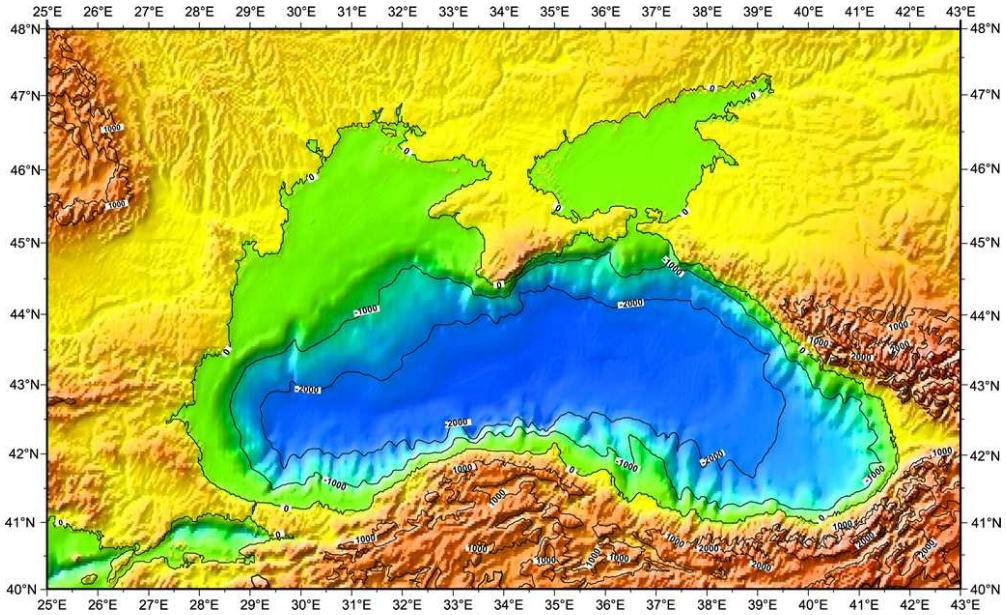

Corresponding author address:
CEC JRC, Institute of Environment and Sustainability
Inland and Marine Water Unit
Ispra (VA) 21020, Italy
elisaveta.peneva@jrc.it

October 2004

Institute for Environment and Sustainability

INLAND & MARINE WATERS

A great deal of additional information on the
European Union is available on the Internet.
It can be accessed through the Europa server
(http://europa.eu.int)

EUR 21504 EN

Printed in Italy

CONTENT

1. Summary of the work plan.

Since many years the Black Sea has been considered as a European sea only when referring to its geographical position. Research has been done only in the neighboring countries (Russia, Ukraine, Bulgaria, Romania, Turkey and Georgia), thus serving mainly to local interests. As the integration of the Black Sea to the European community is getting more and more important, the need of harmonizing the tools for marine management within all European Seas is well recognized by the politicians. In order to assess the ecological status of the marine basins, reliable information on the physical conditions is of crucial importance. Numerical simulations are the most useful tool to integrate environmental data at adequate space/time resolution, as in situ measurements are often too irregular and sparse, while satellite measurements are representative only of the surface conditions. These different points illustrate the reason to direct some efforts in developing a reliable tool to estimate marine environment physical condition in the Black Sea.

Thus the main objective is to set up, test and validate a 3D physical model for the Black Sea. At the end of the study period the model set up should be ready to be used for realistic long term simulations of the Black Sea with realistic forcing data.

Modeling the Black Sea with 3D models is a rather difficult task and the achieved level of simulations up to date is not at all satisfactory. Several simulations using MOM/POM have been done during the last ten years showing severe problems. The first problem is caused by the bathymetry, with a rather small and shallow continental shelf, which rapidly falls of to about 2000 m depth. Especially for z co-ordinate models therefore a good vertical resolution on the shelf and at the same time a sufficient resolution in the deeper parts is hard to obtain. The second problem is the existence of a layer of cold intermediate water that persists during the summer. Usually the applied models were too diffusive, so that this cold intermediate water had the tendency to disappear during the summer.

The work should evolve on several steps as following:
1) Barotropic mode;
2) integration with idealized forcing and initialized with climatological data set;

3) multi-annual integration with realistic forcing and initial conditions.
We aimed at including as much as possible real processes like considering an open boundary at the Bosporus and actual river input.

2. INTRODUCTION

2.1. Black Sea physical characteristics.

The Black Sea has been an object of exploration and intensive scientific research for a historically long period of time. Its unique hydrographic structure originates from a combination of restricted exchange with the Mediterranean Sea through Bosporus Straits supplying a source of salty water, and large fresh water input in the northern shelf part. This determines the strong stratification, which prevents deep convective mixing in the basin interior. As a consequence a permanent anoxic deep layer is formed which makes of the Black Sea the largest anoxic water body in the world. Thus the basin is an excellent case study for oceanographers to observe and investigate the manifestation of many physical processes.

Fig. 2.1. Satellite picture of the Black and Eastern Mediterranean Seas, note the different color.

During the last decade a number of ecological studies have reported that the Black Sea ecosystem is under serious threat of environmental changes. The main reason for that is the increased discharge of nutrients and pollutants, land-based industrial and fisheries activity. An enhanced eutrophication and severe reduction in biodiversity have been observed. That period coincided with a period of significant political and economical changes in the Black Sea region (the crush of several political regimes, the rise of the new independent states, the intensification of oil tanker use). These social changes have had a

profound influence on the Black Sea ecosystem. While in the beginning of 90s a tremendous deterioration of the sea ecological status was observed, lately the measurements show slight improvement, both in the reduction of hypoxia/anoxia events near the sea shelf bottom and recreation of the typical biodiversity species. The main reason is likely to be the sudden collapse of industrial activity, however it is not clear to what extend the factors like natural climate oscillations or the recently taken political measures to reduce the nutrient load from the big rivers contribute to this improvement.

This chapter aims at presenting an overview of the basic Black Sea oceanographic characteristics, highlighting some of the possible mechanism of interaction with neighbor basins, as well as at pointing several not well-understood scientific problems in this area. The Black Sea is a deep (with a depth of down to 2200 m) elongated basin situated between 40°56' and 46°33' in north direction and 27°30 and 42° in east direction. Its maximum zonal length is 1148km. The Crimea peninsula and the Anatolian coast convexity divide the sea into two sub-basins. The minimum width of the sea is 258 km. The broad northwestern shelf (NWS) occupies the northwestern part of the sea. Typical width of the shelf along the other coastlines is 2-12 km. Profiles of density show a well-pronounced permanent pycnocline situated at a depth of 150-300m. The Black Sea is connected with the ocean by the narrow Bosporus Straits, where the minimal width is 1.5 km and depth is 30 m. Density stratification is determined mainly by salinity, which is near 22.5 PSU in the deep-sea against 18-18.5 PSU near the surface. As the sea is in the temperate continental climatic zone the sea surface temperature (SST) presents large seasonal variability, on the contrary the deep-sea temperature is about 9°C as the strong salinity stratification prevents the deep winter convection, thus seasonal variations of temperature can be observed only above the pycnocline. Consequently the winter cooling on the shallow shelf part can reduce SST down to 6°C and produces a distinctive feature of the Black Sea thermal stratification, the so-called cold intermediate layer (CIL) situated at a depth of about 50-90m. A permanent feature of the upper layer circulation is the Rim Current, encircling the entire Black Sea and forming a large-scale cyclonic gyre. Direct observations of the current velocity from surface buoys suggest that the maximum speed of this stream is usually 40-50cm/s increasing sometimes up to 80-100cm/s. The Rim Current is concentrated above the shallow pycnocline and the volume transport of the current is estimated to be 3-4 Sv. There are also two smaller cyclonic gyres in the western and the eastern parts of the basin. Cyclonic circulation and the dooming of the isopycnal surfaces induce the

rise of the sea level toward the coast. The amplitude of sea level variation in space depends on the wind seasonal variability and ranges from 25 to 40 cm. Along with the main Rim current significant mesoscale variability occurs, forming numerous anticyclonic eddies around the coast, and several of them are quasi-permanent like the Batumi and Sevastopol eddies. New observations and numerical simulations with and without real data assimilation made it possible to improve significantly the physical understanding of the Black Sea. Maps of surface currents obtained from altimetry manifest an obvious annual cycle of the circulation. The Rim Current is the most intense in winter-spring seasons, correlating with the wind stress curl seasonal variations. However, the Black Sea circulation also manifests significant intra and inter-annual variability. Major features of mesoscale variability such as planetary waves, meandering of the strong jet and mesoscale eddies, which are well known from oceanic observations, could be found in the Black Sea.

A theory exists that the Black Sea could influence also the neighboring Mediterranean basin, as the large variations of the relatively fresher water input from the upper Bosporus Strait could affect the processes of deep water convection in Aegean and whole Mediterranean Sea (Lascaratos, 1993).

2.2. Numerical modeling problems still to be solved for the area of the Black Sea.

As it was presented above a good numerical model for the Black Sea should represent the main dynamical characteristics like forming of the Rim current and its seasonal intensification, as well as the main elements in the mesoscale variability. The representation of the latter with filaments, meanders and anticyclonic eddies however requires an adequate model grid bathymetry, thus a reasonable smoothing with yet pronounced basic topographic features should be considered.

Apart from the dynamics of the Black Sea another interesting problem is the water mass formation processes. The Black Sea can be regarded as a buffer zone where the fresh water coming from rivers and atmosphere (annually about 300 km^3/yr) is mixed. This water leaves the sea with the surface Bosporus current, approaching Mediterranean conditions in the Marmara and Aegean Seas. Recently it was discovered that the year-to-year fluctuations of the upper Bosporus current could play a significant role in the

deep-water formation processes in the Mediterranean Sea, switching under certain conditions the source of deep waters from the Adriatic to Aegean Sea. The deep Bosporus current closes the conveyor belt from below, providing positive salinity anomaly, thus tending to maintain the salt content of the Black Sea almost constant. Thus the Cold Intermediate Layer (CIL) plays a role of the interface between the surface and deep branch of the ocean conveyor belt in the Black Sea. Its replenishment with cold water is subject to local cooling, slope convection and ocean dynamics basin-wide, as well as at mesoscales.

Most of the numerical Black Sea simulations fail to reproduce fairly the presence of the permanent CIL without a relaxation to the climatological temperature and salinity fields. In addition it is not yet very clear what the source of the CIL is, either local cooling (at the shelf) and subsequent horizontal spreading by advection of these local sources, or is it formed simultaneously at the entire basin surface. After the study of Kolesnikov (1953) most preference is given to the second idea, that is the convection mechanism dominates the formation of CIL. A strong support to this hypothesis has been given also by Filippov (1965) and Blatov et al. (1984). The other idea about the dominating formation of CIL on the shelf stems from the evidence that the Sea Surface Temperature (SST) reaches minimum in these areas in winter (Stanev et all, 2002). An alternative mechanism of the CIL formation was suggested by Ovchinnikov and Popov (1987) assuming that the CIL was formed in the cyclonic eddies in the basin interior. Details on the works about CIL can be found in the works of Staneva and Stanev (1997), Staneva and Stanev (2002), Stanev et al, (2003).

The other problem is the representation of the Bosporus plume, which requires a strong mixing near the Bosporus despite of the stagnant layers structure with poor mixing in the basin interior. This implies the use of a sophisticated turbulence model that should account for different conditions in the different parts of the sea. Not enough studied is also the Kerch Strait plume spreading as most of the model studies do not include the Azov Sea in the model domain.

As a last point but not least important the difficulties in finding reliable data for model comparison and verification need to be noted. Since the last two international large scale expeditions in the framework of HydroBLACK and ComsBLACK (Oguz et al, 1993, Oguz et al, 1994) programs, which took place in 1991 and 1992 only local or hotspots measurements are being

conducted as a part of different projects. Although for example the Danube delta (and more generally the north-western shelf area) is well monitored in the last decade there are places with much poorer observations. The satellite pictures provide data over the whole basin, however it is only representative for the surface and depending on the cloud cover at the moment of observation. Substantial effort was made to obtain an inventory of the existing oceanographic information.

3. Description of the General Estuarine Transport Model.

This section gives a short introduction to the GETM model equations, (for specific details see Burhard et al, 2002)

3.1. Three-dimensional momentum equations.

GETM solves the three-dimensional hydrostatic equations of motion applying the Boussinesq approximation and the eddy viscosity assumption (Bryan, 1969, Cox, 1984, Blumberg, 1987, Haidvogel 1999, Kantha, 2000) In the flux form, the dynamic equations of motion for the horizontal velocity components can be written in Cartesian coordinates as:

$$\frac{\partial u}{\partial t}+\frac{\partial u^2}{\partial x}+\frac{\partial uv}{\partial y}-\frac{\partial}{\partial x}\left[2A_h^M\frac{\partial u}{\partial x}\right]-\frac{\partial}{\partial y}\left[2A_h^M\frac{\partial u}{\partial y}\right]-fv-\int_z\zeta\frac{\partial b}{\partial x}dz+\frac{\partial uw}{\partial z}-\frac{\partial}{\partial z}\left[(\nu_t+\nu)\frac{\partial u}{\partial z}\right]=$$

$$=-g\frac{\partial}{\partial x}\left[\zeta+\frac{1}{\rho_0 P_0}\right]$$

$$\frac{\partial v}{\partial t}+\frac{\partial vu}{\partial x}+\frac{\partial v^2}{\partial y}-\frac{\partial}{\partial y}\left[2A_h^M\frac{\partial v}{\partial y}\right]-\frac{\partial}{\partial x}\left[2A_h^M(\frac{\partial u}{\partial y}+\frac{\partial v}{\partial x}\right]+fu-\int_z\zeta\frac{\partial b}{\partial y}dz+\frac{\partial vw}{\partial z}-\frac{\partial}{\partial z}\left[(\nu_t+\nu)\frac{\partial v}{\partial z}\right]=$$

$$=-g\frac{\partial}{\partial y}\left[\zeta+\frac{1}{\rho_0 P_0}\right]$$

The vertical velocity is given by the continuity equation:

$$\frac{\partial u}{\partial x}+\frac{\partial v}{\partial y}+\frac{\partial w}{\partial z}=0$$

where u, v, w are the ensemble averaged velocity components with respect to the x, y and z direction. The vertical coordinate z ranges from the bottom -H(x,y) to the free surface ζ(t,x,y) with t denoting time.
ν_t is the vertical eddy viscosity, ν- the cinematic viscosity, f - the Coriolis parameter, P_0 is the atmospheric pressure at sea level and g is the gravitational acceleration.

The horizontal mixing is parameterised by terms containing the horizontal eddy viscosity A_h^M, see Blumberg et al, (1987). The buoyancy b is defined as $b=-g\frac{\rho-\rho_0}{\rho_0}$
with the density ρ and a reference density ρ_0.

The last term on the left hand sides of the equations for momentum are the internal (due to density gradients) and the terms on the right hand sides are the external (due to surface slopes and atmospheric pressure variations) pressure gradients. In the latter, the deviation of surface density from reference density is neglected (see Stips et al, 2002).
The derivation of the above equations has been shown in numerous publications, e.g. Pedlosky, (1987), Haidvogel et al, (1999), Burchard, (2002).

The equation of state for seawater (see Foffonoff and Millard, 1983) is used to calculate density as a function of salinity, temperature and pressure.

3.2. Kinematic boundary conditions and surface elevation equation

At the surface and at the bottom, cinematic boundary conditions result from the requirement that the particles at the boundaries are moving along these boundaries:

$$w(z=\zeta)=\frac{\partial\zeta}{\partial t}+u\frac{\partial\zeta}{\partial x}+v\frac{\partial\zeta}{\partial y}$$

$$w(z=-H)=-u\frac{\partial H}{\partial x}-v\frac{\partial H}{\partial y}$$

3.3. Dynamic boundary conditions

At the bottom boundaries, no-slip conditions are prescribed for the horizontal velocity components:
u=0, v=0

With the consideration (3.2) also w=0 holds at the bottom. It should be noted, that the bottom boundary condition is generally not directly used in numerical ocean models, since the near-bottom values of the horizontal velocity components are not located at the bed, but half a grid box above it. Instead, a logarithmic velocity profile is assumed in the bottom layer, leading to a quadratic friction law.

At the surface, the dynamic boundary conditions read:

$$(\nu_t + \nu_t')\frac{\partial u}{\partial z} = \tau_s{}^x$$

$$(\nu_t + \nu_t')\frac{\partial v}{\partial z} = \tau_s{}^y$$

The surface stresses (normalized by the reference density) $\tau_s{}^x$ and $\tau_s{}^y$ are calculated as functions of wind speed, wind direction, surface roughness etc.

3.4. Transport equations for temperature and salinity

The two most important tracer equations are the transport equations for potential temperature T [°C] and salinity S [PSU] (practical salinity units):

$$\frac{\partial T}{\partial t} + \frac{\partial uT}{\partial x} + \frac{\partial vT}{\partial y} + \frac{\partial wT}{\partial z} - \frac{\partial}{\partial z}(\nu_t \frac{\partial T}{\partial z}) - \frac{\partial}{\partial x}(A_h^T \frac{\partial T}{\partial x}) - \frac{\partial}{\partial y}(A_h^T \frac{\partial T}{\partial y}) = \frac{\overline{\partial I}}{c_p' \rho_0}$$

$$\frac{\partial S}{\partial t} + \frac{\partial uS}{\partial x} + \frac{\partial vS}{\partial y} + \frac{\partial wS}{\partial z} - \frac{\partial}{\partial z}(\nu_t \frac{\partial S}{\partial z}) - \frac{\partial}{\partial x}(A_h^T \frac{\partial S}{\partial x}) - \frac{\partial}{\partial y}(A_h^T \frac{\partial S}{\partial y}) = 0$$

The term on the right hand side of the temperature equation is for absorption of solar radiation with the solar radiation at depth z, I, and the specific heat capacity of water is c'_p.
According to Paulson and Simpson, (1977) the radiation I in the upper water column may be parameterised by

$$I(z) = I_0(ae^{-\eta_1 z} + (1-a)e^{-\eta_2 z})$$

Here, I_0 is the albedo corrected radiation normal to the sea surface. The weighting parameter a and the attenuation lengths for the longer and the shorter fraction of the short-wave radiation, η_1 and η_2 , respectively, depend on the turbidity of the water.
Jerlov, (1968) defined 6 different classes of water from which Paulson and Simpson, (1977) calculated weighting parameter a and attenuation coefficients η_1 and η_2 .

At the surface, flux boundary conditions for T and S have to be prescribed. For the potential temperature, it is of the following form:

$$\eta_t' \frac{\partial T}{\partial z} = \frac{Q_s + Q_l + Q_b}{c_p' \rho_0}$$

with the sensible heat flux, Q_s, the latent heat flux, Q_l and the long wave back radiation, Q_b. Here is used the bulk parameterization for calculating the

momentum and heat surface fluxes due to air-sea interactions.

Fig. 3.1 gives an overview of the processes included in GETM. A useful feature is the drying/flooding procedure that is important for tidal events or when due to the strong winds there is an accumulation of water in some part of the basin.

3.5. Vertical turbulent exchange

The eddy viscosity η_t (for momentum) and eddy diffusivity η'_t (for tracers) need to be parameterized by means of turbulence models. Such models may range from simple algebraic prescription of profiles, via zero-, one, or two-equation models to full Reynolds stress closure models. In GETM, a compromise between accuracy and computational effort is made in such a way, that usually two-equation models are used.

The turbulence module of the Public Domain water column model GOTM (General Ocean Turbulence Model, see http://www.gotm.net that has been developed by Burchard et al, (1999) is implemented into GETM. This allows for great flexibility in the choice of the turbulence model and guarantees that a well-tested state-of-the-art turbulence model is always at hand inside GETM.

The features of GOTM have been extensively reported in Burchard, (2002), Bolding et al (2002) and the citations therein. Various comparative calculations with in-situ turbulence measurements have been carried out with GOTM, which gives confidence into the model (Stips et al, 2004).

However, GOTM has various options for turbulence models, but only some of them have been proven to give reasonable results for vertical exchange. The research for improving turbulence models is still ongoing. Presently, better parameterizations for surface wave activity and internal wave activity are under development.

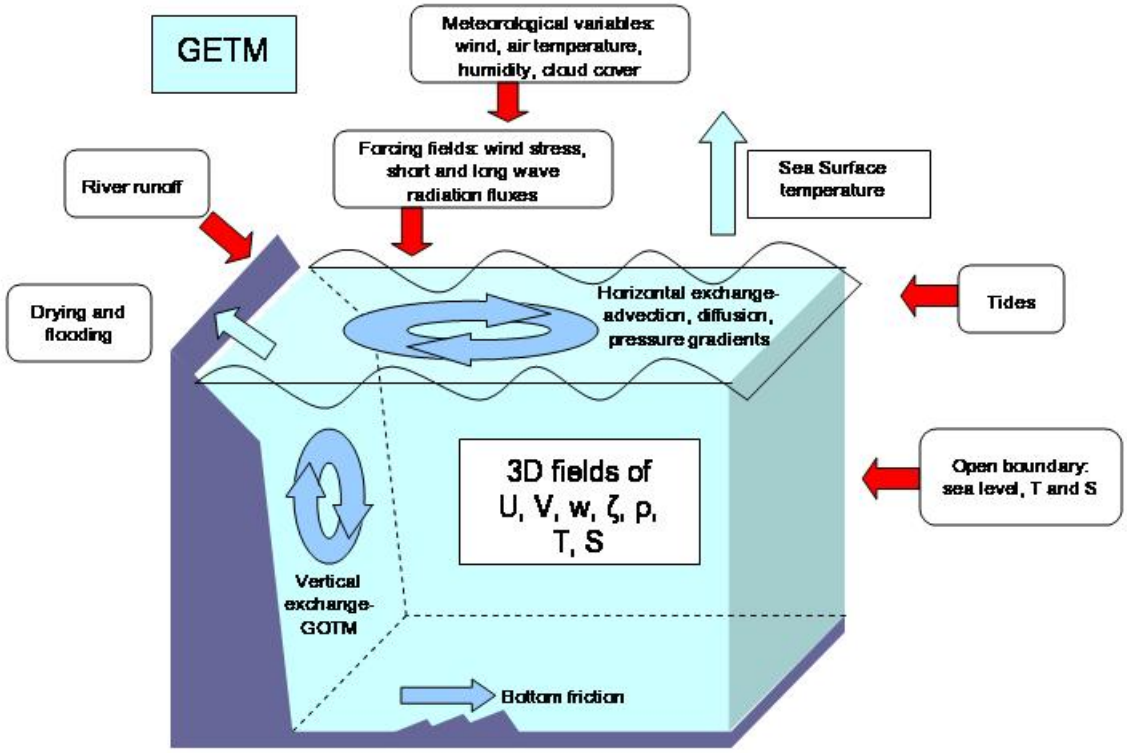

Fig.3.1. Schematic representation of the physical processes in the grid box, included in GETM

The model performance is pretty much depending on the choice of great number of parameters, both for GETM module and for the GOTM vertical exchange block. Usually this is the most time consuming part - to investigate the model sensitivity to parameterization and to choose the proper values. This is also dependent on the basin of interest as these values could vary largely in different seas. Numerous experiments have determined the following configuration (below is printed the input model file getm.inp used in the base experiment):

```
-----------------------------------------------------------------
!$Id: getm.proto,v 1.8 2004/01/06 18:42:54 gotm Exp $
!-----------------------------------------------------------------
! The namelists 'param','time','domain', 'meteo', 'rivers',
! 'io_spec','m2d', 'm3d', 'temp', 'salt', 'eqstate'
! They have to come in this order.
!-----------------------------------------------------------------

!-----------------------------------------------------------------
! General model setup is here - initialise.F90
!
```

```
! dryrun=  Used to test setup - .true. or .false.
! runid=   Used for naming output files
! title=   Title of Simulation
! parallel=     parallel simulation - .true. or .false.
! runtype= 1=2D, 2=3D (no density), 3=3D (frosen density), 4=3D
(full)
! hotstart=     read initial fields from file - .true. or .false.
!-----------------------------------------------------------------
 &param
  dryrun=  .false.,
  runid=   'bs_hot',
  title=   'Black Sea test case',
  parallel=     .false.,
  runtype= 4,
  hotstart=     .true.,
  save_initial= .true.,
 /

!-----------------------------------------------------------------
!Specify time related formats and variables here - time.F90
!
! timestep=     Micro timestep (as a real numer in seconds)
! timefmt= 1,2,3 - implicitly uses timestep=dt
!          1- maxn only - fake start time used.
!          2- start and stop - MaxN calculated.
!          3- start and MaxN - stop calculated.
! nlast=   do loop from n=1,nlast
! start=   Initial time: YYYY/MM/DD HH:MM:SS
! stop=          Final   time: YYYY/MM/DD HH:MM:SS
!-----------------------------------------------------------------
 &time
  timestep=     18,
  timefmt= 2,
  nlast=   30000,
  start=   '1997-09-01 00:00:00',
  stop=          '1997-10-01 00:00:00',
 /

!-----------------------------------------------------------------
!Information on the calculation domain - domain/domain.F90
!
! grid_type=    1:cartesian, 2:spherical, 3:curvi-linear
! vert_cord=    1:sigma, 2:z-level, 3:general
! maxdepth=     maximum depth in active calculation domain
! bathymetry=   name of file holding the bathymetry
! latitude=     used for calculating the Coriolis force
! openbdy= set to .true. if any open boundaries
! bdyinfofile=  read if 'openbdy' equals .true. - contains
boundary info
! crit_depth=   the critical depth - when the drying procedure
starts
! min_depth=    the absolute minimum depth
```

```
! kdum=          number of layers in the vertical - only used when
-DDYNAMIC
! ddu,ddl= upper and lower zooming parameters (in coodinates.F90)
! d_gamma= used to define general vert. cordinates (in
coodinates.F90)
! gamma_surf=    used to define general vert. cordinates (in
coodinates.F90)
!-----------------------------------------------------------------
 &domain
  grid_type=     2,
  vert_cord=     3,
  maxdepth=      2300.,
  bathymetry=    'topo.nc',
  latitude=      0.,
  openbdy= .false.,
  bdyinfofile=   'bdyinfo.dat',
  crit_depth=    2.5,
  min_depth=     0.8,
  kdum=          10,
  ddu=           10.,
  ddl=           -1.,
  d_gamma= 100.,
  gamma_surf=    .true.,
  il=      -1,
  ih=      -1,
  jl=      -1,
  jh=      -1,
 /

!-----------------------------------------------------------------
! Specify variables related to meteo forcing - meteo/meteo.F90
!
! metforcing=    .true. or .false.
! on_grid= .true. or .false.
! calc_met=      .true. or .false.
! step_calc_met= number of time step between calculation of
fluxes.
! method=  1 = constant, 2 = from file
! spinup=  spin forcing up over 'spinup' micro time steps
! metfmt=  format of meteofile: 1-ASCII, 2-NetCDF
! meteo_file=    'meteofiles.dat',
! tx=      constant x stress
! ty=      constant y stress
! swr_const=     constant short wave radiation
! shf_const=     constant surface heat flux
!-----------------------------------------------------------------
 &meteo
  metforcing=    .true.,
  on_grid= .false.,
  calc_met=      .true.,
  step_calc_met=200,
  method=  2,
```

```
  spinup=  1000,
  metfmt=  2,
  meteo_file=    'meteofiles.dat',
  tx=      0.,
  ty=      0.,
  swr_const=    0.,
  shf_const=    0.,
 /
! southpole (lon,lat) - default 0,90
! name_u10
! name_v10
! name_airp
! name_t2
! name_hum
! name_cc
! name_tausx
! name_tausy
! name_swr
! name_shf
! name_time
! time_fmt
! scan_axis - integer
!

!-----------------------------------------------------------------
! Specify variables related to rivers - 3d/rivers.F90
!
! river_method= 0:none,1:const,2:from file
! river_info=   name of file with river specifications
! river_format= 1=ASCII,2=NetCDF
! river_data=   name of file with actual river data
! river_factor= to be apllied to all read values - e.g. m3/day --
> m3/s
!-----------------------------------------------------------------
 &rivers
  river_method= 2,
  river_info=   'riverinfo.dat',
  river_format= 2,
  river_data=   'rivers.nc',
  river_factor= 1.0,
 /

!-----------------------------------------------------------------
!Format for output and filename(s) - output/output.F90.
!
! out_fmt= 1=ASCII, 2=NetCDF, 3=GrADS
! in_dir=  path to input directory
! out_dir= path to output directory
! save_meteo=    .true. or .false.
! save_2d= .true. or .false.
! save_3d= .true. or .false.
! save_vel=     .true. or .false.
```

```
! save_strho=    .true. or .false.
! save_s=  .true. or .false.
! save_t=  .true. or .false.
! save_rho=      .true. or .false.
! save_turb=     .true. or .false.
! save_tke=      .true. or .false.
! save_eps=      .true. or .false.
! save_num=      .true. or .false.
! save_nuh=      .true. or .false.
! first_2d=      the first (micro) time step to save 2D fields
! step_2d= save 2D fields every 'step_2d'
! first_3d=      the first (micro) time step to save 3D fields
! step_3d= save 3D fields every 'step_3d'
! hotout=  save hot file every 'hotout' timestep - < 0 - no
saving
!-----------------------------------------------------------------
 &io_spec
  out_fmt= 2,
  in_dir=  '.',
  out_dir= '/scratch2/penevel/light_kde_hor/',
  save_meteo=    .true.,
  save_2d= .true.,
  save_3d= .true.,
  save_vel=      .true.,
  save_strho=    .true.,
  save_s=  .true.,
  save_t=  .true.,
  save_rho=      .true.,
  save_turb=     .true.,
  save_tke=      .true.,
  save_eps=      .true.,
  save_num=      .true.,
  save_nuh=      .true.,
  first_2d=      0,
  step_2d= 144000,
  first_3d=      0,
  step_3d= 4800,
  hotout=  4800,
  meanout= 144000,
 /

!-----------------------------------------------------------------
! Specify variables related to 2D model - 2d/m2d.F90
!
! MM=      number of micro timesteps between call to
bottom_friction()
! z0_const=      constant bottom roughness (m)
! vel_depth_method=
!          0: using mean value of neigboring H points (default)
!          1: using minimum value of neigboring H points
!          2: a mixture of 0,1: see code for details
```

```
! Am=      constant horizontal momentum diffusion coefficient
(m2/s)
! An=      constant horizontal numerical diffusion coefficient
(m2/s)
! bdy2d=   .true. or .false.
! bdyfmt_2d=    1 (ascii), 2 (NetCDF)
! bdyramp_2d=   spin elevation bdy up over ramp time steps
! bdyfile_2d=   name of file with boundary data
!-------------------------------------------------------------------
 &m2d
  MM=           40,
  z0_const=          0.02,
  vel_depth_method=  1,
  Am=           -1.,
  An=           1000.,
  residual=          -1,
  bdy2d=        .false.,
  bdyfmt_2d=         2,
  bdyramp_2d=        -1,
  bdyfile_2d=        'bdy_2d.nc',
/

! Advection methods implemented sofar:
1=UPSTREAM,2=UPSTREAM_SPLIT,3=TVD

!-------------------------------------------------------------------
! Specify variables related to 3D model - 3d/m3d.F90
!
! M=       number of micro timesteps between call to 3D model
! cnpar=   Cranck - Nicolson number - between 0. and 1. - close
to 1.
! cord_relax=   Coordinate relaxation time scale (HB to explain)
! bdy3d=   .true. or .false.
! bdyfmt_3d=    1 (ascii), 2 (NetCDF)
! bdyramp_3d=   spin bdy up over ramp time steps
! bdyfile_3d=   name of file with boundary data
! vel_hor_adv=  horizontal advection method for momentum
! vel_ver_adv=  vertical advection method for momentum
! vel_adv_split=
!          if vel_hor_adv=1: 3D first-order upstream
!    For all other setting -DUV_TVD has to be set in Makefile
!          0: 1D split --> full u, full v, full w
!          1: 1D split --> half u, half v, full w, half v, half u
!               hor_adv and ver_adv may be 2,3,4,5,6
!               2: upstream (first-order, monotone)
!               3: P2-PDM   (third-order, non-monotone)
!               4: TVD-Superbee (second-order, monotone)
!               5: TVD-MUSCL    (second-order, monotone)
!               6: TVD-P2-PDM   (third-order, monotone)
!          2: 2D-hor-1D-vert split --> full uv, full w
!               hor_adv must be 2 (2D-upstream) or 7 (2D-FCT)
! calc_temp=    .true. or .false.
```

```
! calc_salt=    Suspended particulate matter - .true. or .false.
!-----------------------------------------------------------------
 &m3d
  M=             40,
  cnpar=         1.0,
  cord_relax=          0.,
  bdy3d=         .false.,
  bdyfmt_3d=           2,
  bdyramp_3d=          -1,
  bdyfile_3d=          'bdy_3d.nc',
  vel_hor_adv=         1,
  vel_ver_adv=         1,
  vel_adv_split=1,
  calc_temp=           .true.,
  calc_salt=           .true.,
  calc_spm=            .false.,
  avmback=               1.8e-6,
  avhback=               1.8e-7,
  ip_method=             1,
 /

!-----------------------------------------------------------------
! Specify variables related to temperature - 3d/temperature.F90
!
! temp_method= 1:const, 2:homogeneous stratification, 3:from 3D
field
! temp_const=   constant initial temperature
! temp_file=    name of file with initial salinity distribution
! temp_format=  1=ASCII,2=NetCDF
! temp_name=    name of the temperature variable (used if NetCDF
format)
! temp_field_no=what number to read initial data from (used if
NetCDF format)
! temp_hor_adv= horizontal advection method for temperature
! temp_ver_adv= vertical advection method for temperature
! temp_adv_split=
!          temp_hor_adv=1: 3D first-order upstream
!          0: 1D split --> full u, full v, full w
!          1: 1D split --> half u, half v, full w, half v, half u
!               hor_adv and ver_adv may be 2,3,4,5,6
!               2: upstream (first-order, monotone)
!               3: P2-PDM   (third-order, non-monotone)
!               4: TVD-Superbee (second-order, monotone)
!               5: TVD-MUSCL    (second-order, monotone)
!               6: TVD-P2-PDM   (third-order, monotone)
!          2: 2D-hor-1D-vert split --> full uv, full w
!               hor_adv must be 2 (2D-upstream) or 7 (2D-FCT)
! temp_AH= horizontal diffusion for temperature.
!-----------------------------------------------------------------
 &temp
  temp_method=        0,
  temp_const=         20.0,
```

```
  temp_format=        2,
  temp_file=          'climatology.nc',
  temp_name=          'temp',
  temp_field_no=1,
  temp_hor_adv=       6,
  temp_ver_adv=       6,
  temp_adv_split=     0,
  temp_AH=       -1.,
 /

!-----------------------------------------------------------------
! Specify variables related to salinity - 3d/salinity.F90
!
! salt_method= 1:const, 2:homogeneous stratification, 3:from 3D
field
! salt_const=   constant initial salinity
! salt_file=    name of file with initial salinity distribution
! salt_format=  1=ASCII,2=NetCDF
! salt_name=    name of the salinity variable (used if NetCDF
format)
! salt_field_no=what number to read initial data from (used if
NetCDF format)
! salt_hor_adv= horizontal advection method for salinity
! salt_ver_adv= vertical advection method for salinity
! salt_adv_split=
!          salt_hor_adv=1: 3D first-order upstream
!          0: 1D split --> full u, full v, full w
!          1: 1D split --> half u, half v, full w, half v, half u
!               hor_adv and ver_adv may be 2,3,4,5,6
!               2: upstream (first-order, monotone)
!               3: P2-PDM   (third-order, non-monotone)
!               4: TVD-Superbee (second-order, monotone)
!               5: TVD-MUSCL    (second-order, monotone)
!               6: TVD-P2-PDM   (third-order, monotone)
!          2: 2D-hor-1D-vert split --> full uv, full w
!               hor_adv must be 2 (2D-upstream) or 7 (2D-FCT)
! salt_AH= horizontal diffusion for salt.
!-----------------------------------------------------------------
 &salt
  salt_method=        0,
  salt_const=         35.0,
  salt_format=        2,
  salt_file=          'climatology.nc',
  salt_name=          'salt',
  salt_field_no=1,
  salt_hor_adv=       6,
  salt_ver_adv=       6,
  salt_adv_split=     0,
  salt_AH=       -1.,
 /

!-----------------------------------------------------------------
```

```
! Specify variables related to the equation of state.
!
! method =
!          1: Linearisation of equation of state with
T0,S0,dtr0,dsr0
!          2: UNESCO equation of state no pressure adjustment.
!             See -DUNPRESS for pressure effect
! T0=      Reference temperature (deg C) for linear equation of
state
! S0=      Reference salinity (psu) for linear equation of state
! p0=      Reference pressure (bar) for linear equation of state
! dtr0=    thermal expansion coefficient for linear equation of
state
! dsr0=    saline expansion coefficient for linear equation of
state
!--------------------------------------------------------------------
 &eqstate
  eqstate_method= 2,
  T0=             9.5,
  S0=             21.5,
  p0=             0.,
  dtr0=           -0.13,
  dsr0=           0.78,
!--------------------------------------------------------------------
```

The complete view of the results from different tuning experiment will require much effort both to the writer and reader. For this reason only a list of the parameters, to which the model sensitivity is investigated before setting the above printed values, is given:

```
time_step, grid_type, vert_coord, ddu, ddl, d_gamma,
min_depth,     crit_depth,     vel_hor_adv,     tem_hor_adv,
salt_hor_adv,   vel_ver_adv,   tem_ver_adv,   salt_ver_adv,
vel_adv_split, tem_adv_split, salt_adv_split, M, MM, Am, An,
cnpar, ip_method, eqstate_method, river_method, avm_back,
avh_back
```

Several experiments with different turbulence models have also been performed and from the point of view of best representation of stagnant vertical exchange in the Black Sea the k-ε model is chosen.

4. Initial and boundary data.

4.1. Bathymetry.

The bathymetry data are of crucial importance when aiming at adequate model simulations that is why particular attention was made to find a reliable data set with fine resolution. The main data source used in this study is the new developed GEBCO global bathymetric grid with horizontal resolution of 1'. The compilation of the different elevation data and producing this final grid was initiated in NOAA National Geophysical Data Center and represents at the moment one of the most sophisticated products on global bathymetry. The input sources for the creation of the grid are digitized current GEBCO GDA contours, GLOBE land elevations, WVS coastlines, SCAR (Antarctic) coastlines, additional shallow-water contours and soundings, additional intermediate contours in featureless areas and additional individual echo-soundings. More information on the product could be found at http://www.ngdc.noaa.gov/mgg/gebco/grid/1mingrid.html

Fig. 4.1. Model bathymetry with 5' horizontal resolution

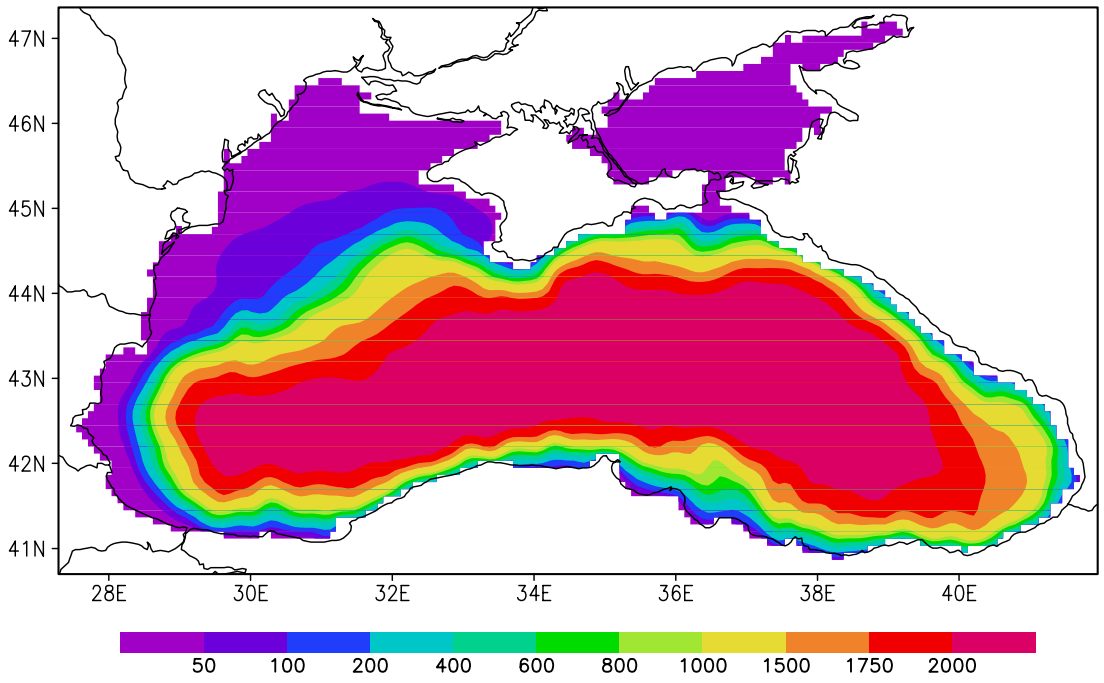

From this large file the data for the Black Sea region was extracted in a rectangular domain and 3 data sets were created with different horizontal resolution - 1', 2' and 5'. Until now only the 2' and 5' model set up are run, as the finer resolution integration would require substantial computing

resources. Note that the Azov Sea is included in the model domain. The Kerch Strait is represented only by several grid boxes in the 5' grid, but much better in the 2' grid.

Fig. 4.2. Model bathymetry with 2' horizontal resolution

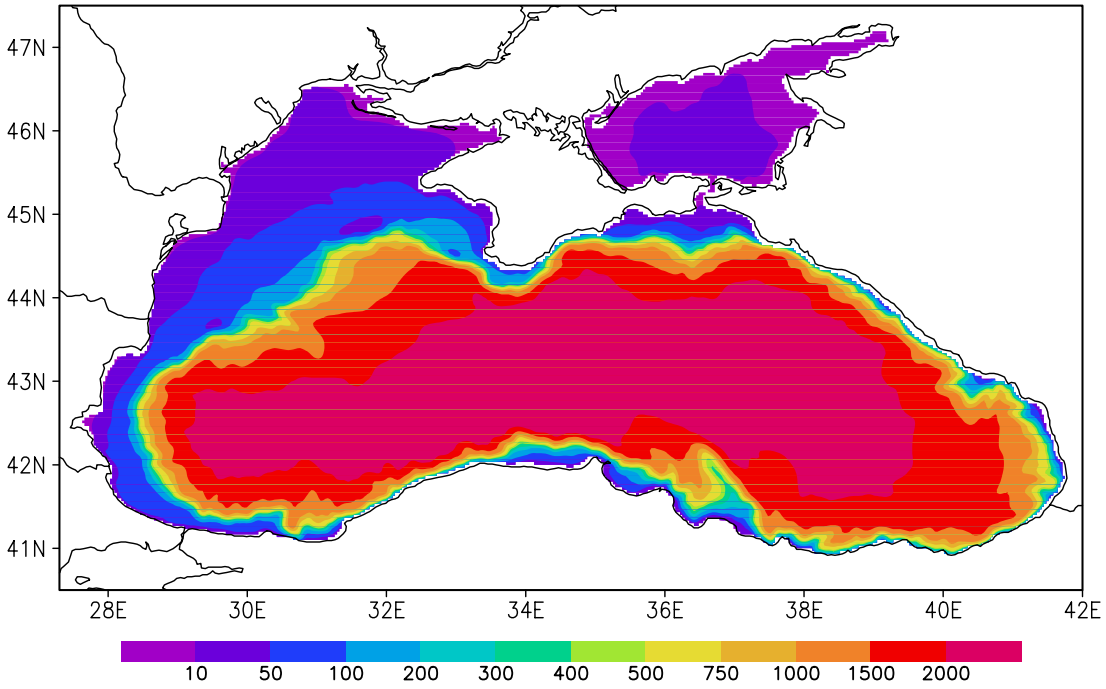

The comparison between Fig.4.1 and Fig.4.2 gives clear conclusion that the better horizontal resolution the better representation of the small-scale topography features like for example the local canyons on the continental slope.

A typical problem in models with a sigma-vertical coordinate system is a relatively large error coming from the calculation of the internal baroclinic force on a steep slope that is, why smoothing of the original data has to be done, in a way that the horizontal gradients are limited. The measure for the smooth degree is the so-called R-value, which is defined as

$$Rvalue = \frac{\max(\Delta_x H, \Delta_y H)}{H} < 0.4$$

One can easily see that a steep slope in the shallow parts of the sea is more dangerous than in the deep sea. The aim is to smooth selectively only these dangerous slopes. In Fig. 4.1 and Fig. 4.2 the smoothed bathymetry is

shown. In the Black Sea the continental slope areas near the shelf in the northwestern part and on the Turkish coast had to be smoothed to fulfill this criterion.

4.2. Thermohaline fields for model initialization.

The model is initialized by means of temperature and salinity 3D fields coming from the recently completed project MEDAR/MEDATLAS II. The objective of this project was to make available a comprehensive data product of temperature, salinity and bio-chemical data in the Mediterranean and Black Sea, through a wide co-operation of the Mediterranean countries. The partners in this project were 20 institutes from the Mediterranean and Black Sea countries. For more information on the data set look at http://www.ifremer.fr/medar

It was decided to start the simulations in the winter month thus the January climatological temperature (T) and salinity (S) fields are used. As the Azov Sea is not covered by this data set, there are used climatic values for temperature and salinity, taken from the literature, assuming a homogeneous basin. On Fig. 4.3 are given the monthly mean January SST and SSS (a and b) and in addition the cross-section along the 31ºE meridian (c and d). It is important that the initial T and S fields are consistent, otherwise this could cause model problems and it could be impossible to reach an adaptation of the model currents (steady state). Thus the same source should be used for the two fields and a careful check of the data must be performed. The MEDAR data set for the Black Sea reflects the main features known from observations – the strong halocline at 70-150 m, the Cold Intermediate Layer at ~70m and the dooming of the isohalines due to the cyclonic Rim current.

When the simulations with real atmospheric forcing were run, several experiments on the choice of initial moment were conducted, starting in July and April, with no substantial influence on the results.

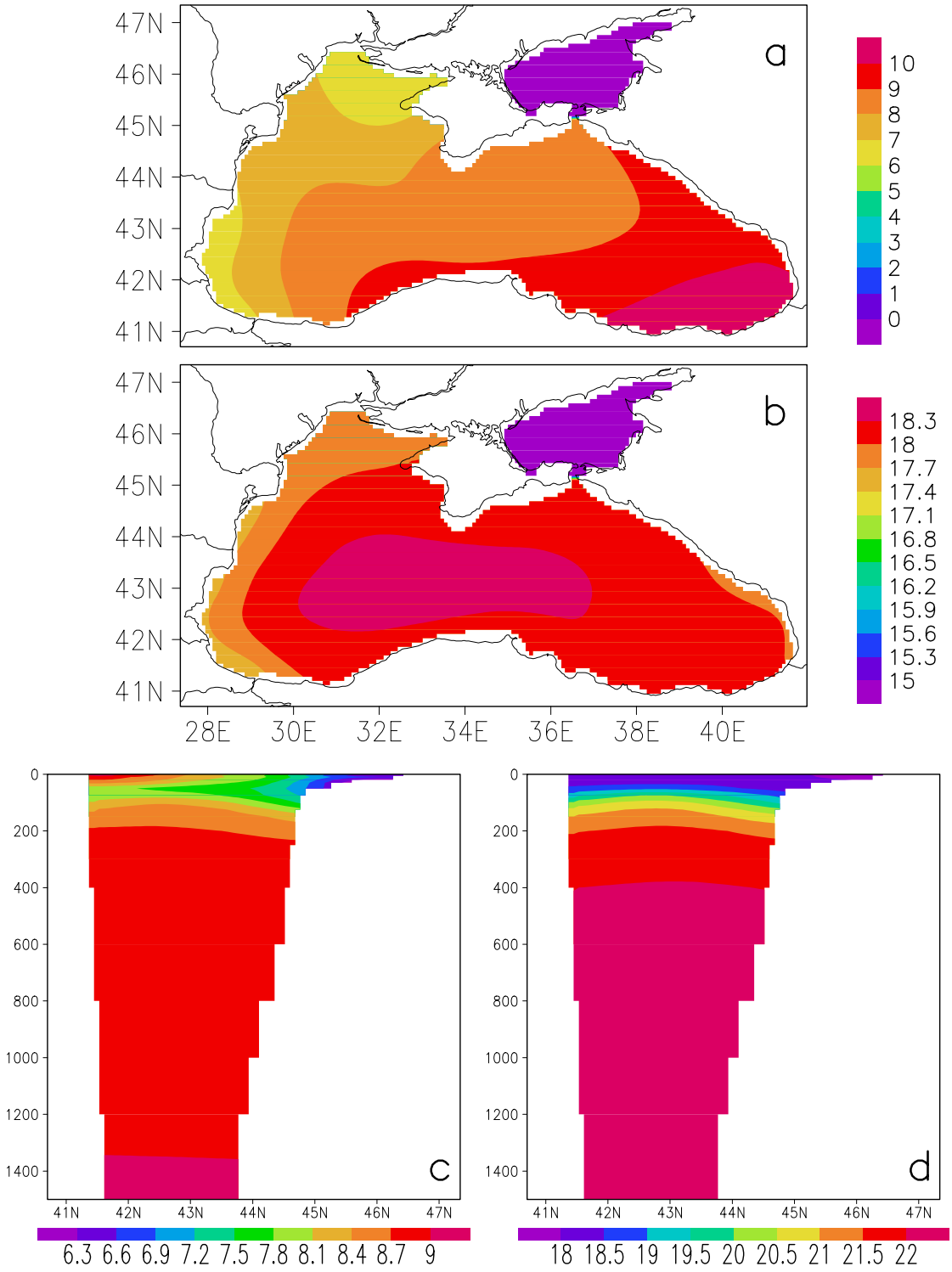

Fig. 4.3. Initialization fields.

4.3. Vertical resolution.

The choice of the proper vertical resolution is of crucial importance for the Black Sea. The presence of the Cold Intermediate Layer requires a good number of vertical layers to adequately represent the processes between the constant halocline and seasonal thermocline. Exploiting the GETM feature of providing general vertical co-ordinates we tested many different layer distributions, with the layer number ranging from 10 to 60 layers, and applying different refinements at the surface and at the bottom. Best results were obtained by using about 25-30 layers and a uniform distribution of layers down to 100 m, by applying a strong surface zooming (ddu=5) (see Fig. 4.4).

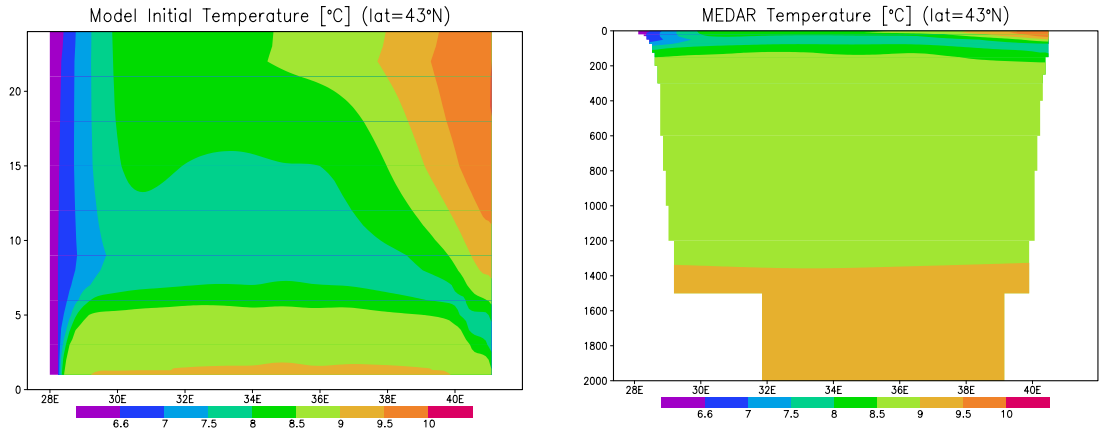

Fig. 4.4. The vertical coordinate system

4.4. Climatological forcing.

The atmosphere climatic data set is described in Sorkina (1974) and consists of monthly long-term mean 2D fields of air temperature [C], relative humidity [%] and wind velocity [m/s] zonal and meridional components. It was compiled using data from observations on the coastal stations and ships. Part of the Azov Sea is not covered by the data and there an extrapolation of the values from the Black Sea was done.

The model subroutine which calculates the air-sea heat fluxes in principal needs also the cloud cover as an input. The authors of the climatic data do not give this meteorological element, thus the calculations are done for a cloudless sky, therefore overestimating the solar radiation. The other

simplification is setting the atmospheric pressure to a constant value of 1013 HPa. Fig. 4.5, 4.6 and 4.7 give the maps of the monthly mean winds, temperature and relative humidity. Dominating through the year is the northeastern wind, which is stronger in the winter months.

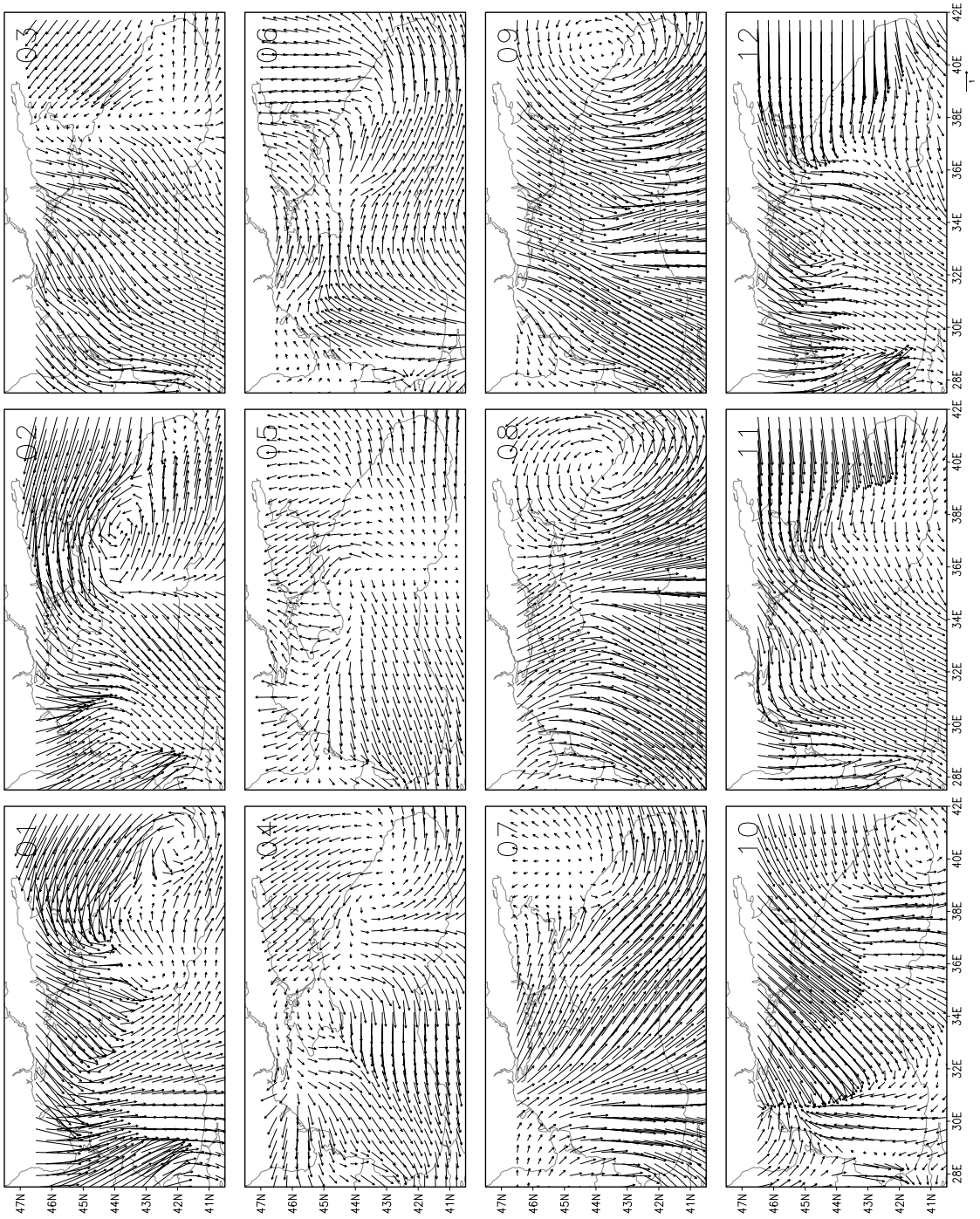

Fig. 4.5. Monthly mean climatological fields of wind. The arrow scale is 1 m/s.

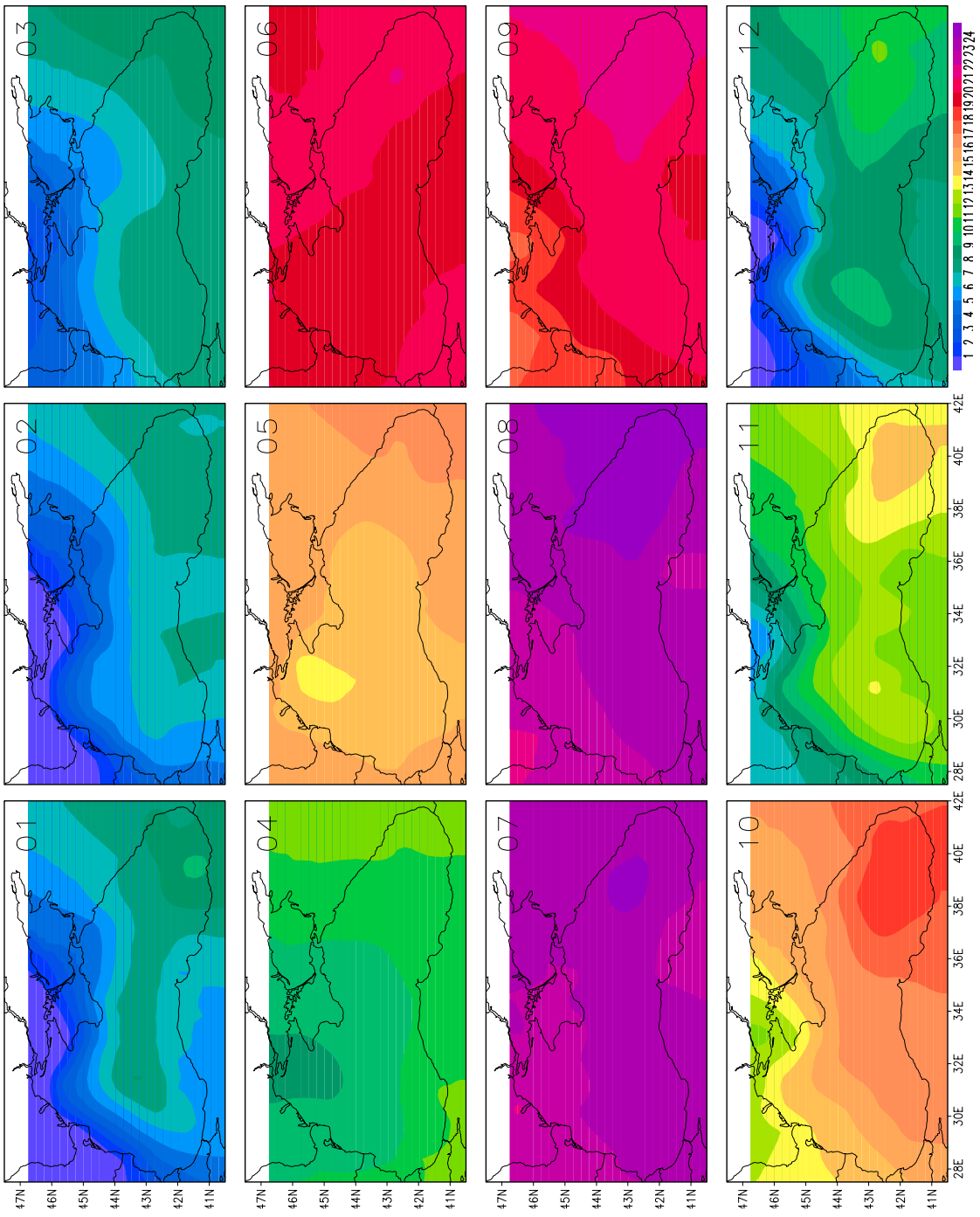

Fig. 4.6. Monthly mean climatological field of air temperature [°C].

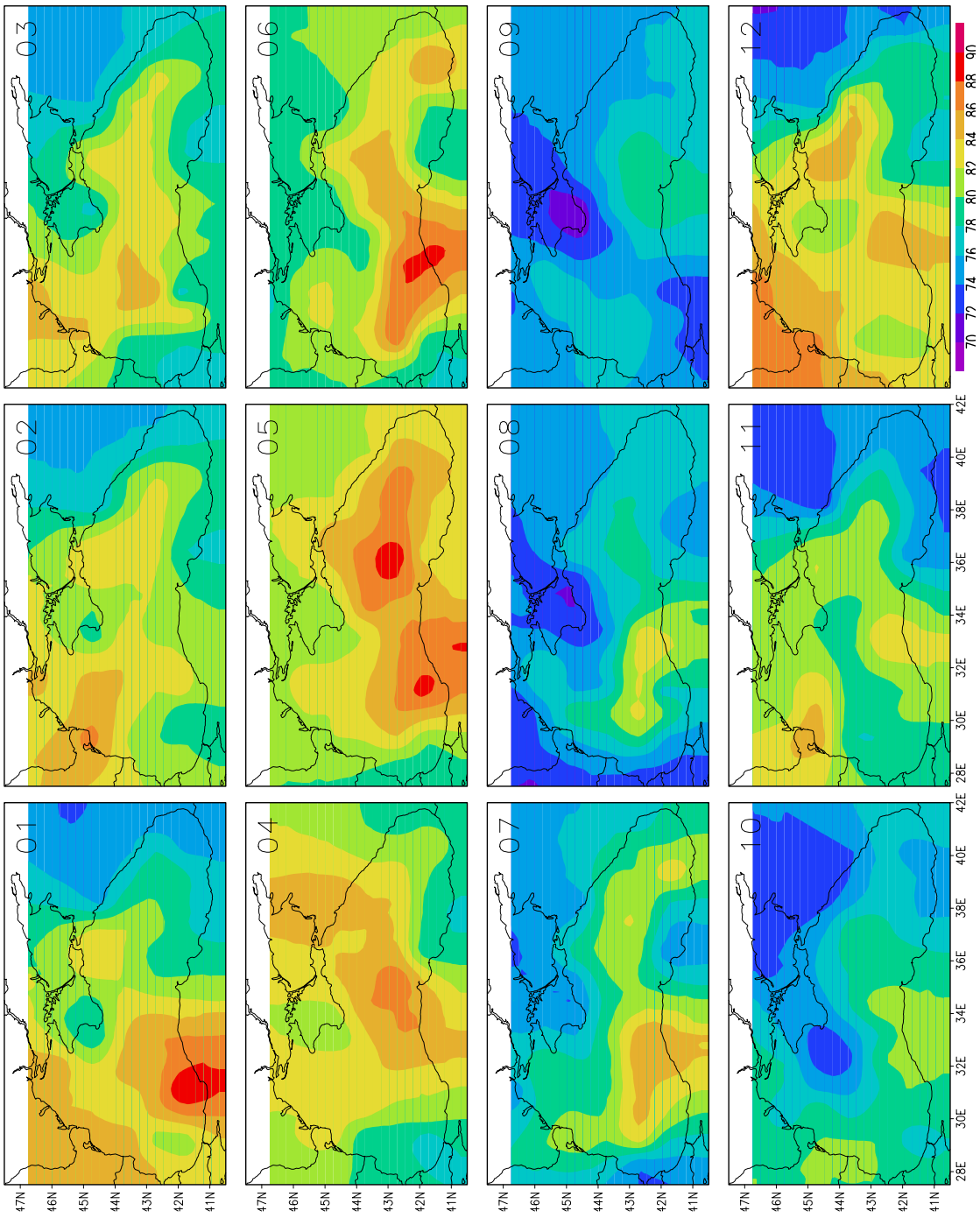

Fig. 4.7. Monthly mean climatological fields of air relative humidity [%].

4.5. Meteorological reanalyzes forcing.

ECMWF 40 Year Re-analysis (ERA-40) Data Archive.

The new re-analysis project ERA-40 covers the period from mid-1957 to mid-2002, overlapping the earlier ECMWF re-analysis, ERA-15, 1979 to 1993.

The whole period from September 1957 to August 2002 is now available. These data sets contain data at the resolution of the data assimilation and forecast system used by ERA-40. The resolution is (TL159 for spectral fields and N80 Quasi-regular Gaussian grid (80 lines with varying numbers of points along each row) for Gaussian fields). Data Services associated with these data sets include the provision of interpolation to requested resolutions and representation forms.

Eight data sets are supported separately: * Surface analysis * Pressure level analysis Model level analysis * Isentropic level analysis * Potential vorticity level analysis * Surface daily forecast * Pressure level daily forecast * Model level daily forecast

More information can be found on http://www.ecmwf.int

The model reads the meteorological ECMWF data every 6h, however in order to illustrate the data variability several maps of the monthly averaged 2D fields are presented. The consistency with the climatological data set is checked. The dominating winds here are also north-easterlies but the better horizontal resolution allows for representing more elements of the typical air circulation above the Black Sea (e.g. the wind curl in the southeastern part of the sea, near Batumi). Important is also the presence of two more meteorological variables, the atmosphere pressure and total cloud cover, thus the estimation of air-sea heat and momentum fluxes is more accurate. One more significant advantage is the complete data coverage of the region, with more realistic winds in the Aral Sea

On Fig. 4.8-11 the monthly mean 2D fields of the wind velocity, air temperature, total cloud cover and air pressure are presented.

To prove that the ECMWF data set represents also the inter-annual variability Fig. 4.12 is prepared – annual means of surface meteorological values, which are averaged for the Black Sea area.

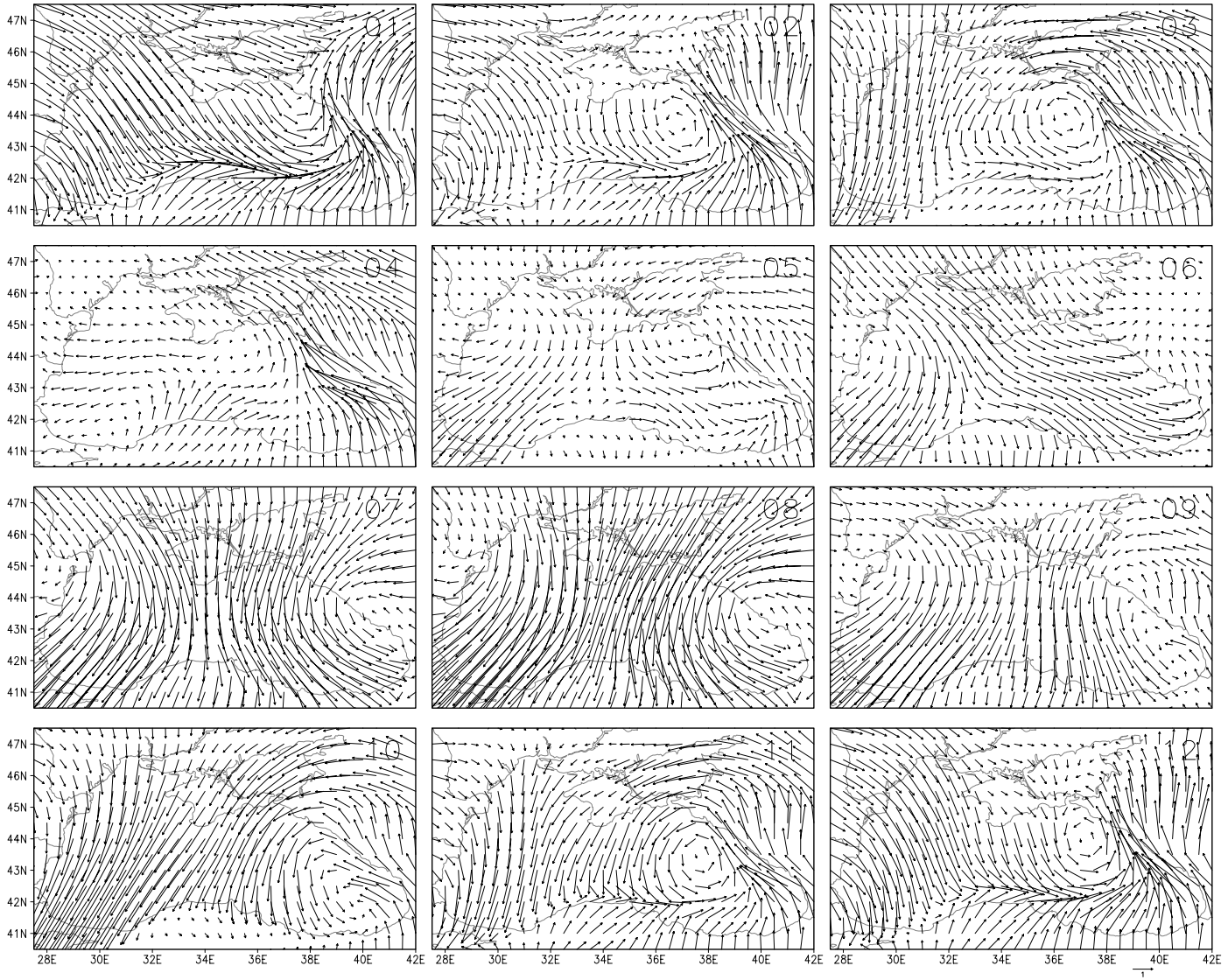

Fig. 4.8. Monthly ECMWF wind fields averaged for the period 1990-2000 [m/s].

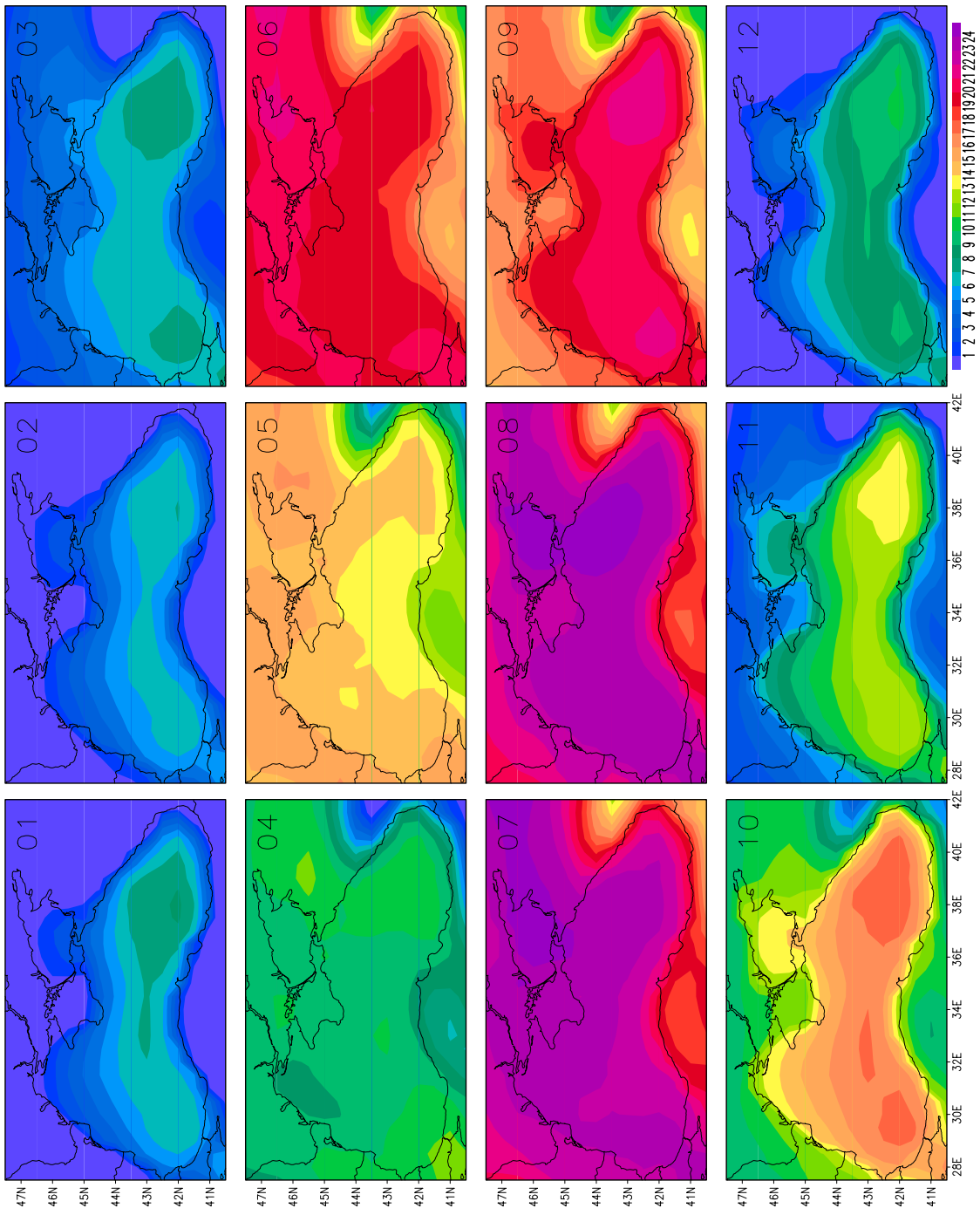

Fig. 4.9. Monthly ECMWF air temperature fields averaged for the period 1990-2000 [°C].

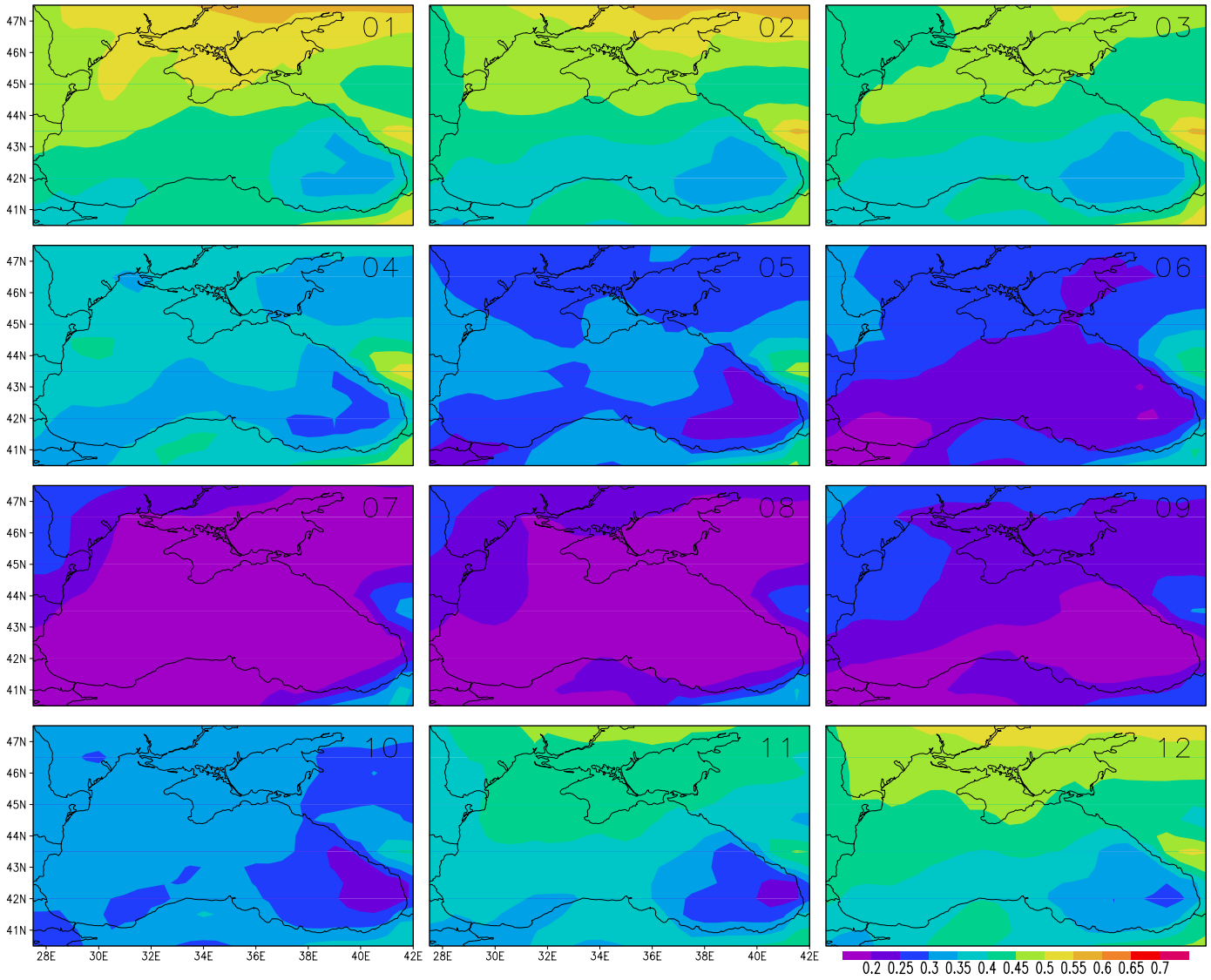

Fig. 4.10. Monthly ECMWF cloud cover averaged for the period 1990-2000 [°C].

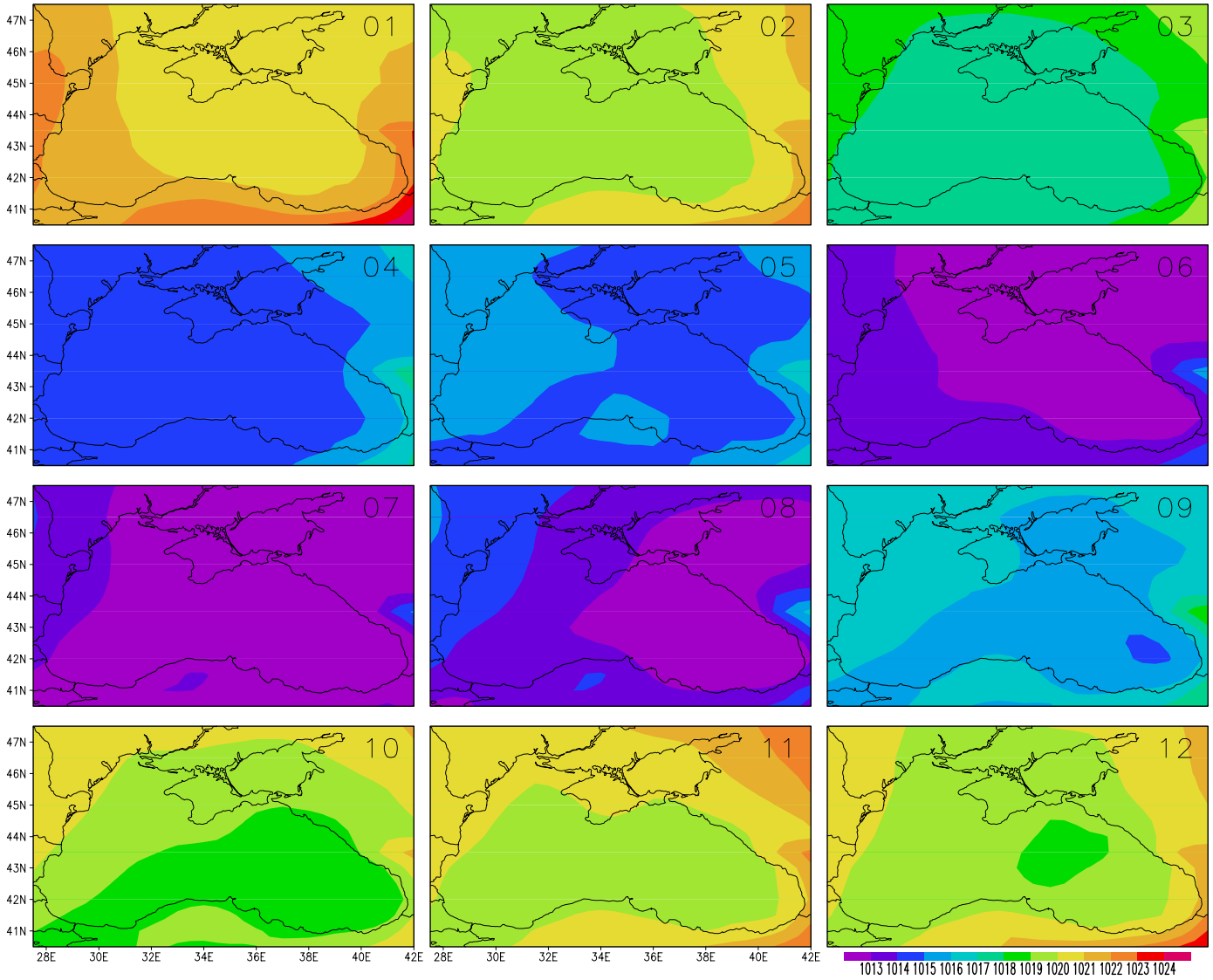

Fig. 4.11. Monthly ECMWF air pressure fields averaged for the period 1990-2000 [HPa].

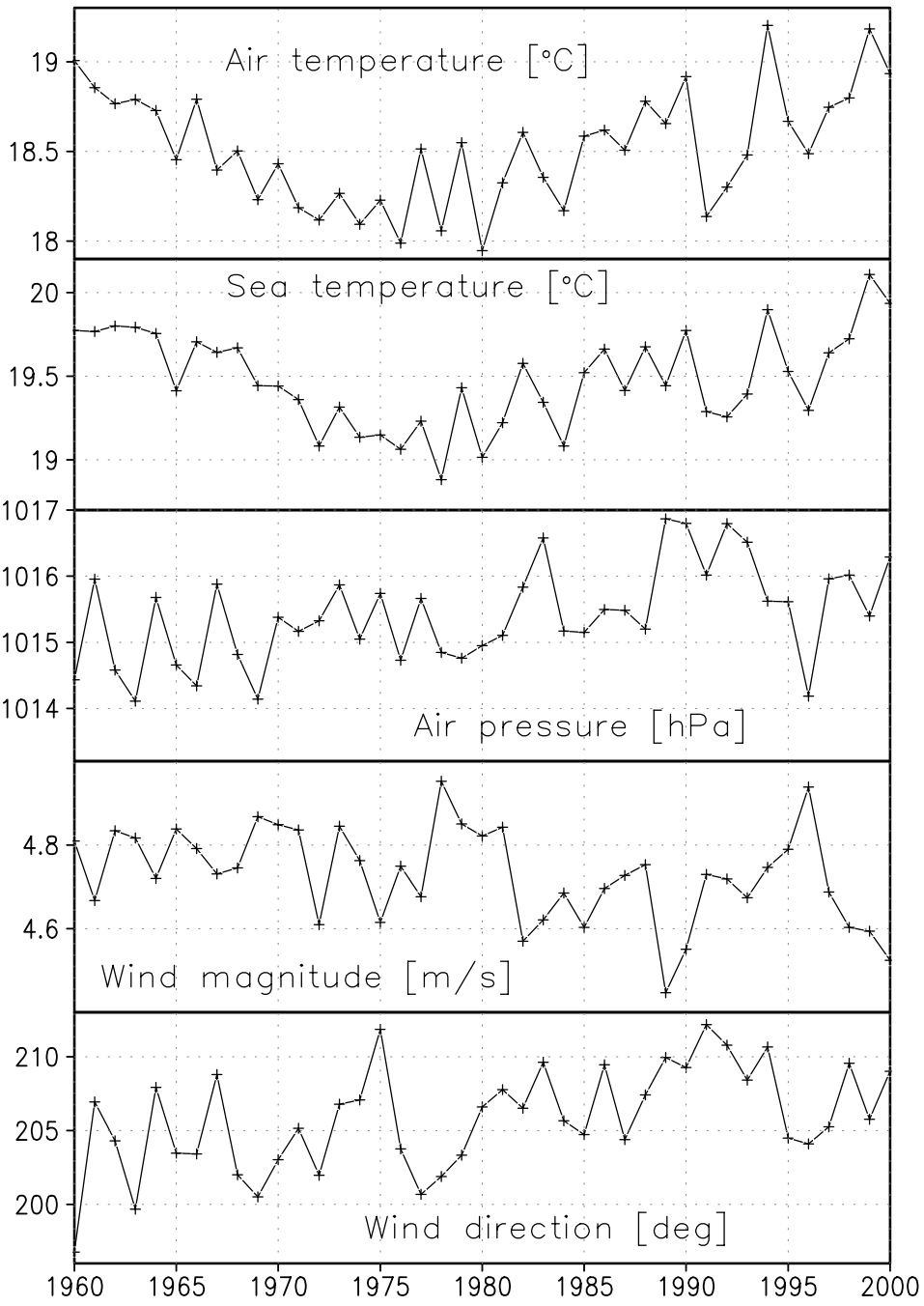

Fig.4.12. Interannual variability of the ERA40 meteo-forcing components. The data cover the period 1960-2000.

4.6. Rivers.

Global Runoff Data Centre (GRDC) Freshwater discharge from continents into the oceans is of major interest in research concerned with global monitoring of freshwater resources, the flux of matter into coastal areas and the open oceans, and the influence of freshwater fluxes on circulation patterns in the ocean and the atmosphere on regional and global scales.

Following two previous publications of estimated Mean Annual Freshwater Surface Water Fluxes into the World Oceans based on 161 and 181 discharge stations, respectively (GRDC, 1996 and GRDC, 1998) the GRDC has reworked this exercise for a third time, now based on 251 discharge stations close to the estuary, featuring basin areas greater than 25.000 km^2. The report is expected for publication in the course of the year 2004.

Discharge from land areas not integrally captured by GRDC stations has been determined via estimating mean annual runoff coefficients (RC) by means of regionalisation from nearby monitored areas, taking into account data from another 1378 GRDC stations and applying precipitation data from the Global Precipitation Climatology Centre (GPCC).

Application of GIS analysis on a 0.5 degree elevation grid, optimised for flow path detection allowed to determine the catchments of the entire individual grid cells that form the fringe of the continents (around

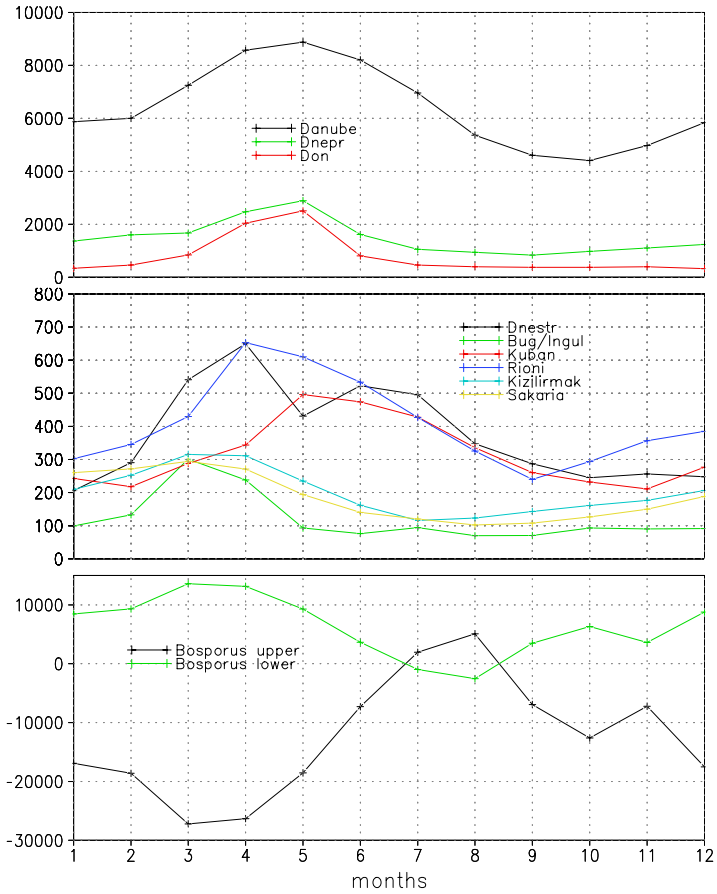

Fig. 4.13. River forcing varying seasonally. There are 9 rivers included and the Bosporus barotropic transport is calculated from their values.

12.000), i.e. all continental grid cells were co-registered with their respective fringe grid cell through which they drain to the oceans. Furthermore, each grid cell was assigned either a calculated or estimated RC. Thus, it is possible to calculate for each fringe grid cell the integral flux from its adjacent catchment as the spatially weighted product of RC and precipitation over all co-registered grid cells. Summarizing the fluxes of subsets of continental fringe cells allows estimating fluxes for arbitrary coastline sections.

For further information http://grdc.bafg.de/

Fig. 4.13 shows the river run-off used in the model simulations. Every river varies seasonally and adds a fresh water volume to the model grid box which is nearest to its geographical position. Thus it affects the sea level and currents, but also the salinity in this grid box, which is calculated as a mean from the salinity of the previous moment and the total mixed volume.

The graph shows the well known facts from the studies of Simonov and Altman, (1991), that the Danube contribution is ~90% of the total river discharge. The period with maximum fresh water input is April-May, and November is the month with minimum river discharge. The included 9 big rivers in the Black Sea are – Danube, Dnestr, Ingul+Bug, Dnepr, Don, Kuban, Rioni, Sakarya and Kizilirmak.

Having the river runoff monthly values, the Bosporus barotropic transport is easily calculated. This is done to remove the constant increase of the sea level caused by the rivers. The effect for the model is as if one more river with negative transport and no influence on the salinity of the grid box is included. This barotropic transport is vertically separated in two parts representing the lower and upper Bosporus Strait. The lower Bosporus Strait is considered as an inflowing river with salinity of 36 PSU.

4.7. Initial "spin-up" simulations.

At the beginning of the integration the numerical model needs initial values for all model variables. Unfortunately it is not possible to provide initial conditions for the currents. Though temperature and salinity are measured relatively easy and observational material usually is available, the currents are much more difficult to measure. One possible solutions of this problem

is to use some idealized current velocity solution (geostrophic velocity) or to integrate the model in so called “spin-up” mode.

During such type of integration the 3D water density field is “frozen”, and the subroutines for the evolution of T and S are skipped. Thus after some number of model time steps a stable model state is reached. In other words this preliminary run serves to adapt the fields of the zonal and meridional velocity components to the density field.

The number of time steps before this adaptation occurs is different for each basin and each choice of the model parameters, described in Paragraph 3. In

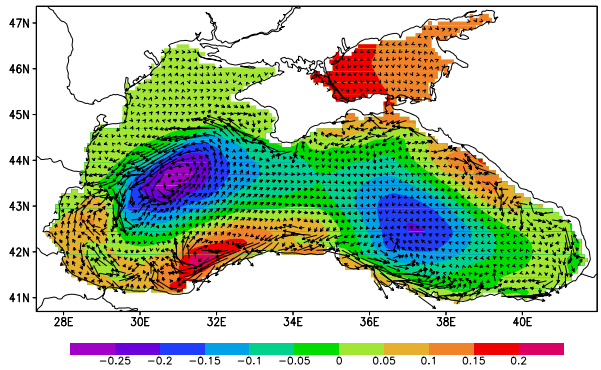

Fig. 4.14. The Sea Surface Elevation after the spin-up run.

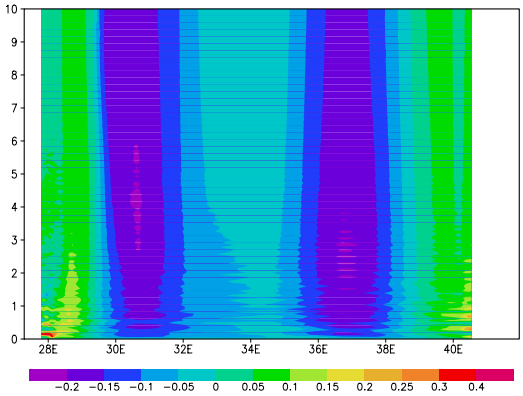

Fig. 4.15. Zonal Hoevmoller diagram of the Sea Surface Elevation [m] during the spin-up run.

the case of the Black Sea a spin-up period of 10 days is chosen. Fig. 4.14 shows the reached stable state for the sea elevation and the velocity field (the vectors). The typical situation for a basin with a cyclonic circulation is observed – lower level in the center of the sea and higher level in the coastal zones. From the Hoevmuller diagram on Fig. 4.15 it is clear that the initial oscillations and perturbations disappear after 10 days and the state can be considered as stable.

4.8. Water transparency.

As it was described in Paragraph 3 the model performance is dependent on a great number of parameters, including the water transparency. Three

parameters (a, η_1 and η_2) are available in the equation for light propagation in the water: $I(z) = I_0(ae^{-\eta_1 z} + (1-a)e^{-\eta_2 z})$

However it is considered usually that these parameters are constant for the whole basin because in order to have most accurate space varying estimate of a, η_1 and η_2 special and rather expensive measurements have to be conducted. For the base numerical Black Sea experiment we have chosen constants according to Jerlov type 6 (a=0.67, $1/\eta_1$ =0.67m and $1/\eta_2$=17m, which are the attenuation coefficients for short and long wave radiation), which corresponds to a rather turbid water. Recent measurements have shown that the water in the Black Sea is rather turbid, Secchi disk depths of about 5 m are reported in the shelf part, which justify such a parameterization.

More accurate measures for optical water properties could be obtained from satellite data (Paulson and Simpson, 1977). Using the SeaWIFS ocean color data base an estimate of the water optical depth is done on monthly bases. Further these values are used in the model and several sensitivity experiments are conducted. Fig. 4.16 shows the annual optical depth calculated from the monthly mean values (see maps on Fig. 4.17). The mean value for the whole sea is about 10 m, which is the depth where the light intensity decreased by e-times. During the year it varies from 5 to 15 m.

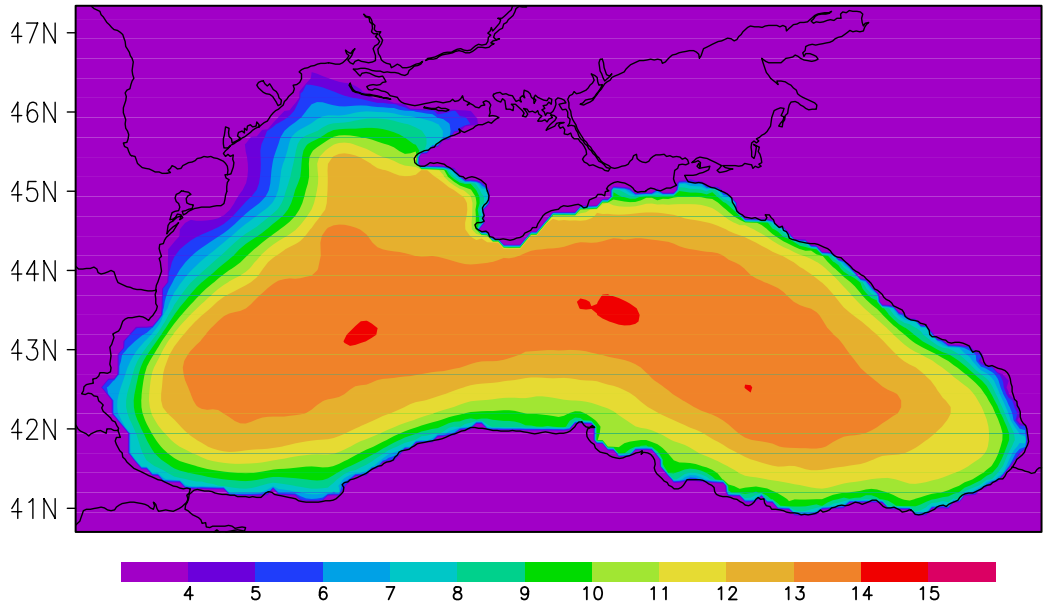

Fig. 4.16. The annual mean water optical depth [m], used further in the experiments for sensitivity to optical properties.

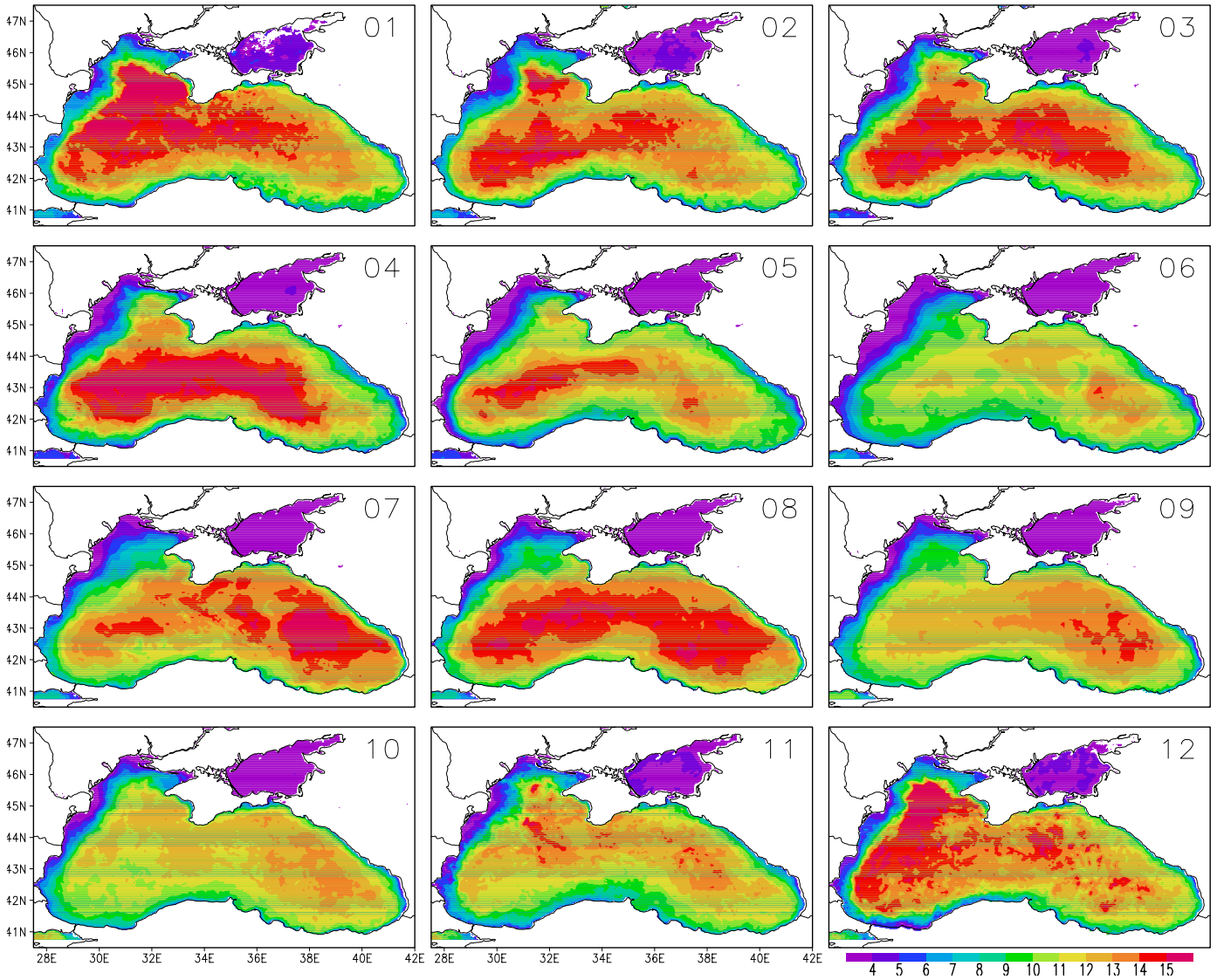

Fig. 4.17. Monthly mean optical depth fields calculated from the satellite [m].

5. Results from climatological simulations.

When setting up the model for a new basin the first step to do is the integration with atmospheric climatological forcing, thus one can scale the importance of the different physical processes in the region and obtain an idea about the seasonal variability.

The integration with the model configured as explained in Paragraph 3 for 12 months with constant atmosphere forcing is done and the monthly mean fields of the model variables are obtained. The forcing was already described in section 4.3.

From the model simulations the characteristics of the mixed layer are calculated and the results are given on several figures. These are important parameters when estimating the ecological status of marine ecosystems.

The monthly mean mixed layer depth, temperature and salinity seasonal variations are given on Fig. 5.1. The depth varies from 5m in the summer to 40 m in winter. The salinity is rather constant ~17.5 PSU and the temperature oscillates between 6 and 20 °C. There is however a large spatial variability as seen from the 2D maps (Fig. 5.2-5)

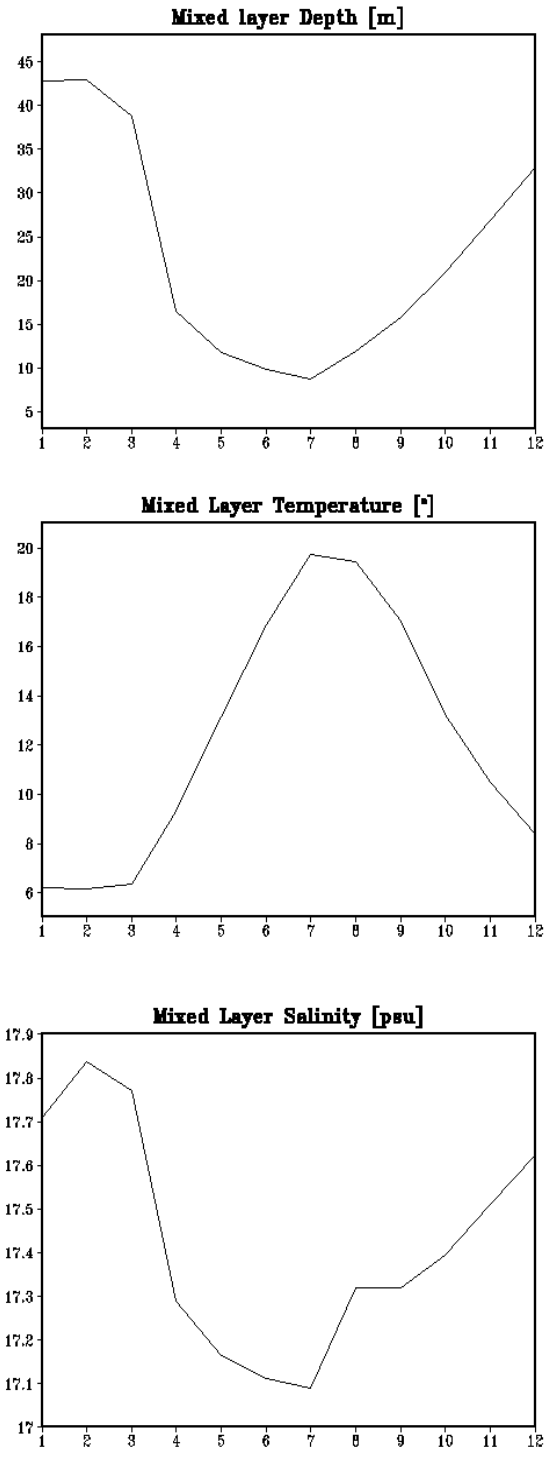

Fig. 5.1. Seasonal variations.

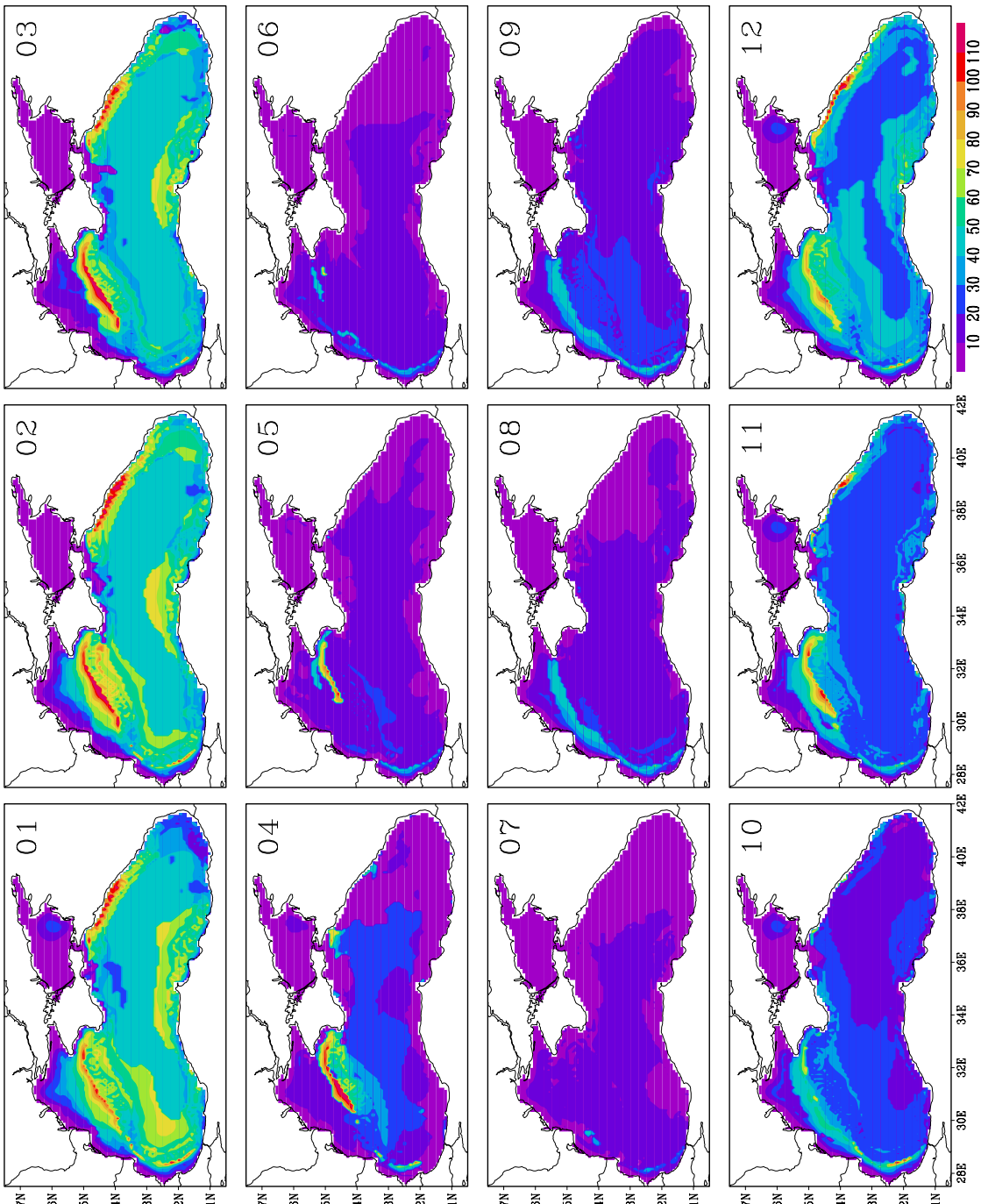

Fig. 5.2. Monthly mean maps of the mixed layer depth from the climatological run [m].

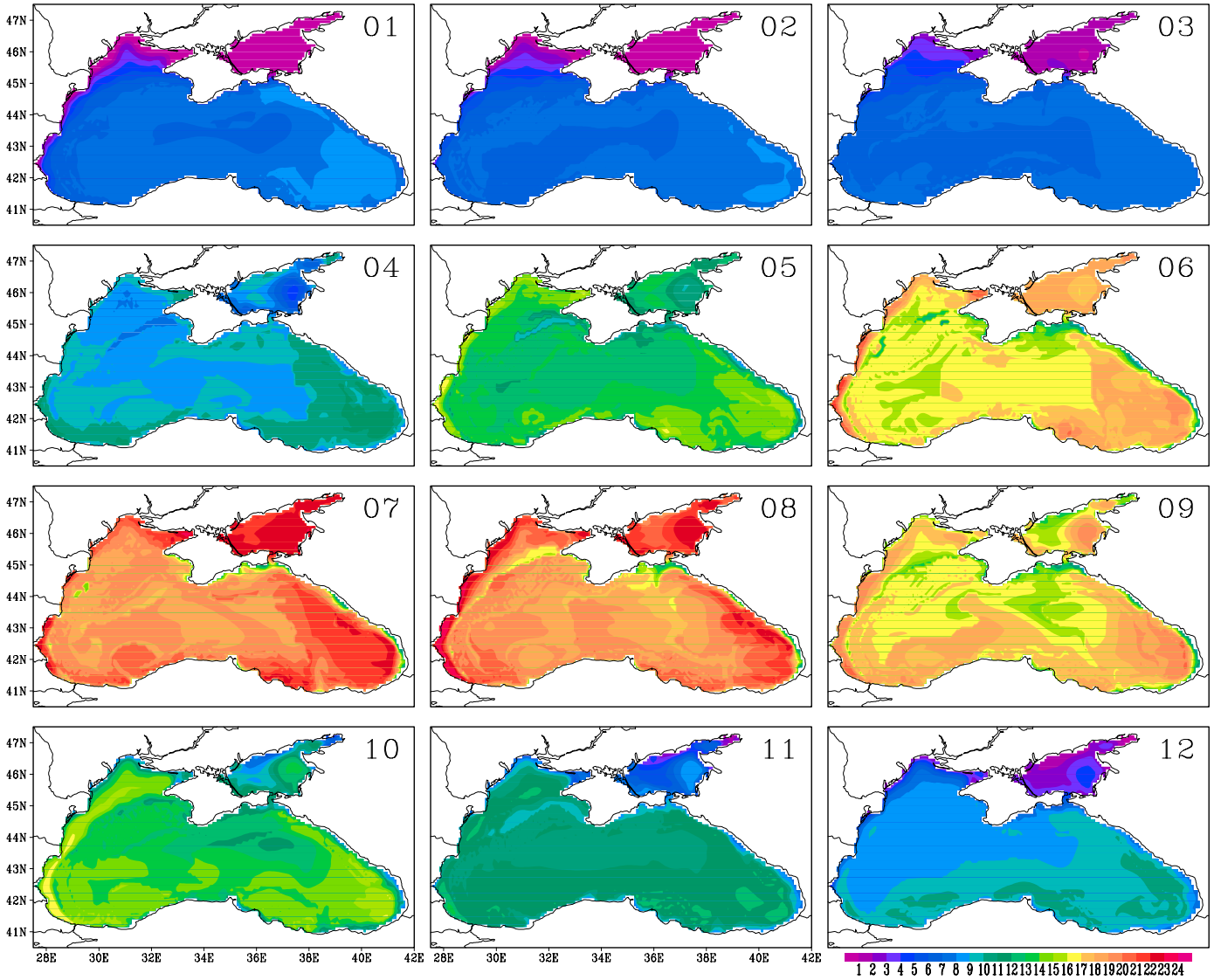

Fig. 5.3. Monthly mean mixed layer temperature from the climatological run [°C].

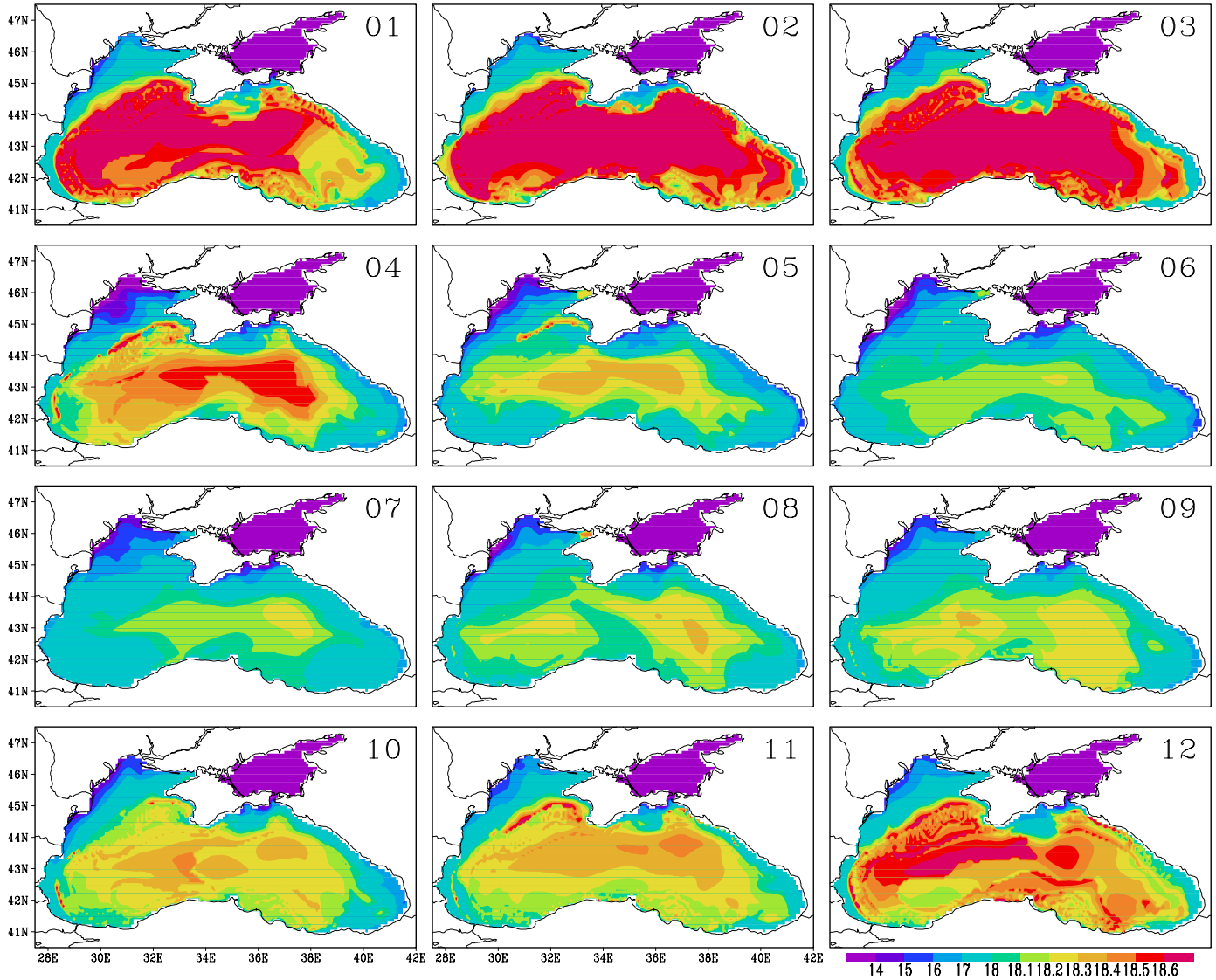

Fig. 5.4. Monthly mean maps of the mixed layer salinity from the climatological run [PSU].

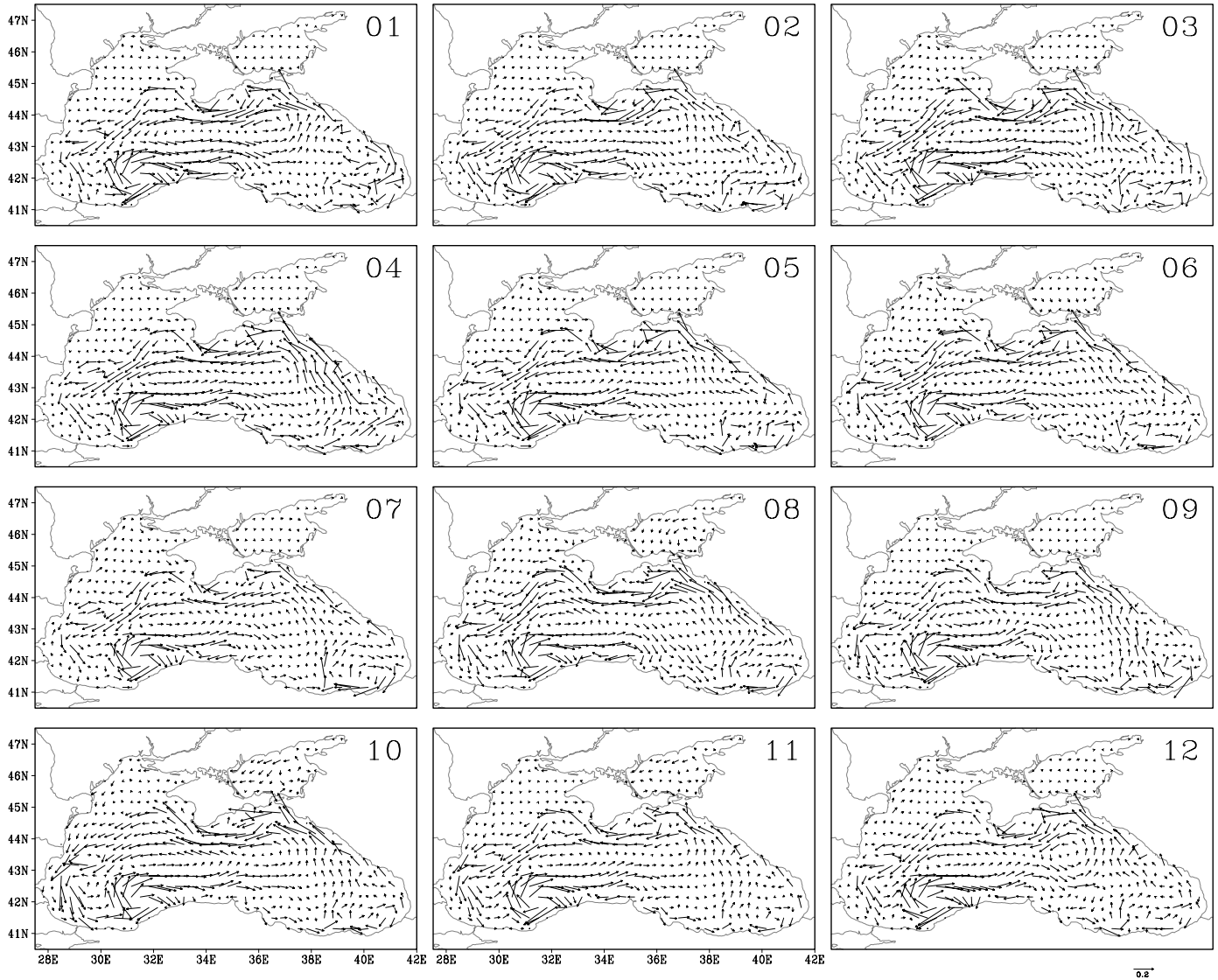

Fig. 5.5. Monthly mean maps of the mixed layer current from the climatological run [m].

6. Results from real-forcing simulations. Base experiment.

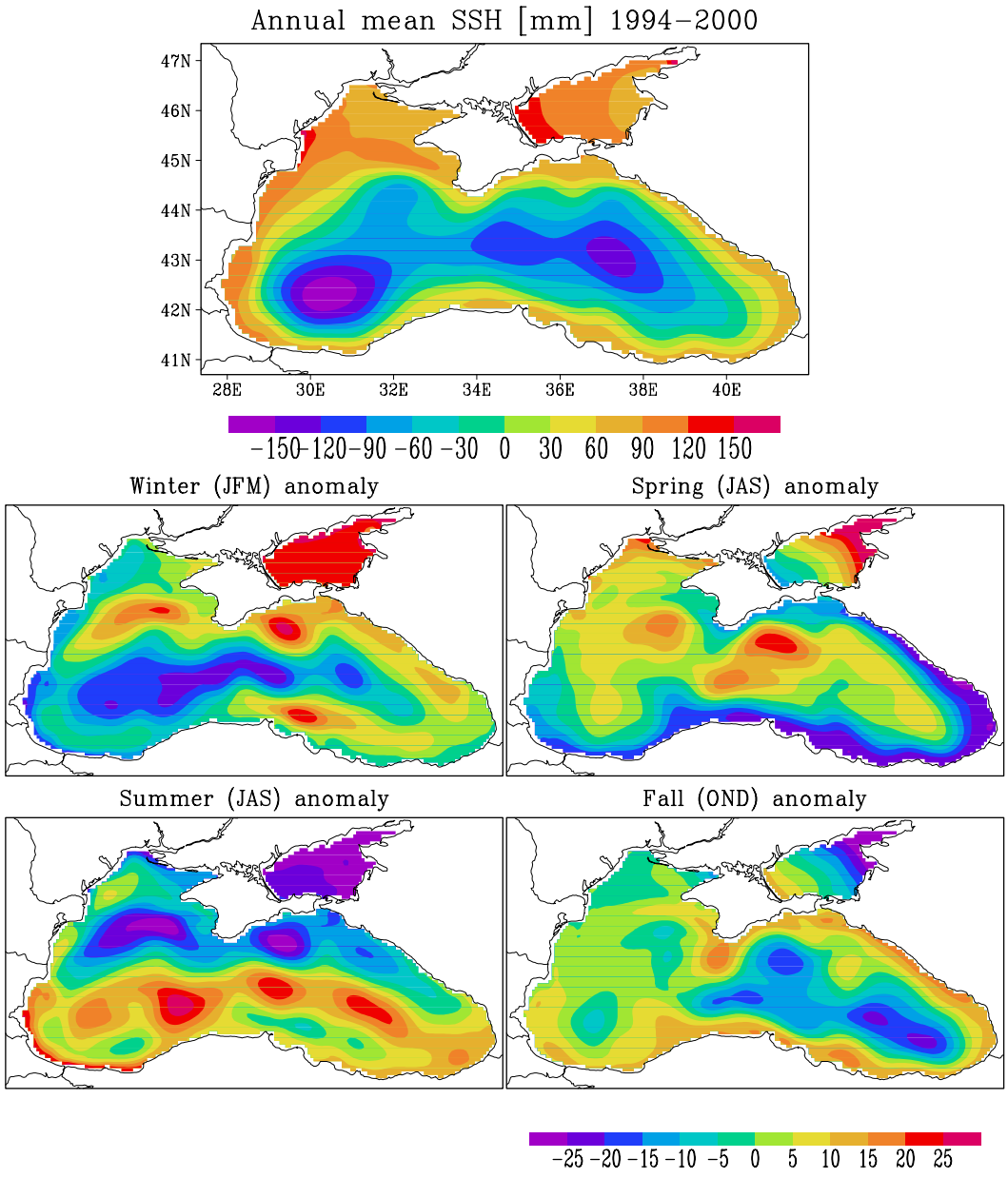

Fig. 6.1. Annual mean Sea Surface Elevation [mm] calculated from the model averaged for the period 1994-2000. The seasonal means are also calculated and the difference to the annual mean field is shown.

The base numerical experiment is denoted from here on as “J6”. This refers to the choice of water optical properties (equation for the light propagation follows Jerlov formulation and the coefficients correspond to the proposed type 6).

The horizontal resolution is 5’ in both zonal and meridional directions, the grid dimensions are 177x81 grid points with the coordinates of the starting point at 27.33ºE and 41.74ºN and the number of vertical layers is 25. For the rest of the input parameters see the file getm.inp printed in Paragraph 3. The meteorological forcing is ECMWF re-analysis data, referred as ERA40 data set. The model data are available as daily values and monthly mean fields. For the complete list of the produced files and variables see the Appendix 1.

In this Chapter an overview is given over the seasonal variability of the basic physical parameters – temperature, salinity and currents. Note that there is much to be done in analyzing the great amount of produced data in regard to the spatial and interannual variability.

First we discuss the dynamics of the model results. On Fig. 6.1 the annual mean Sea surface elevation (SSE), averaged from the model results, is shown. The main Rim cyclonic current is well represented, which can be seen by comparison with Fig. 6.2, where the sea surface height is calculated by the dynamical heights method from climatological data for T and S. The seasonal anomalies from the model compare well to the climatological ones and to the altimeter TOPEX/Poseidon data (Fig. 6.3). The seasonal intensification of the Black Sea circulation is identified by the reverse sign of SSE anomalies in the central and coastal sea in the warm part of the year comparing to the cold part (these results are known from the works of Bulgakov and Korotaev, 1984, Stanev, 1990, Ducet et al, 1999, Stanev et al, 2000). Weaker variability is observed however in the easternmost part where theory and observation have proven the existence of a pronounced anycyclonic circulation (Rachev and Stanev, 1998, Stanev and Rachev, 1999, Stanev and Staneva, 2000). This partially might be due to the wind forcing – in the easternmost Black Sea the wind curl seems to be underestimated. Fig. 6.4 shows the wind in July 1992 from ECMWF data set and calculated by a regional climate model, showing that the regional model captures better the eastern wind curl feature. This might be one direction to improve the simulations, by obtaining better meteorological data from regional models.

Fig. 6.5 illustrates the seasonal and inter-annual variability of the Sea Surface Temperature and Salinity (SST and SSS) averaged for the whole Black Sea. The seasonal amplitude is around 18ºC for the SST and 0.6 PSU for SSS. What could be noted is that the SST variations do not show a pronounced trend, during 1991 and 1999 the summer is warmer and the winter in 1993 was the coldest one. However, after 4 years of integration the SSS experiences a large trend of 0.1 PSU per year. This is an indication that the model tends to overestimate the mixing in the surface layer.

The model validation continues with comparison of annual mean 2D fields of the model and data from observations. The climatological data are given on Fig. 6.6 as surface map and area mean values. Fig. 6.7 presents the annual mean fields for SST, SSS and surface currents (the first column is J6 experiment, the others are experiments denoted KDE and E10 which will be described in the next paragraph). Both, the amplitude of the seasonal signal and the horizontal features of the fields show comparable values.

Fig. 6.8 and Fig. 6.9 also serve to prove that the model results are consistent regarding the surface and deep layers. A vertical cross-section in zonal direction 43ºN for annual mean temperature is given on Fig 6.8. On Fig. 6.9 the meridional vertical cross-sections around 31ºE meridian presents model and observational data for September 1991 and July 1992. The observations have taken place during the HydroBlack and ComsBlack expeditions (Oguz). Both pictures show rather encouraging consistency between simulations and measurements.

The next three figures Fig. 6.10-12 aim at presenting the monthly 2D fields of the model SST, SSS and surface currents in order to reveal the horizontal variability. The SST maps represent well the general meridional gradient with a considerably warmer eastern part. The SSS shows larger values in the central parts following the dooming of the isohaline surfaces due to the cyclonic Rim gyre.

The next interesting question is about the mesoscale and intra-annual variability which is reported from theoretical and observational studies (Rachev and Stanev, 1997, Stanev and Rachev, 1999). For this purpose several figures are prepared. Fig. 6.13 presents the Sea Surface Elevation (SSE) in several consecutive weeks in April 2004. The prepared video animation shows more clearly the mesoscale variability, like moving eddies and oscillations of the main Rim gyre, but with some imagination it could be

also seen on the plot. Fig. 6.14 illustrates basin oscillations, on the zonal Hoevmuller diagram a wave propagating from east to west can be easily identified. Mesoscale variability can be also observed on the maps of salinity (Fig.6.16) as the mesoscale eddies and filaments can be well distinguished by its different salinity.

Fig. 6.15 is showing the seasonal variation of the temperature profile at a single location. Different meteorological events like summer heating and winter cooling can be identified.

Fig. 6.17-19 present the SST, SSS and surface currents zoomed on the shelf NW part of the Black Sea as this is an area of particular interest.

Fig. 6.2. Annual mean dynamic height [cm] calculated from climatological temperature and salinity fields. The seasonal means are also calculated and the difference to the annual mean field is shown.

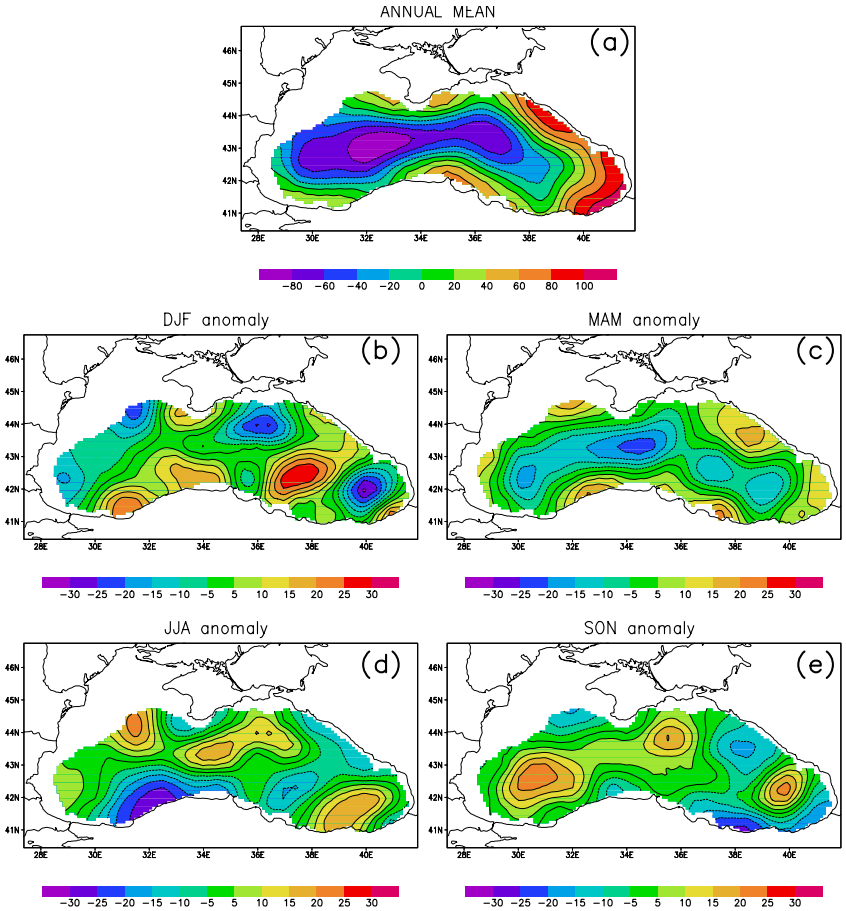

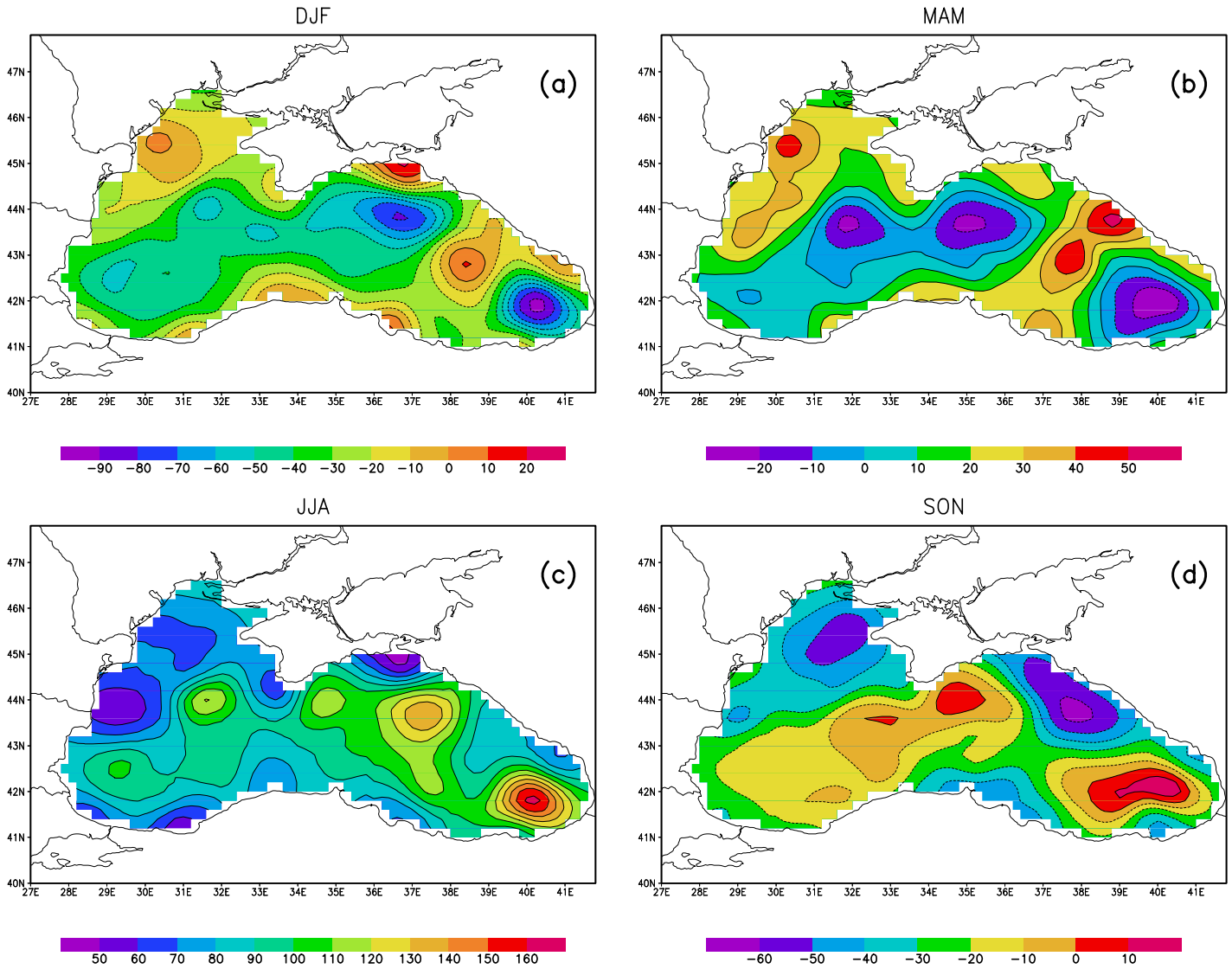

Fig. 6.3. Seasonalaveraged maps of the sea level calculated from the TOPEX/Poseidon [cm].

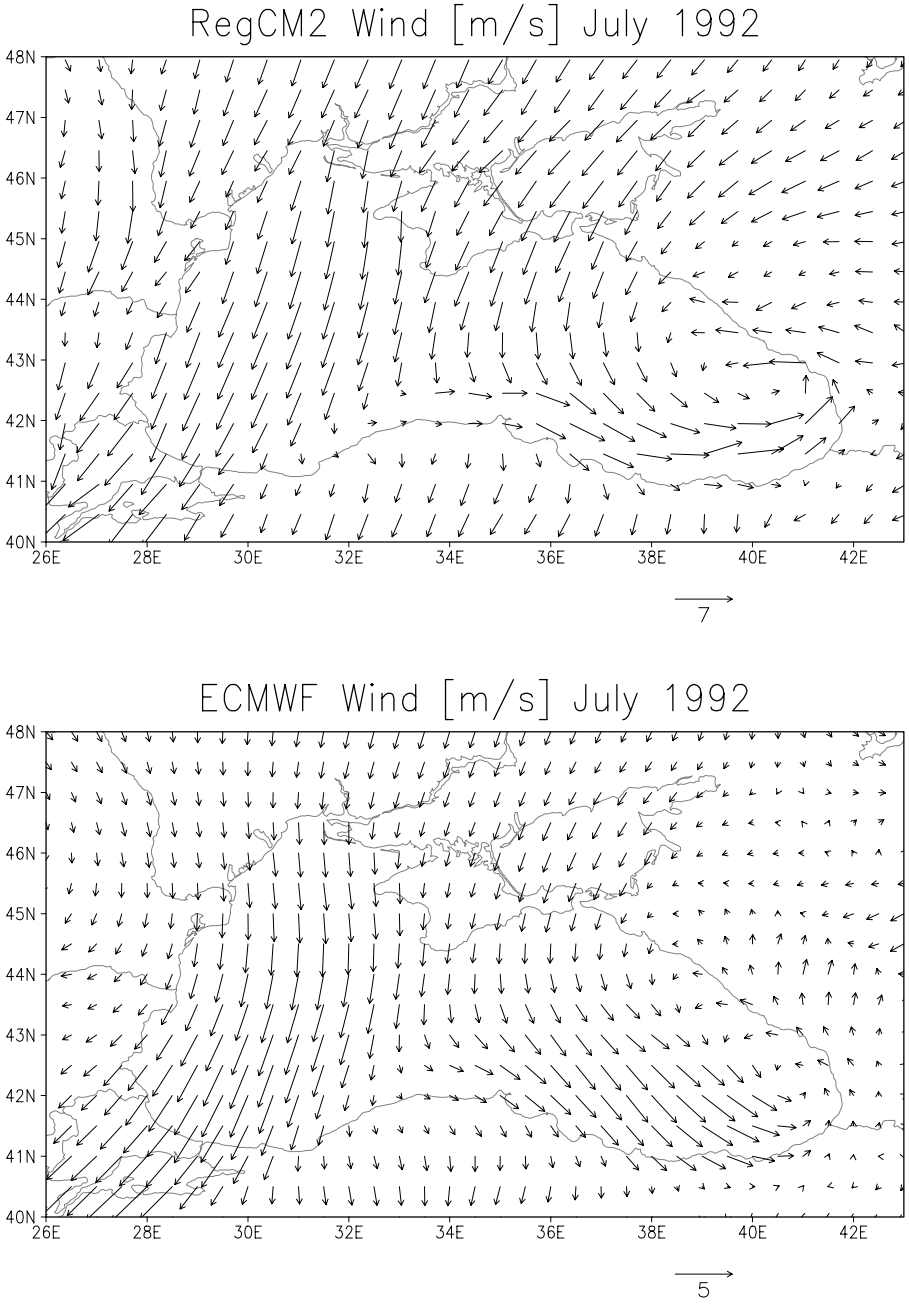

Fig.6.4. Monthly mean winds [m/s] for July 1992 calculated from a Regoinal climate model (RegCM2) and ECMWF dataset.

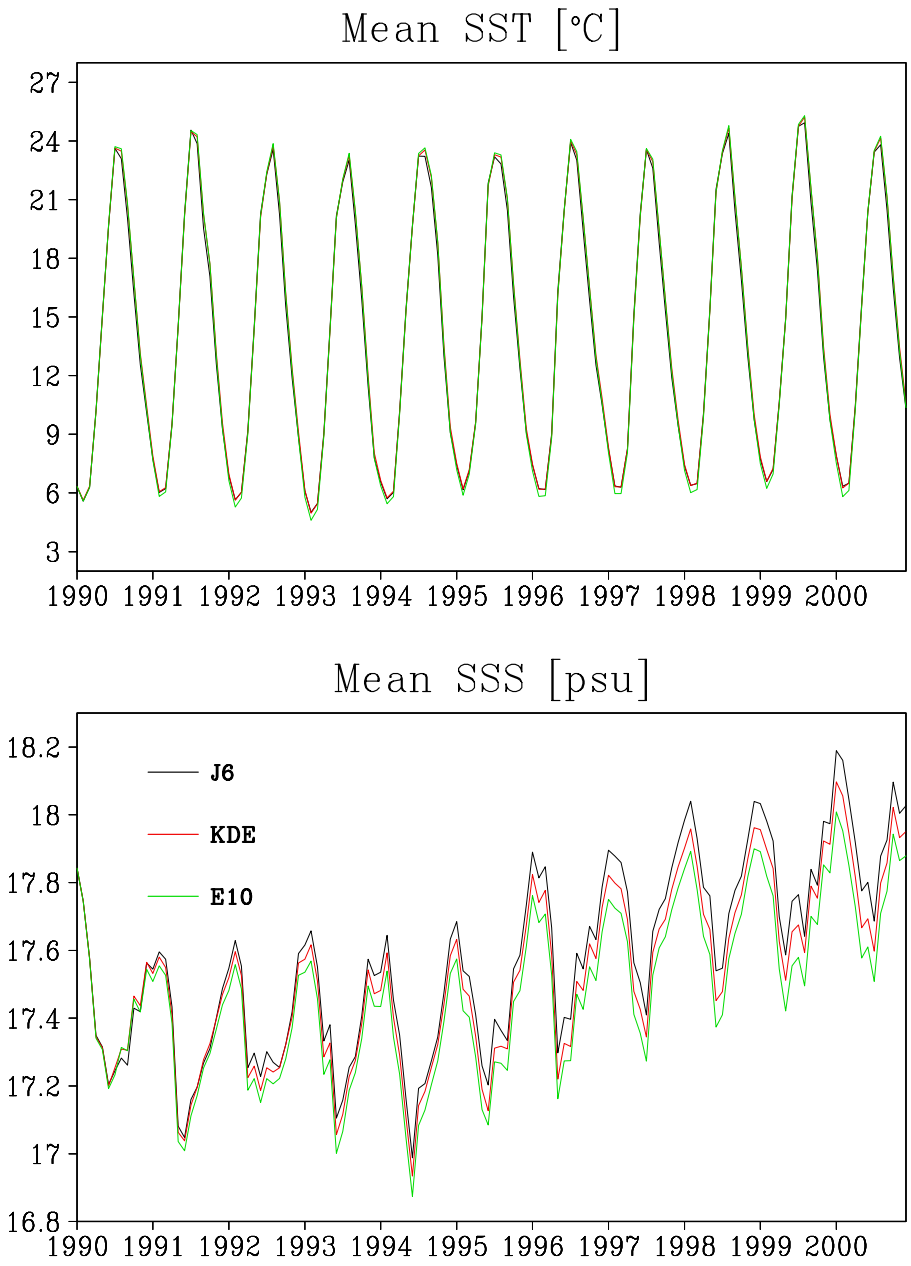

Fig.6.5. Sea surface mean values of temperature [°C] and salinity [PSU] for the integration period 1990-2000.

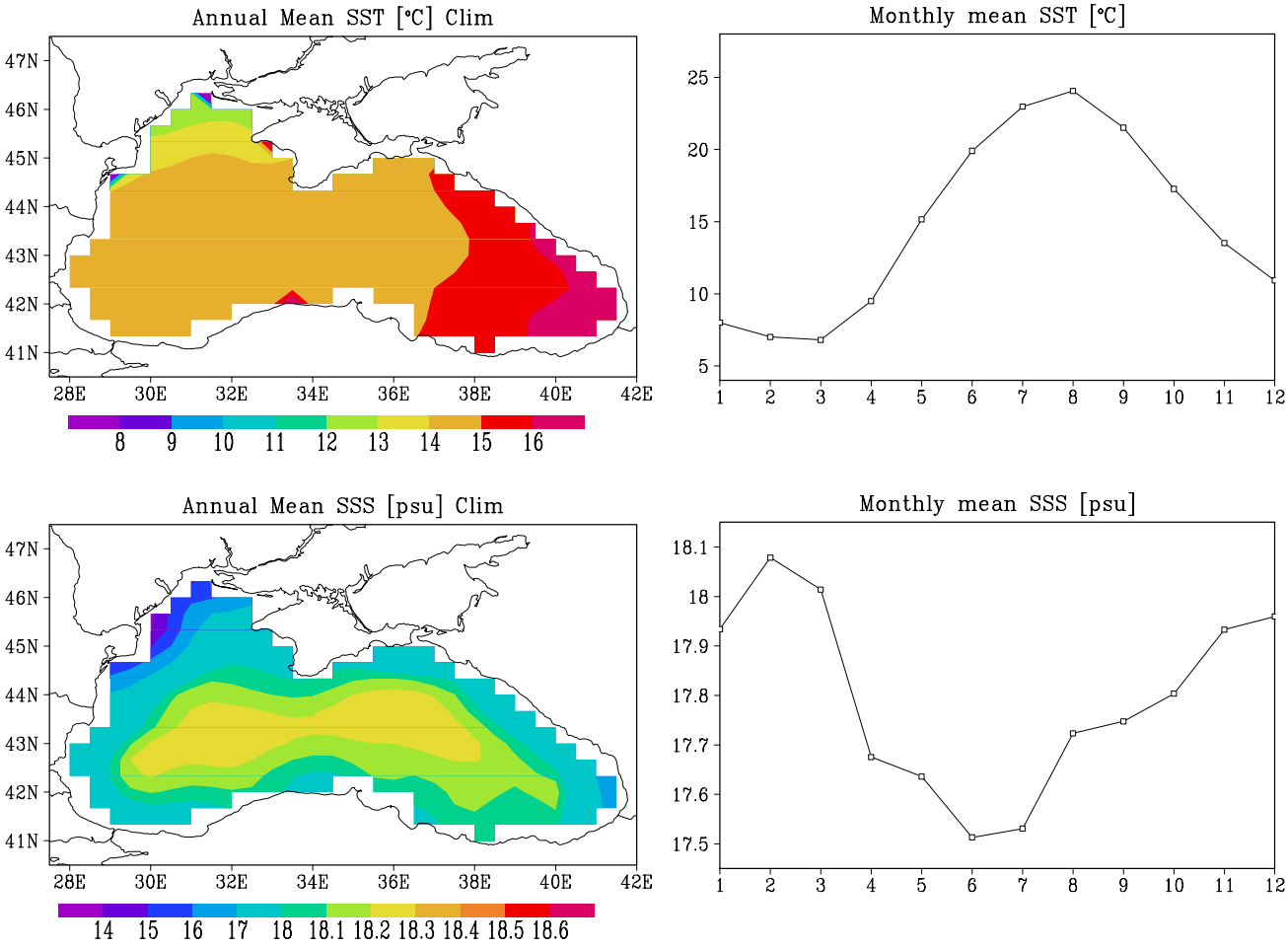

Fig.6.6. Sea surface temperature [°C] and salinity [PSU] (left panels) and their seasonal variations (right) given by the climatological dataset BSHM

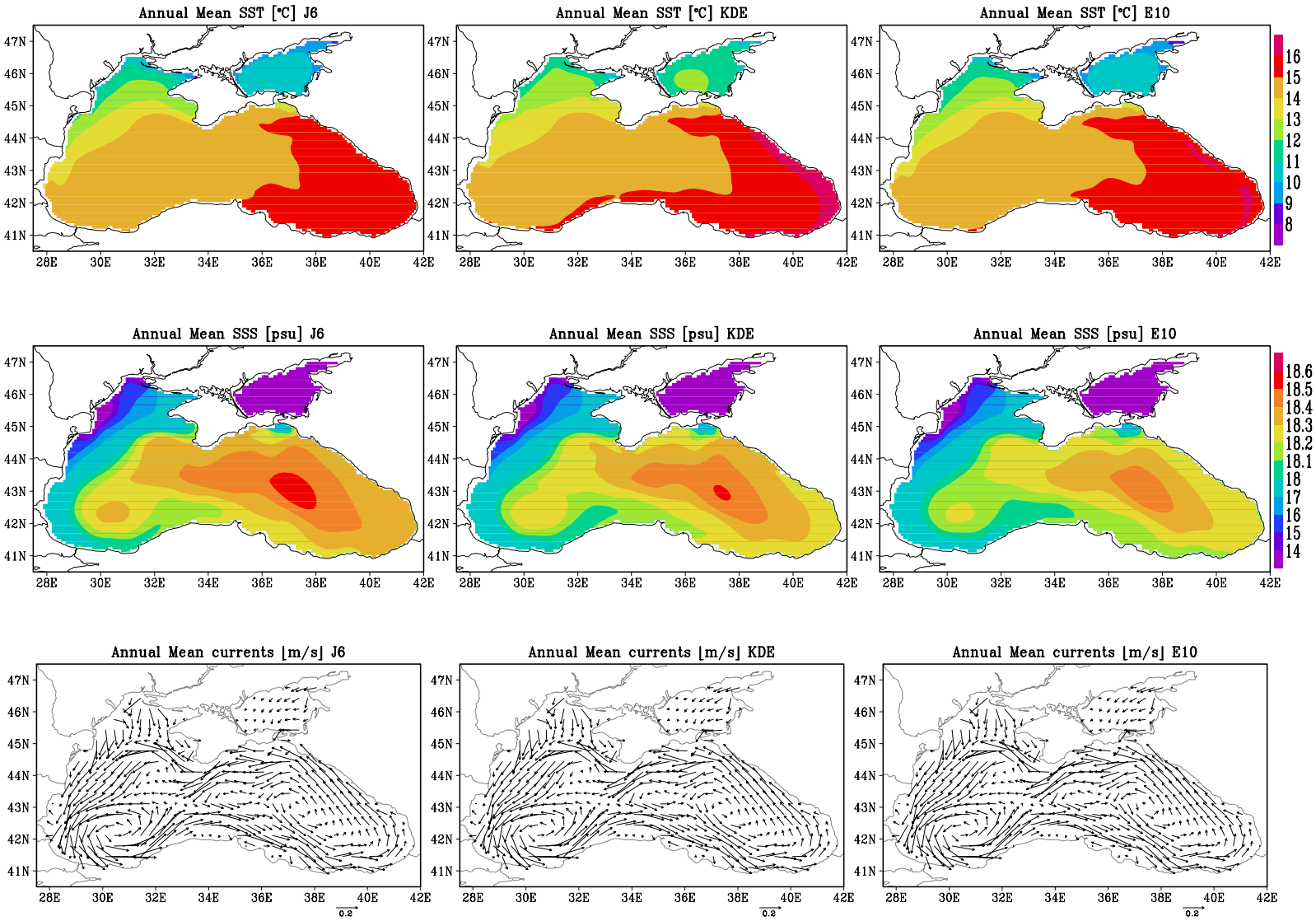

Fig. 6.7. Annual maps of surface temperature, salinity and currents for 1990-2000.

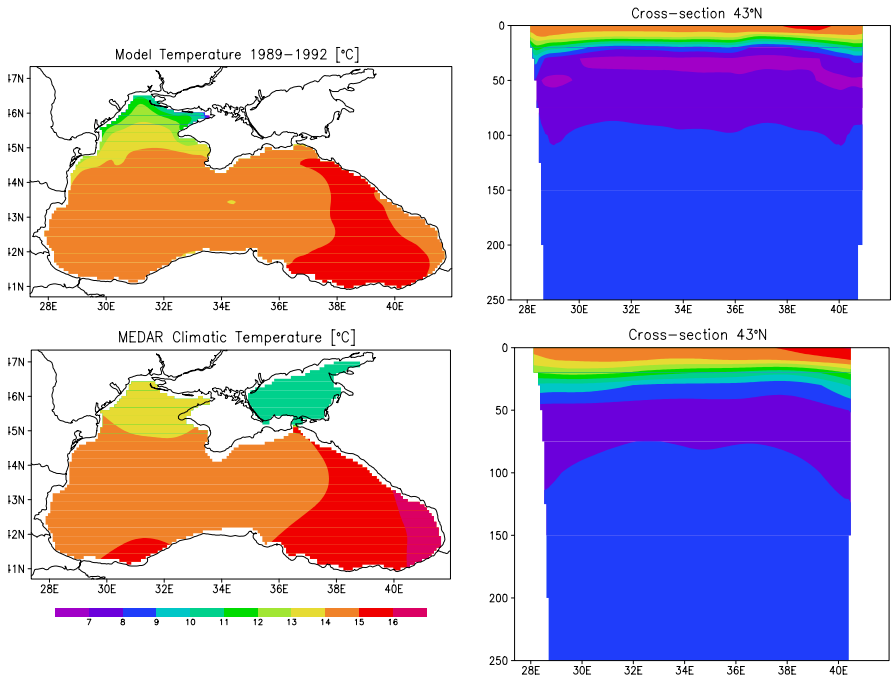

Fig.6.8. Model validation: Temperature [°C] simulated by the model and from the climatological MEDAR dataset.

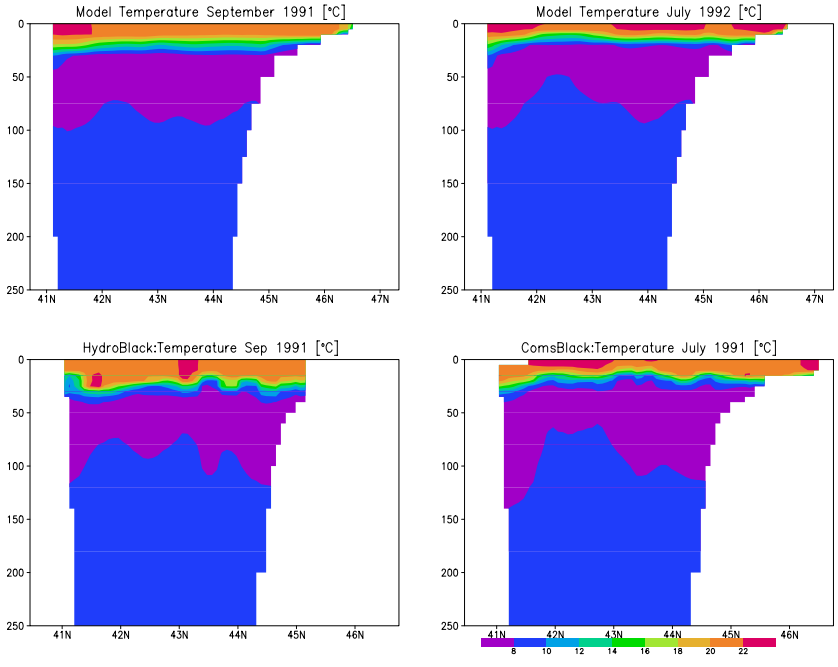

Fig. 6.9. Meridional cross-section of the temperature [°C] for September 1991 and July 1992 simulated by the model and from the HydroLACK and COMSBlack expeditions observations.

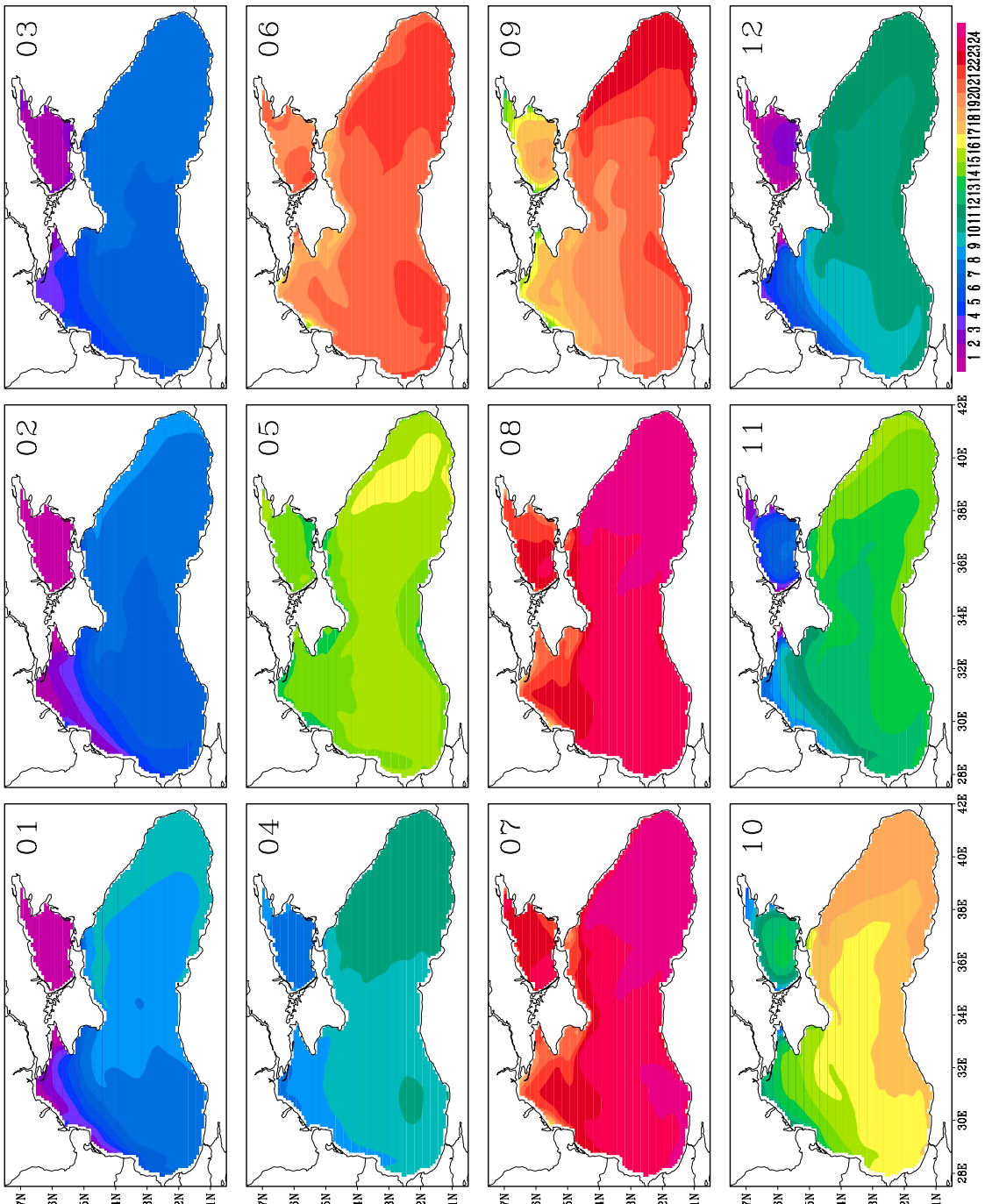

Fig. 6.10. Monthly sea surface temperature [°C] for 1990-2000.

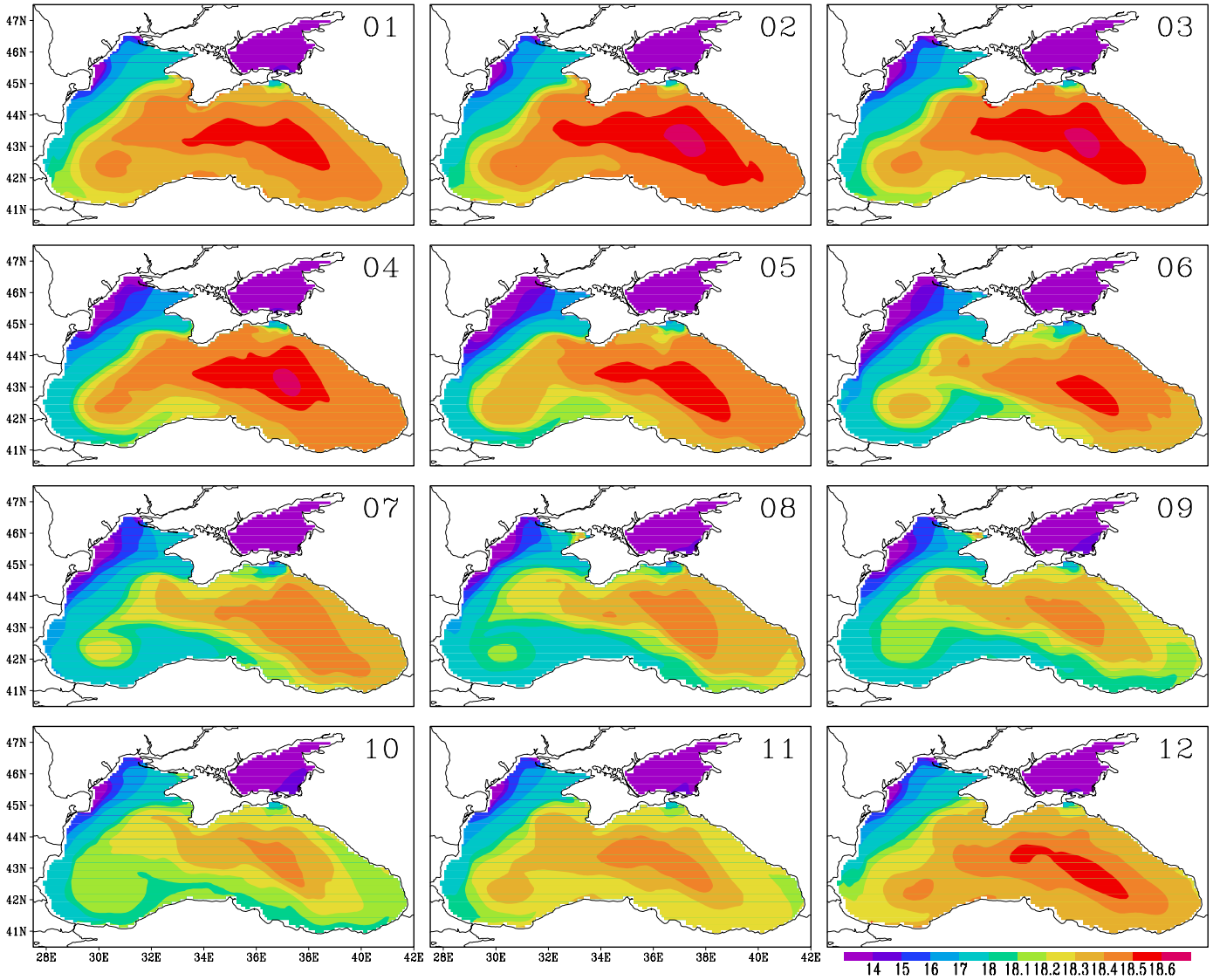

Fig. 6.11. Monthly sea surface salinity [PSU] for 1990-2000.

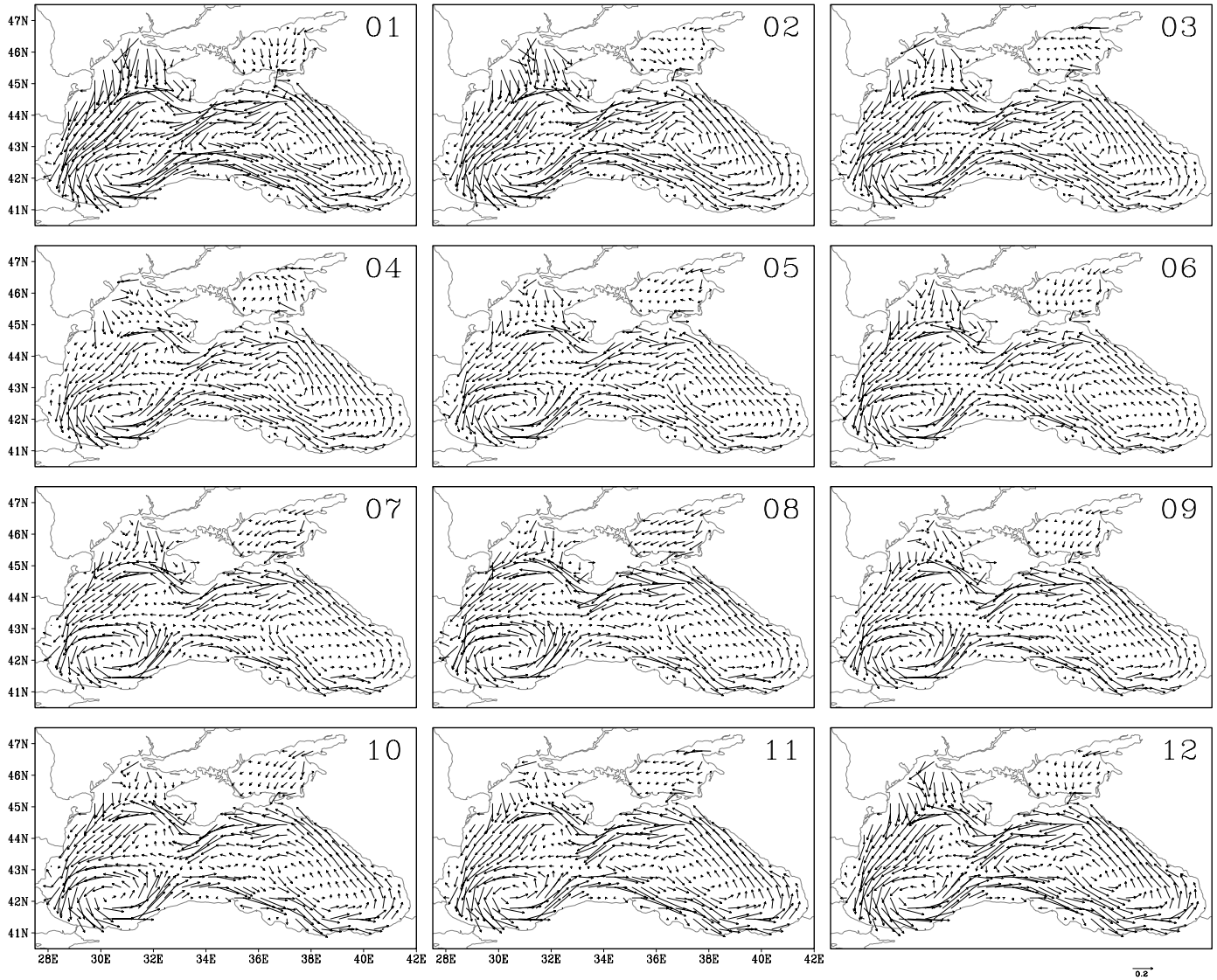

Fig. 6.12. Monthly sea surface currents [m/s] for 1990-2000.

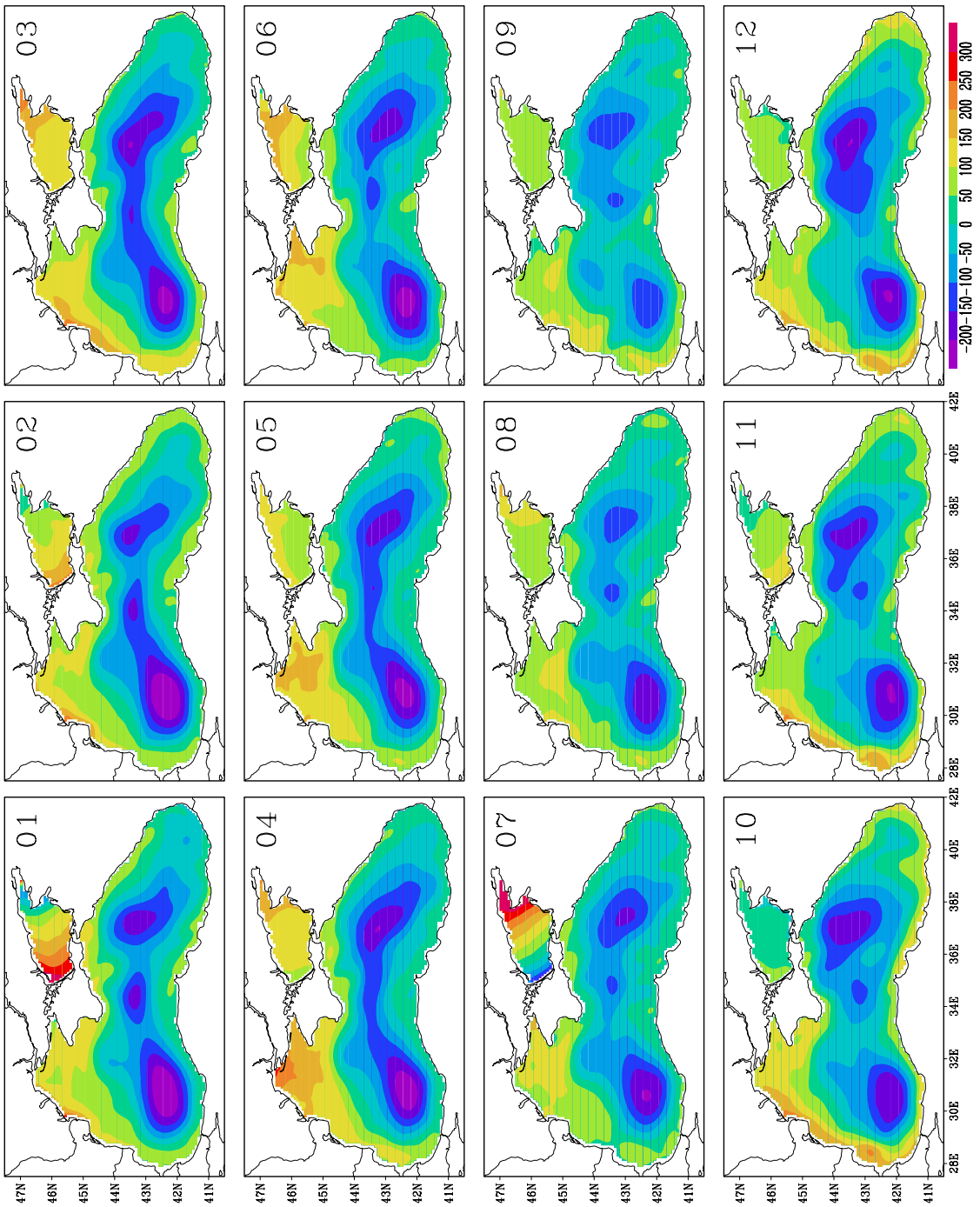

Fig. 6.13. Maps of the sea elevation [mm] for 12 subsequent weeks in April and May 1994.

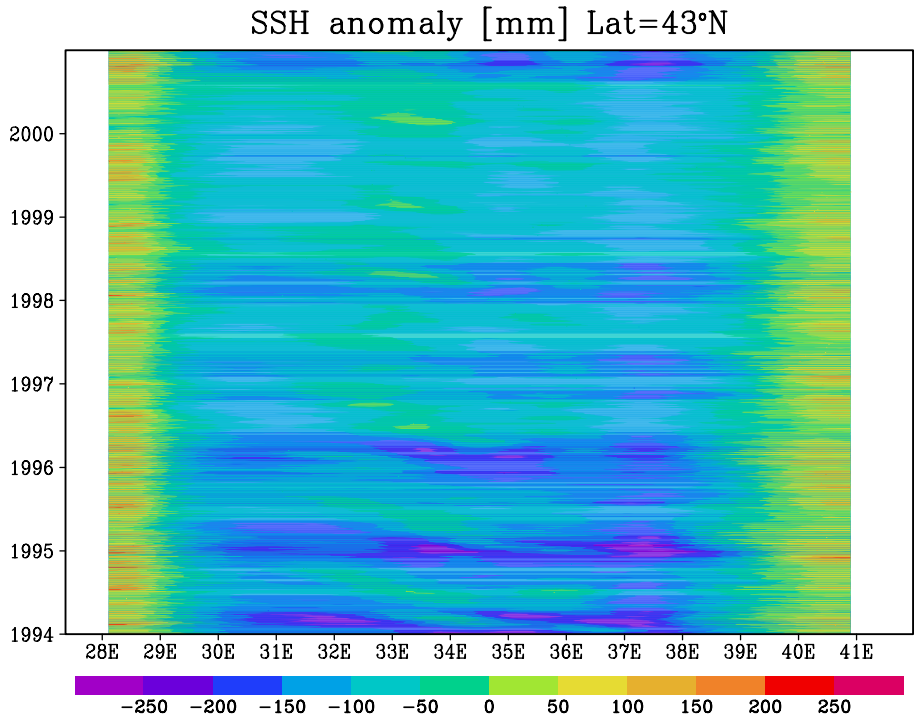

Fig.6.14. Zonal Hoevmuller diagram of the sea surface elevation [mm] for 1994-2000 simulated by the model.

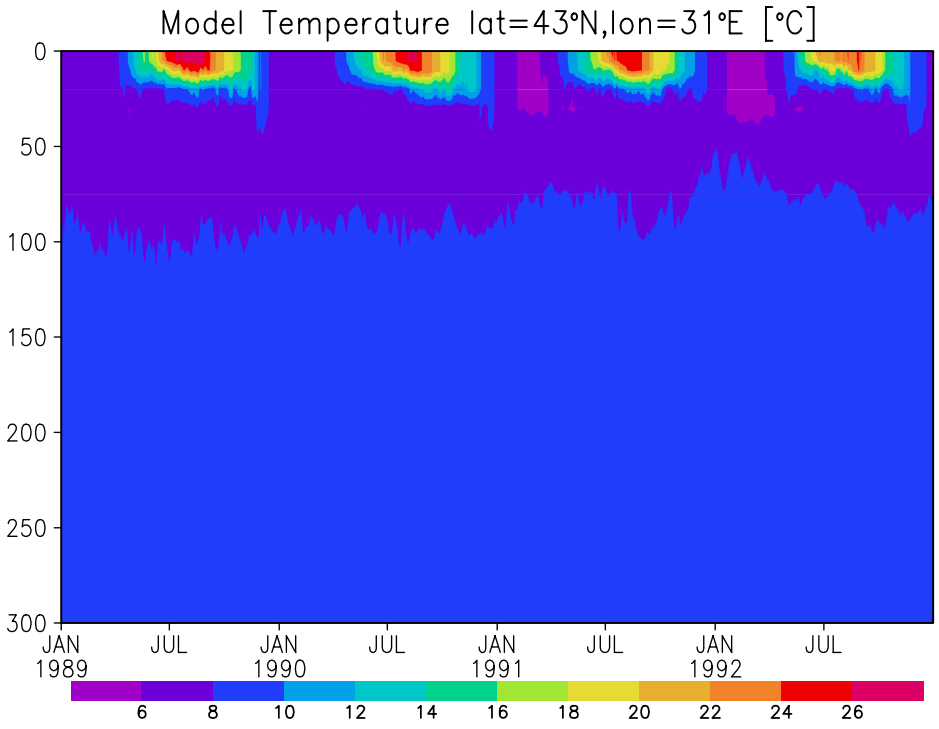

Fig.6.15. Vertical Hoevmuller diagram of simulated temperature [°C] in the beginning of the integration 1989-1993.

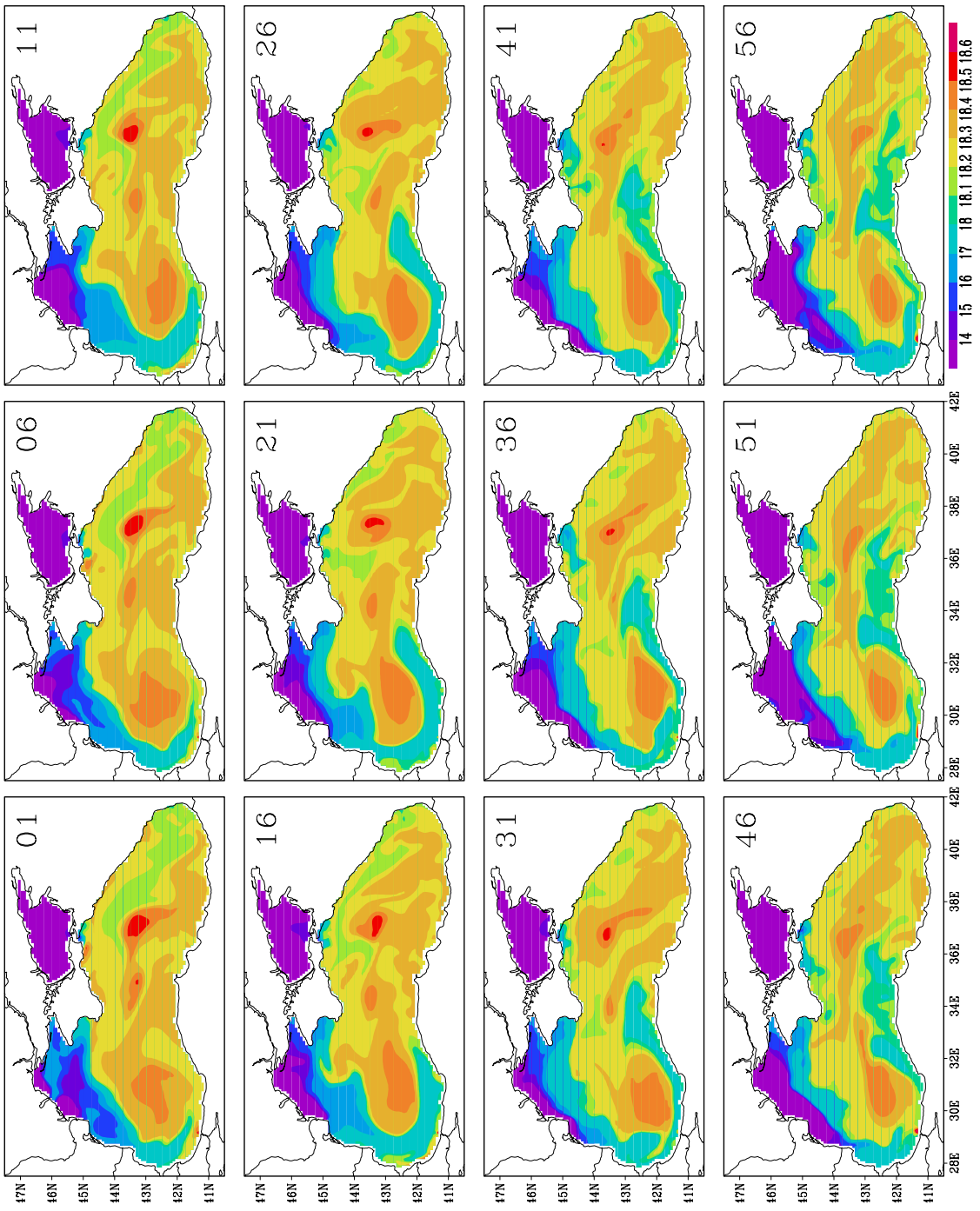

Fig. 6.16. Maps of the sea surface salinity [PSU] for several days (April and May 1994).

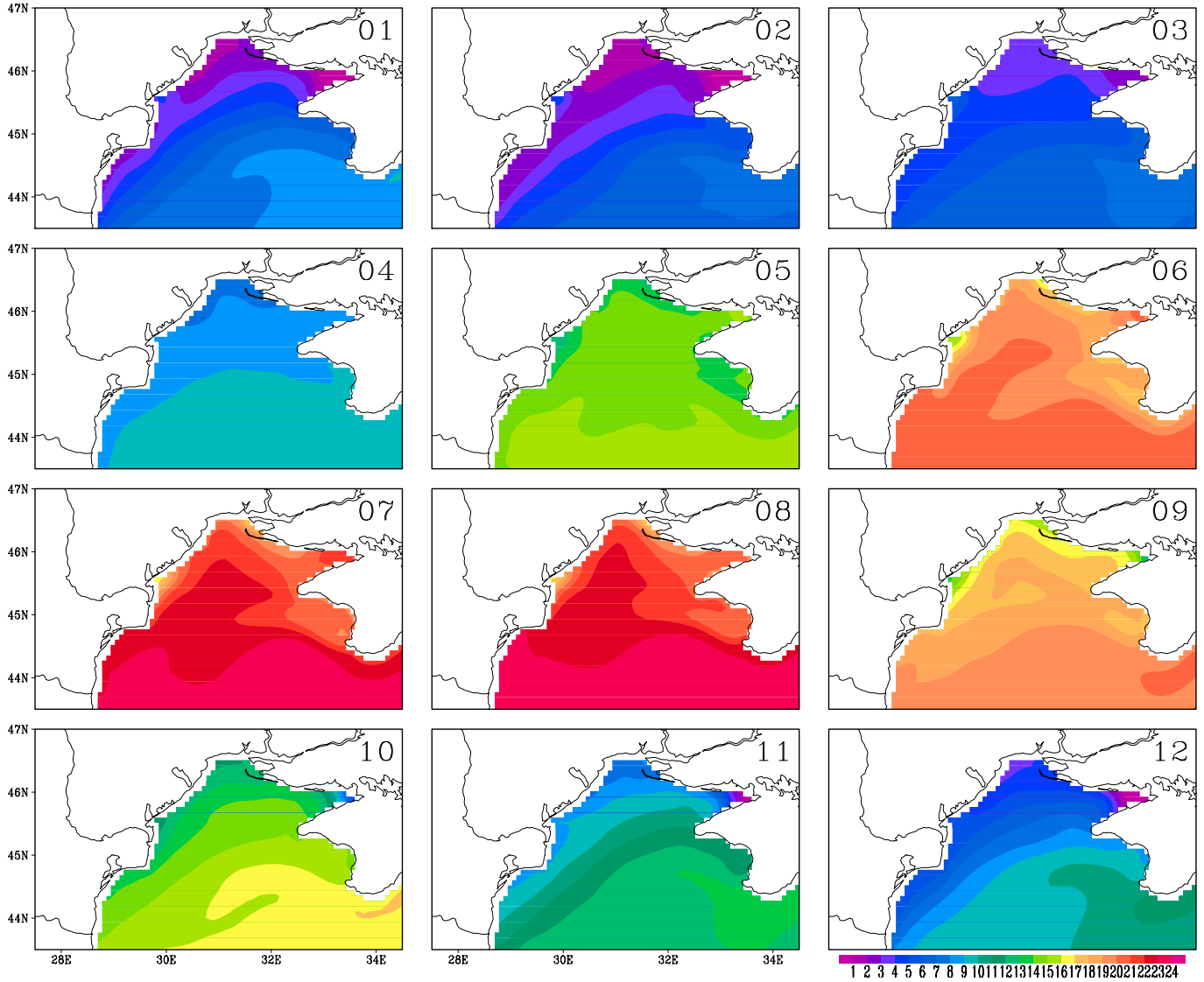

Fig. 6.17. Shelf zone: monthly sea surface temperature [°C] for 1990-2000.

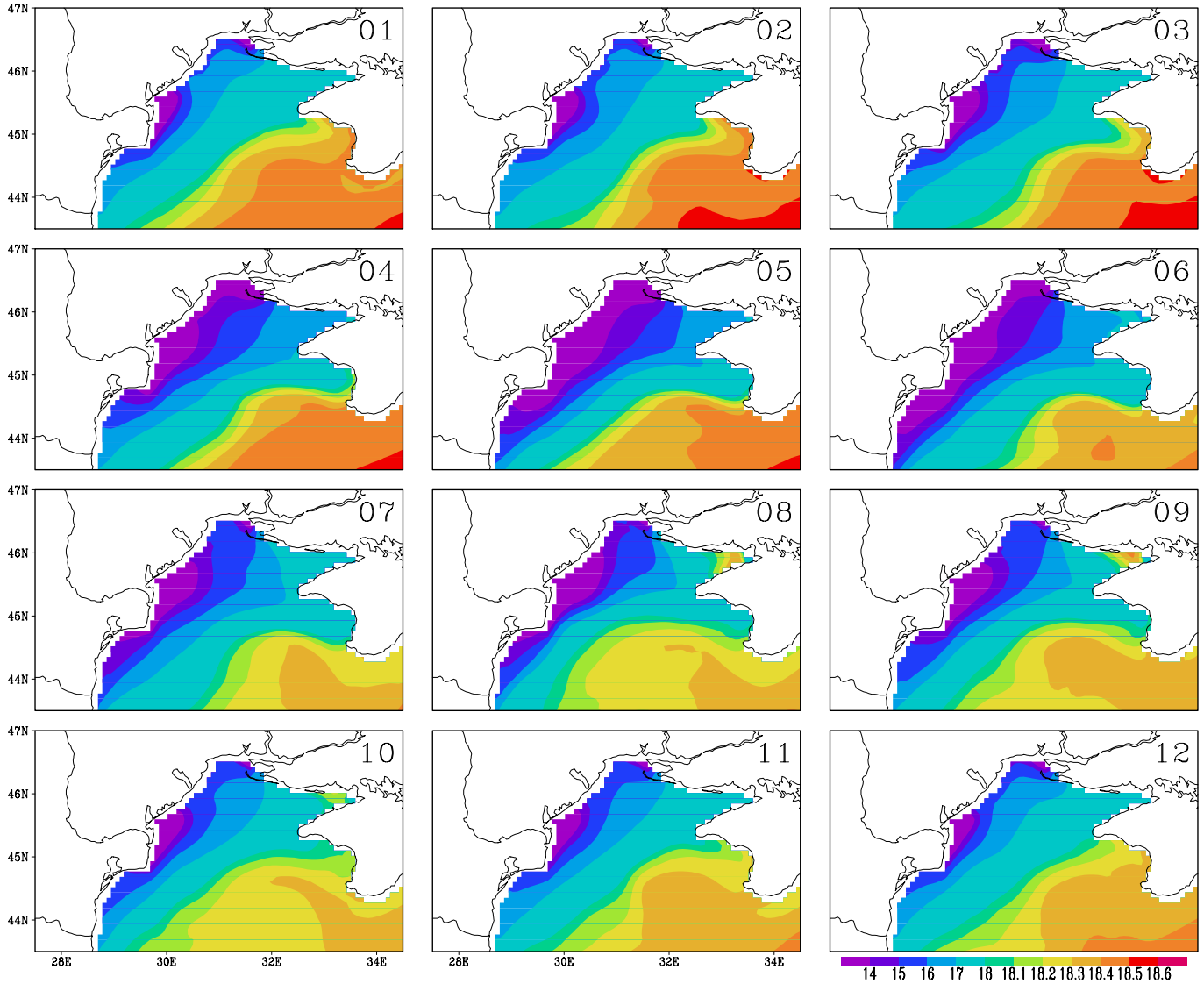

Fig. 6.18. Shelf zone: monthly sea surface salinity [PSU] for 1990-2000.

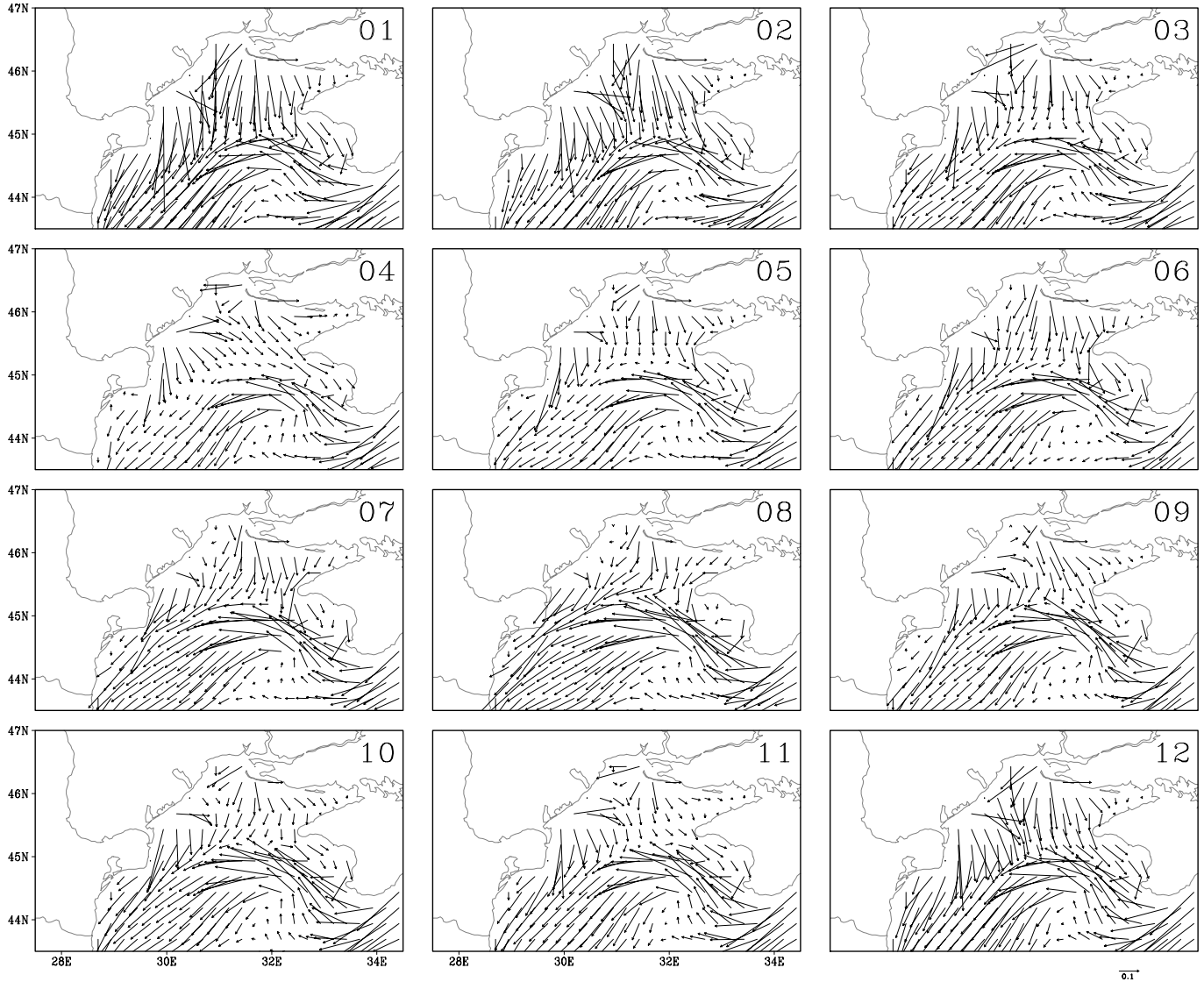

Fig. 6.19. Shelf zone: monthly sea surface currents [m/s] for 1990-2000.

7. Sensitivity to water optical properties.

It was mentioned already in Paragraph 4.6 that one of the simplifications in the model is to consider the same optical properties in each grid point. In reality this is not the case as the ships and satellite measurements prove. The problem is how to implement the measured values of the optical depth in the model. The formulation of Jerlov types (used in the model) distinguishes between the short and long wave radiation and the measurements usually give one common extinction coefficient for the light in general. Thus the equation of light propagation in the water has a simpler form with a single exponent

$I(z)=I_0\, a \exp(-z/\eta)$,

where I is the light intensity (I_0 is the surface value), z is the depth, η is the optical depth and a is coefficient dependent on the geographical latitude (Paulson and Simpson, 1977). For the Black Sea this coefficient is taken as a=0.45.

The changing of the light propagation equation in the model is expected to affect the temperature 3D field and as a consequence the baroclinic gradients and velocities. Two numerical experiments differing from J6 only by light propagation properties are designed in order to account for horizontal inhomogeneity of the water transparency.

The first experiment is denoted “KDE” and $\eta(x,y)$ is set to be dependent on the grid point location and data are taken from satellite measurements (Fig. 4.16). In the second experiment, referred here “E10”, η is constant set to the area mean value of Fig. 4.16 η=10 m.

The same 10-year integrations with the model as for the experiment J6 are completed and the same variables are calculated with the same spatial and temporal resolution as explained in Paragraph 7. Here several figures aim to help the intercomparison of model results for J6, KDE and E10 experiments. Two figures have been already shown in the previous paragraph 6 (Fig. 6.5 and Fig. 6.7). One interesting result is that there is no significant difference between the monthly area mean SST’s (Fig. 6.6). However the SSS in the three experiments differ, the largest trend show the J6 results. From Fig. 6.7 the horizontal maps are rather similar and differences are in the eastern basin.

Fig. 7.1 shows in more detail the evolution of the temperature and salinity profiles in a single location in the center of the western basin (31ºE, 43ºN). The seasonal temperature signal propagates down only in the surface, but some warming of the deeper parts is also observed in J6 and KDE experiments after 1994, to a lesser degree in E10. The tendency of mixing the surface layers and increasing their salinity is seen in all three experiments. This is an indication that it might be important to include not only the rivers but also the fresh water flux at the sea surface (e.g. precipitation and evaporation).

The next figures show the seasonal maps of sea surface temperature, salinity and currents for the KDE and E10 experiments in the same way as it was done for the J6 on Fig. 10-12. The KDE results are shown on Fig. 7.2-4 and E10 – on Fig. 7.5-7. The SST again does not differ much between the three experiments, greater differences are in the salinity field.

Larger differences are found below the surface and in the deeper basin. To demonstrate this, 6 pictures for the all three experiments J6, KDE and E10 are prepared. They show seasonal maps of the vertical meridional cross-section of T and S (Fig.7.8-13, see the caption under the figures). The subsurface layers are warmer in J6 and KDE compared to E10, which mean that the warming propagates to greater depth (compare Fig. 7.8 7.9 and 7.10). There are indications for larger mixing in the J6 run, as the salinity of the near surface layers is larger than in the maps for KDE and E10 results. For maintaining the stagnant stratification (CIL) of the Black Sea without using relaxation, there is still much to be done, the results in this respect are not satisfactory in none of the three experiments.

The reason for this inconsistency is most probably that the coefficients in the equation of light propagation for the Black Sea (both, in the Jerlov type form and in that with a single exponent) have to be carefully checked and tuned using real expeditions measurements. Thus a space for improvement is still left.

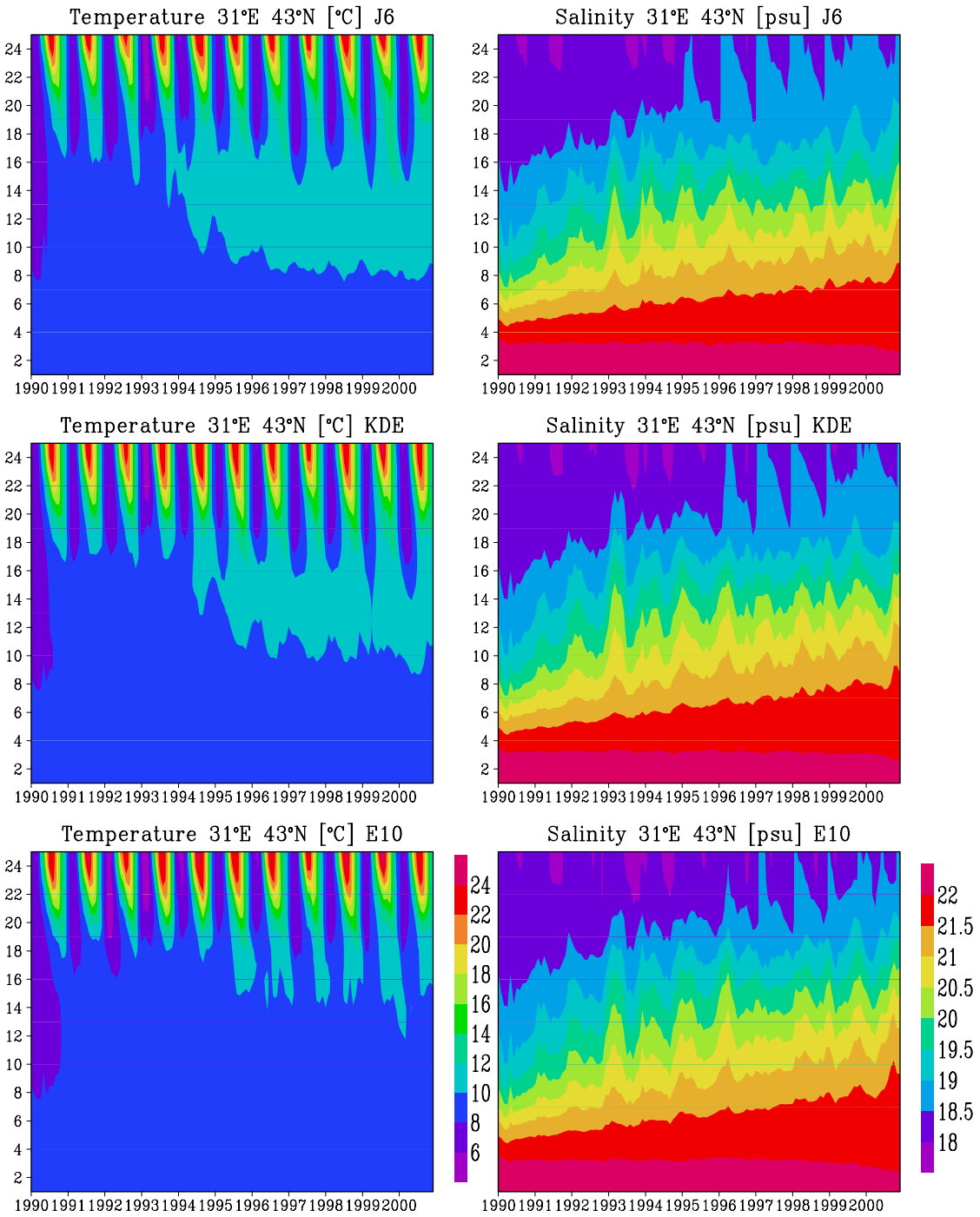

Fig. 7.1. Vertical Hoevmuller diagrams for the monthly mean temperature [°C] and salinity [PSU] simulated by the three experiments J6, KDE and E10.

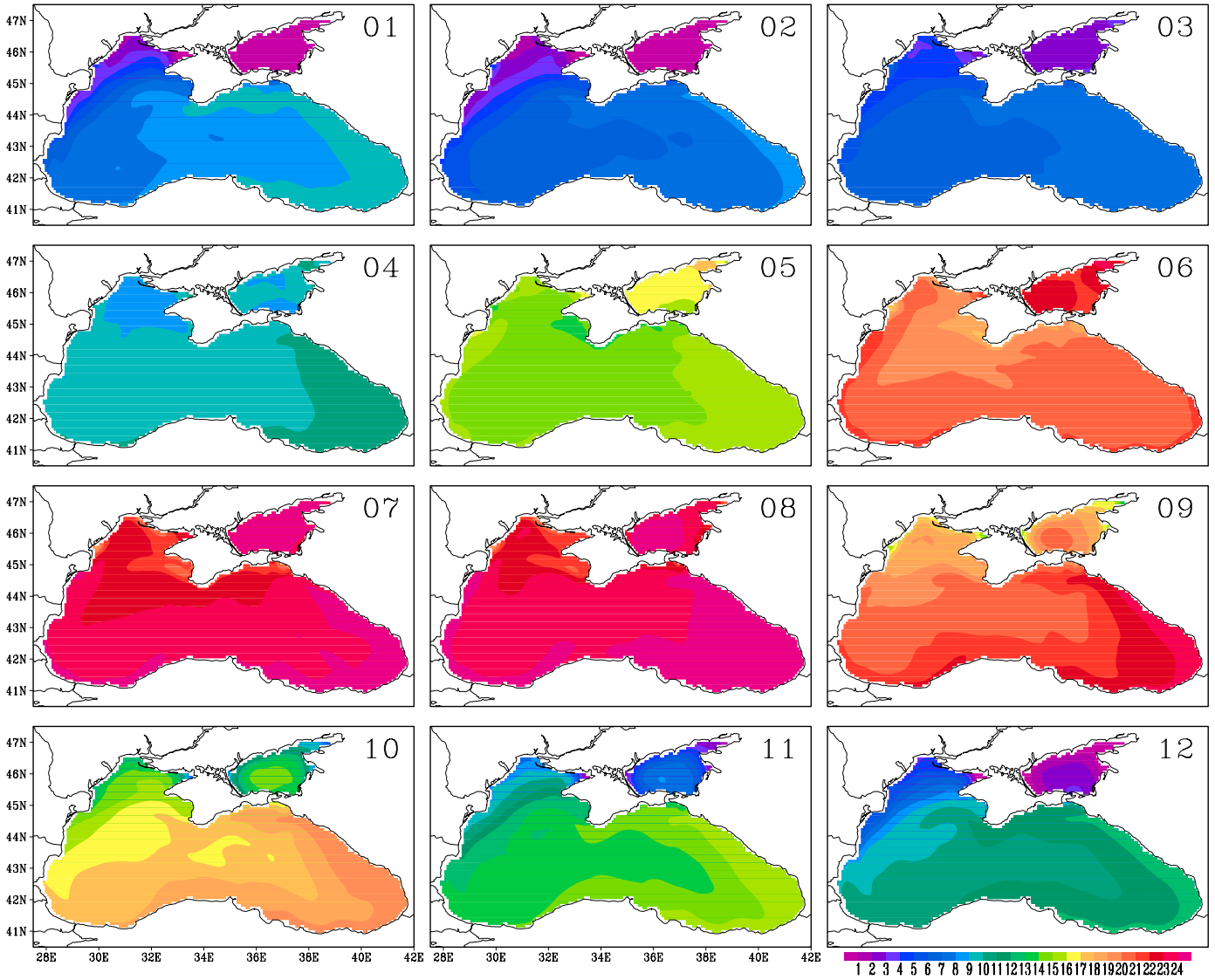

Fig. 7.2. Monthly sea surface temperature [°C] for 1990-2000 for the experiment KDE.

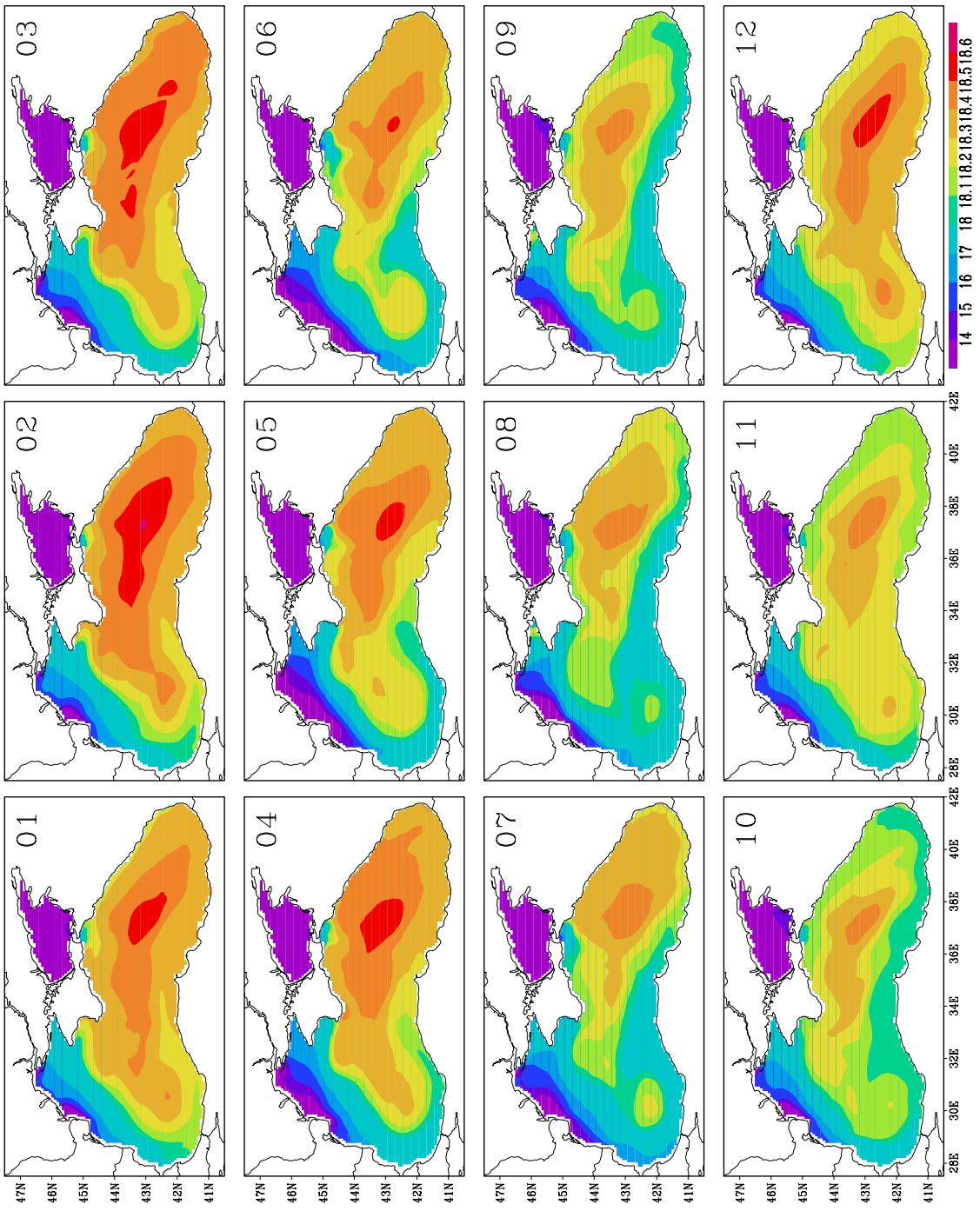

Fig. 7.3. Monthly sea surface salinity [PSU] for 1990-2000 for the experiment KDE.

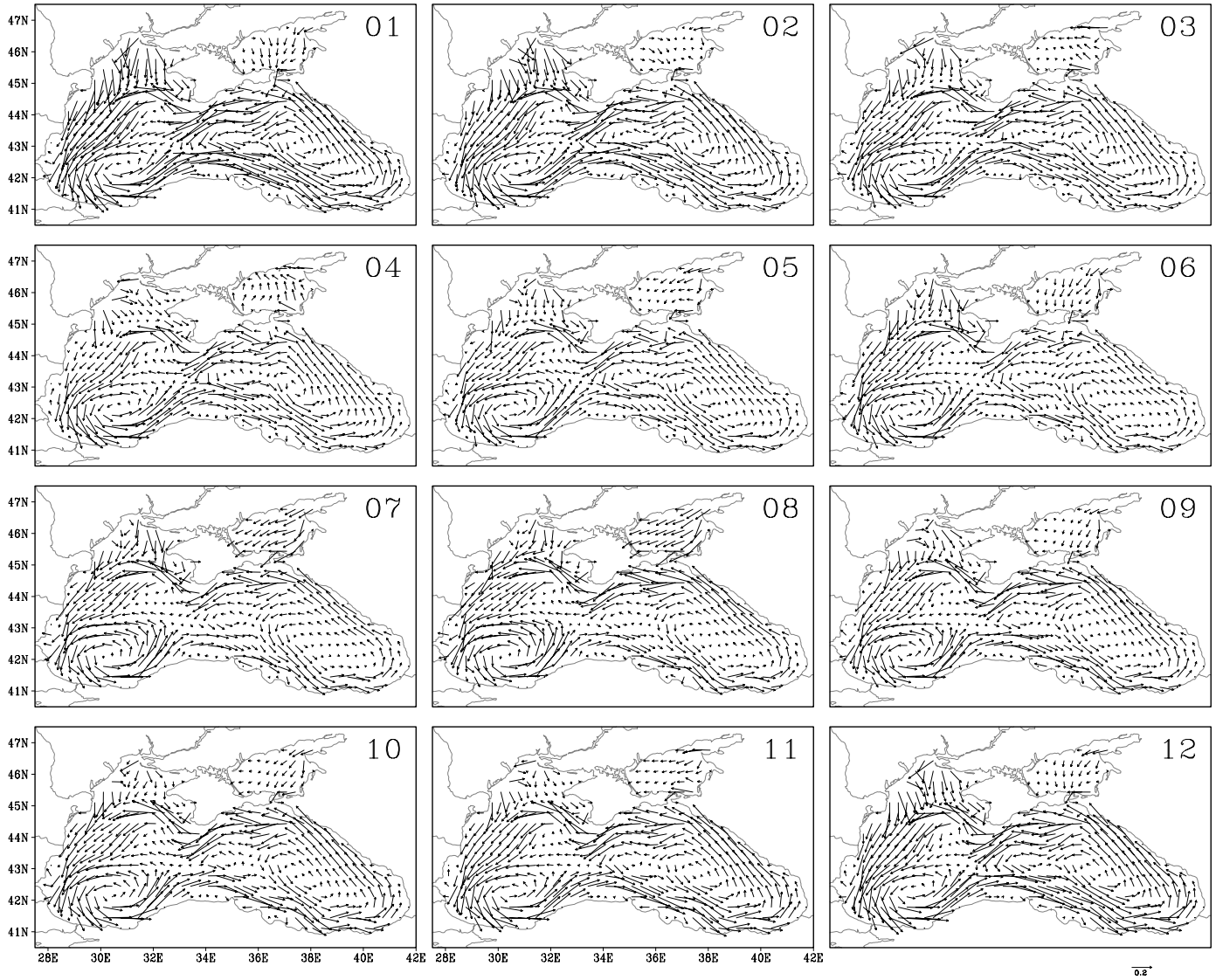

Fig. 7.4. Monthly sea surface currents [m/s] for 1990-2000 for the experiment KDE.

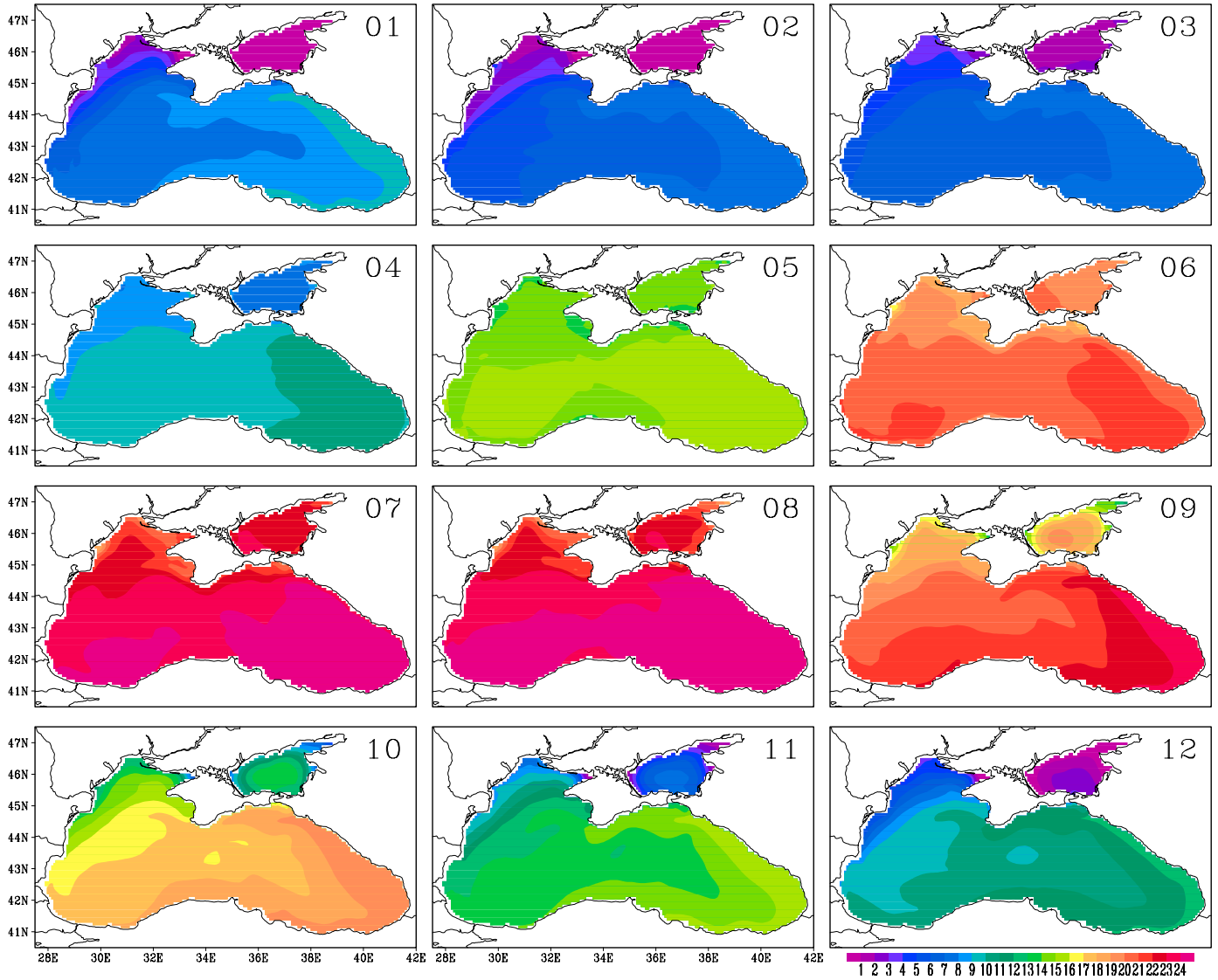

Fig. 7.5 .Monthly sea surface temperature [°C] for 1990-2000 for the experiment E10.

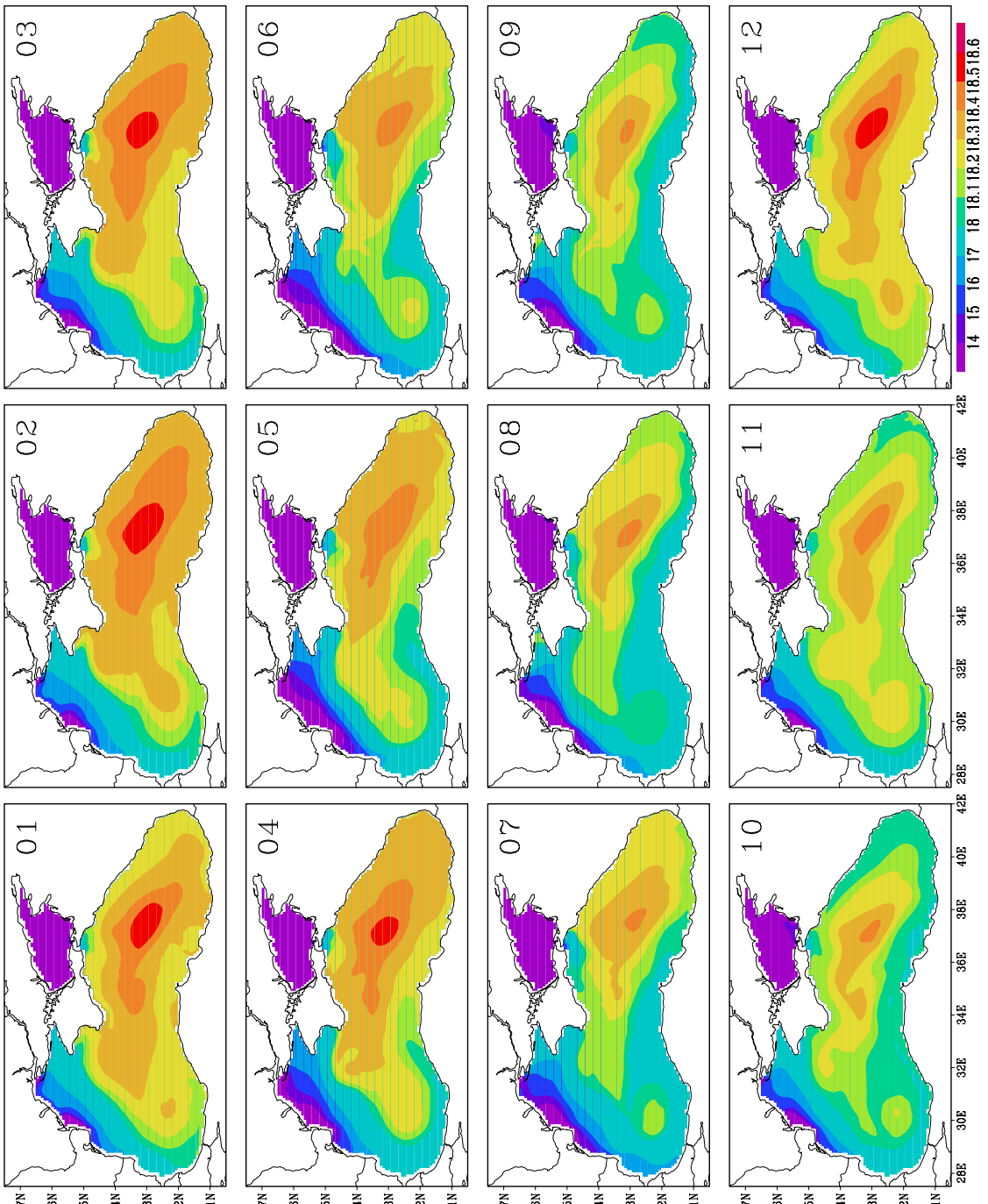

Fig. 7.6. Monthly sea surface salinity [PSU] for 1990-2000 for the experiment E10.

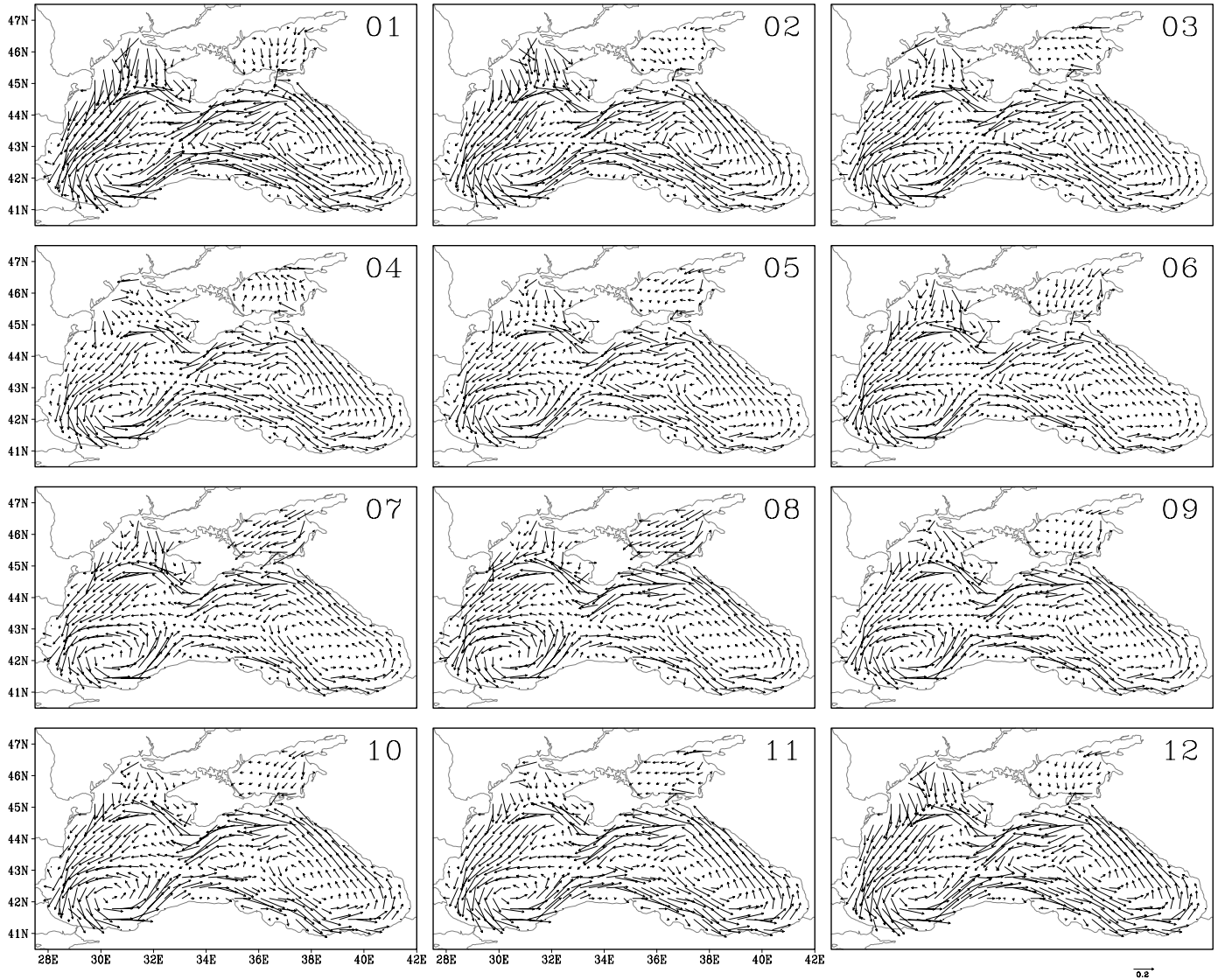

Fig. 7.7. Monthly sea surface currents [m/s] for 1990-2000 for the experiment E10.

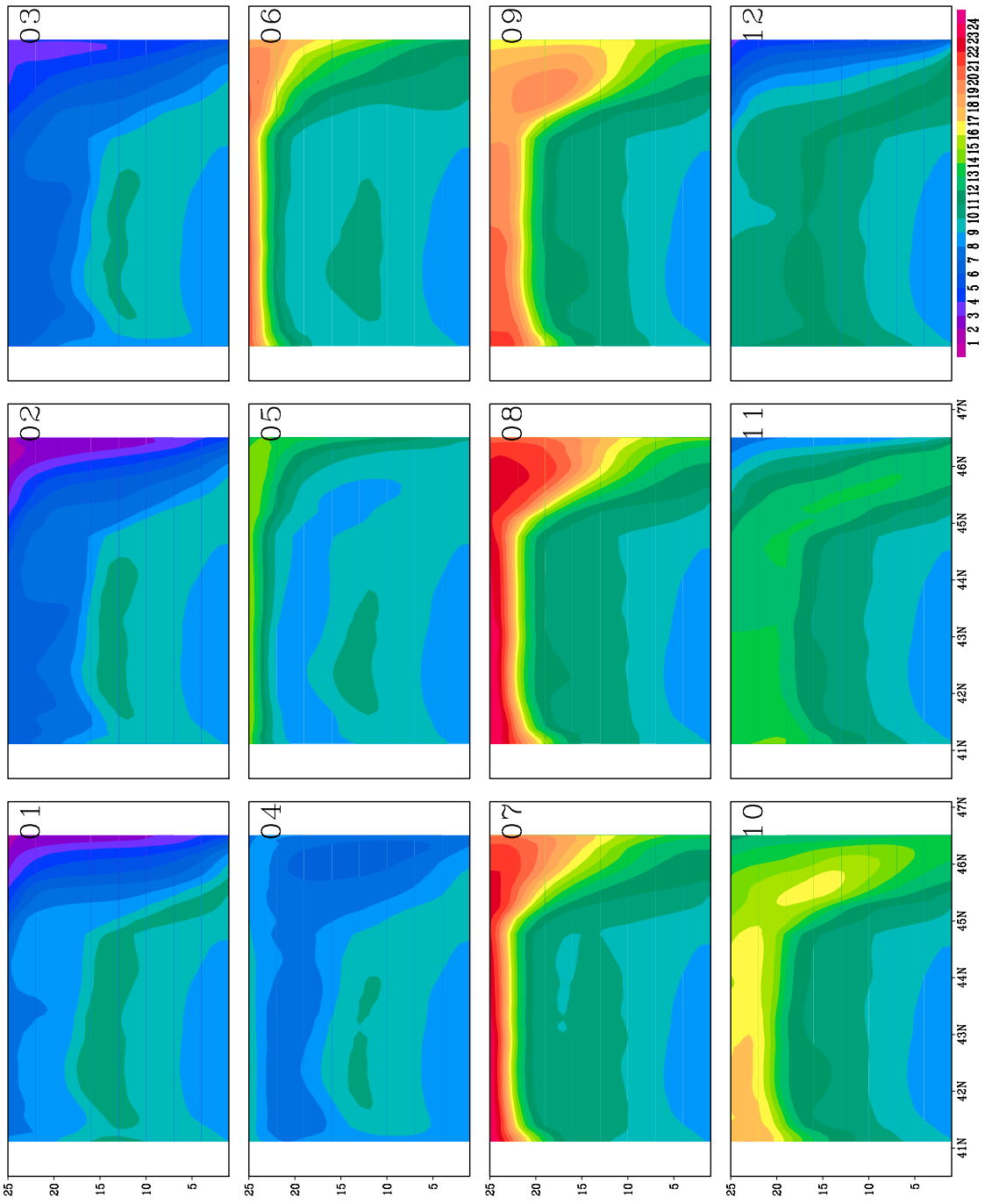

Fig. 7.8. Meridional cross-section of the temperature [°C] for 1990-2000 J6 experiment.

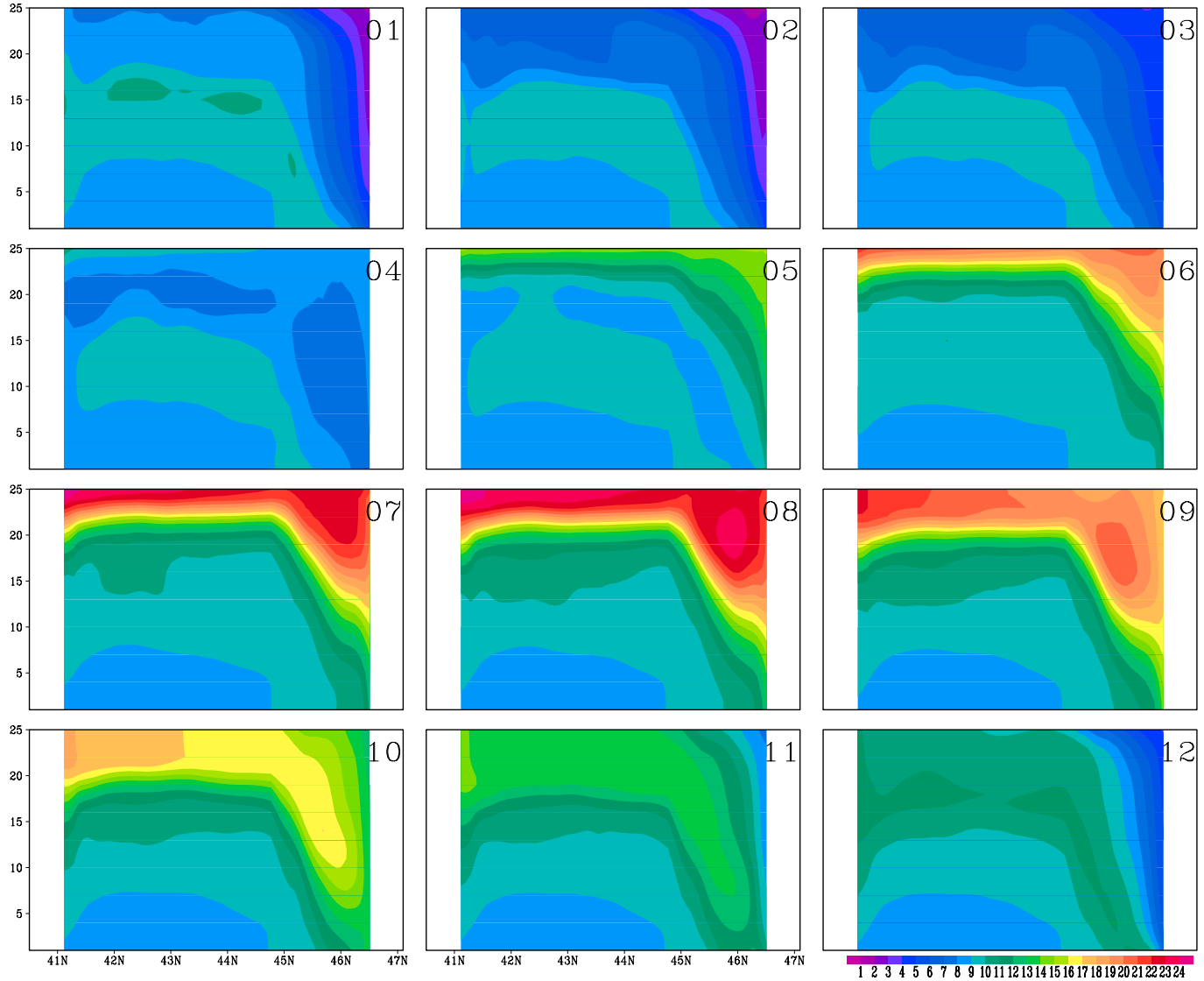

Fig. 7.9. Meridional cross-section of the temperature [°C] for 1990-2000 KDE experiment.

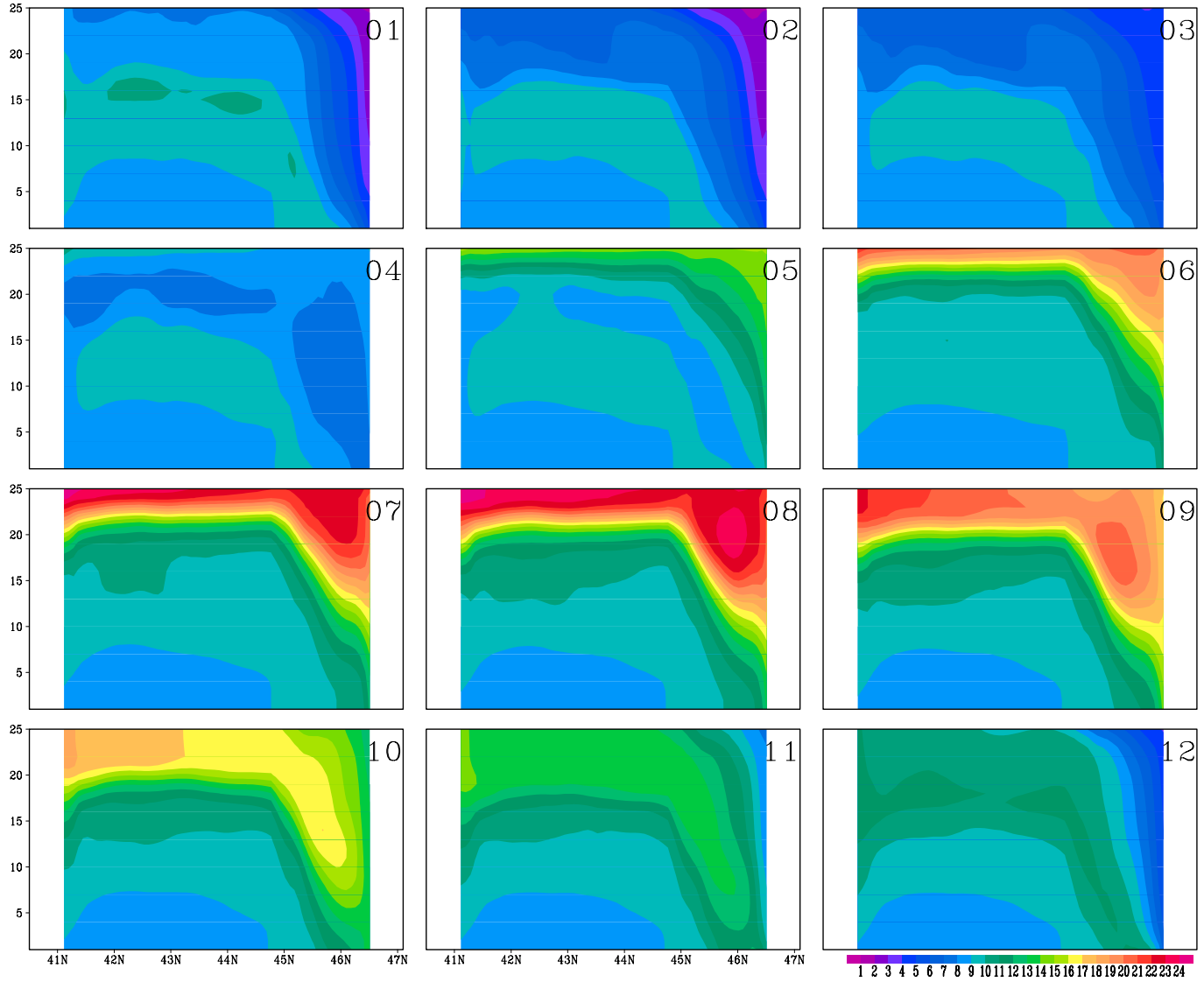

Fig. 7.10. Meridional cross-section of the temperature [°C] for 1990-2000 E10 experiment.

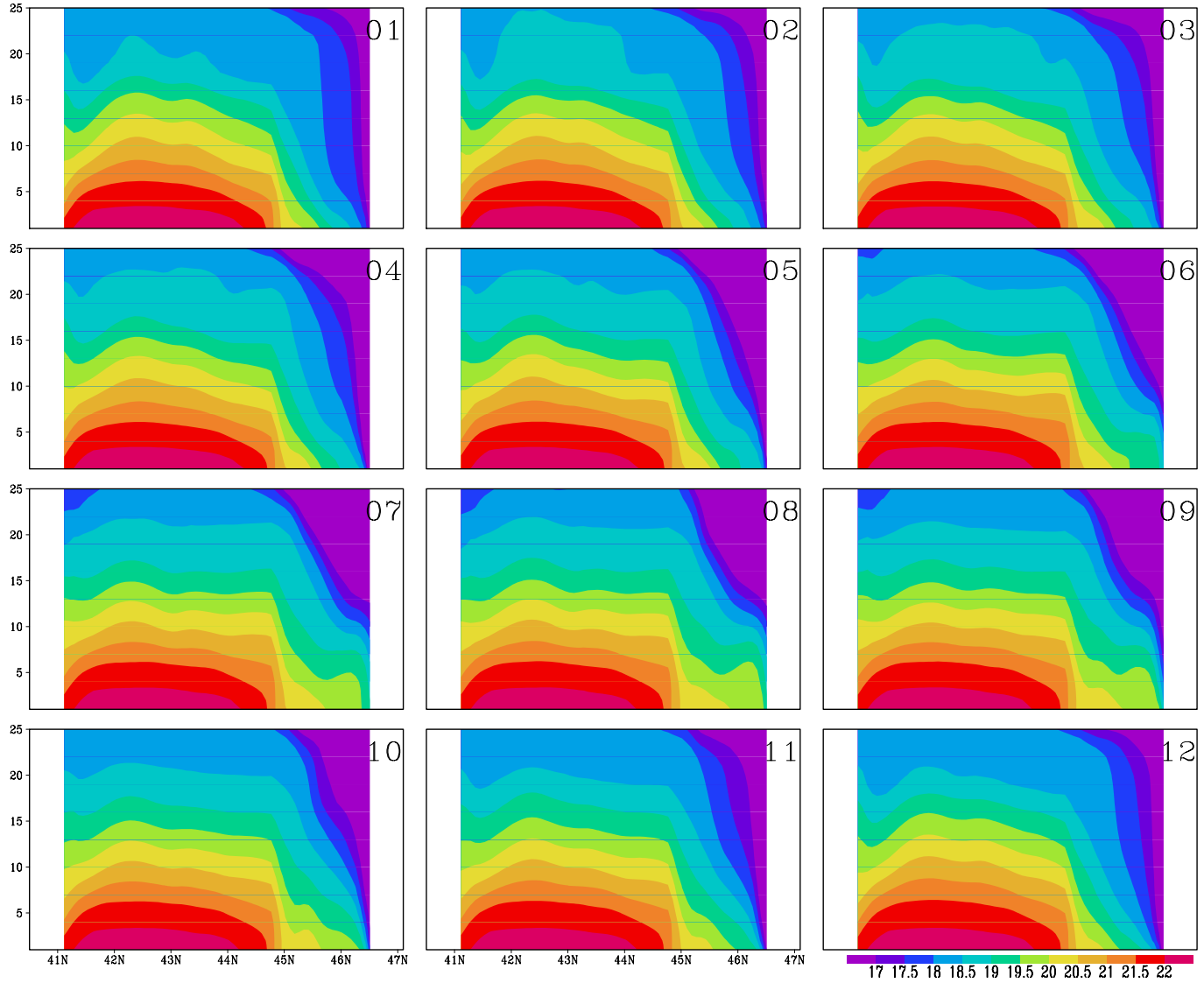

Fig. 7.11.Meridional cross-section of the salinity [PSU] for 1990-2000 J6 experiment.

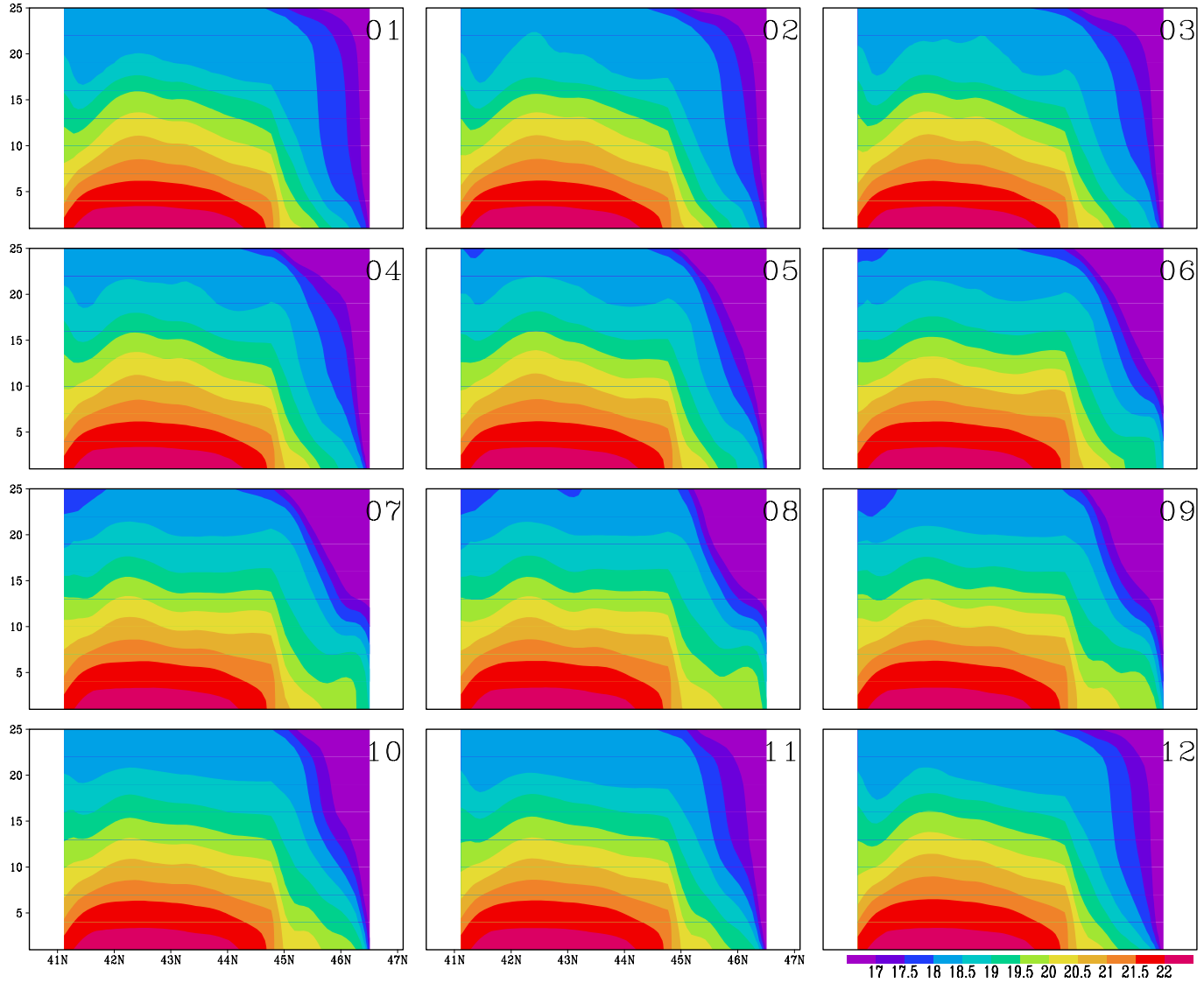

Fig. 7.12. Meridional cross-section of the salinity [PSU] for 1990-2000 KDE experiment.

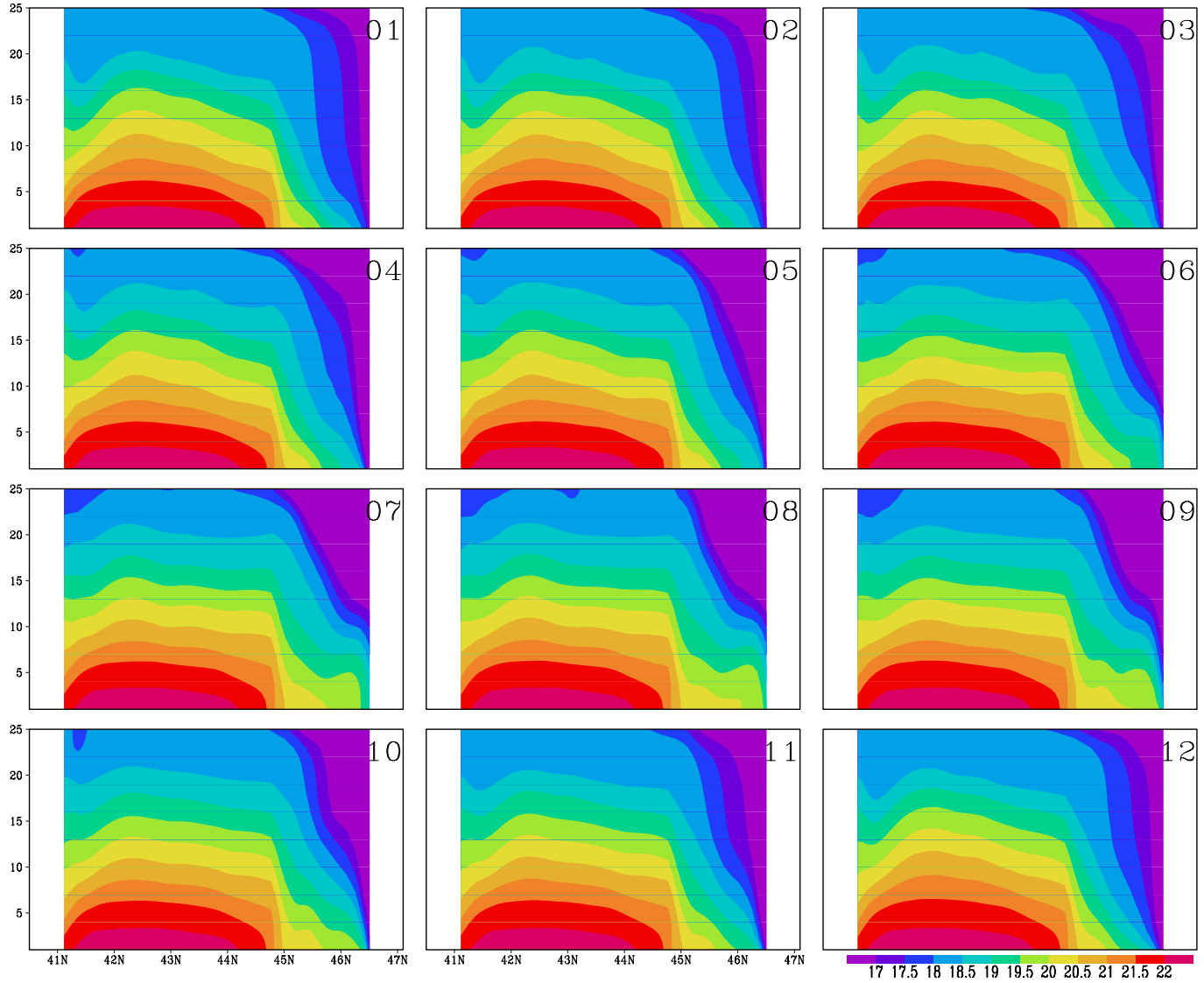

Fig. 7.13. Meridional cross-section of the salinity [PSU] for 1990-2000 E10 experiment.

8. Model set-up for the high resolution simulations.

The resolution of numerical simulations is usually limited by the available computer resources. The additional problem is that decreasing the horizontal resolution one is obliged to decrease also the time step (the criterion of Courrant-Fridrich-Levi) and therefore integrating a fine resolution model for the same period as a coarse resolution model will require much more time. The entire Black Sea in the numerical studies reported in the literature until now is resolved usually with 5' (or ~9km).

The GETM parallel setup version which was recently made available by the developers gave the possibility to separate the model basin into different parts (domains), thus to considerably speed up the integration process. The integration of each model "cell" is done by a different processor.

A test run of GETM configured for the Black Sea with 2' horizontal resolution in zonal and meridional direction was performed. The grid dimensions are 428x107 grid points; the starting point coordinates are at 21.33ºE and 40.74ºN. The number of vertical layers is still kept to be 25. The model topography was already presented in paragraph 4.1. The micro time step was decreased to 4s (instead of 18s for the 5' configuration). The meteorological forcing is derived again from the ECMWF re-analysis data.

The efficiency of the parallel integration is very much dependent on the way the model area is separated. The run was tested on 4, 6, 8 and 12 processors and finally it was decided to use the setup with 8 processors. This was a compromise between number of available free processors and the time needed to complete the integration.

The experiment with 2' resolved Black Sea in parallel mode is denoted as "2min". The integration of 1 year (1990) was fulfilled and the results are written in the same format as the other described experiments – as monthly mean fields and daily snapshots. The interesting question is, whether the finer resolution will represent the different mesoscale circulation features better. Several snapshots of Sea Surface Elevation and Salinity from December 1990 are presented on Fig. 8.1 and 8.2 respectively. Much more details in the fronts, Rim current filaments and eddies compared to the results from J6, KDE and E10 experiments are easily seen.

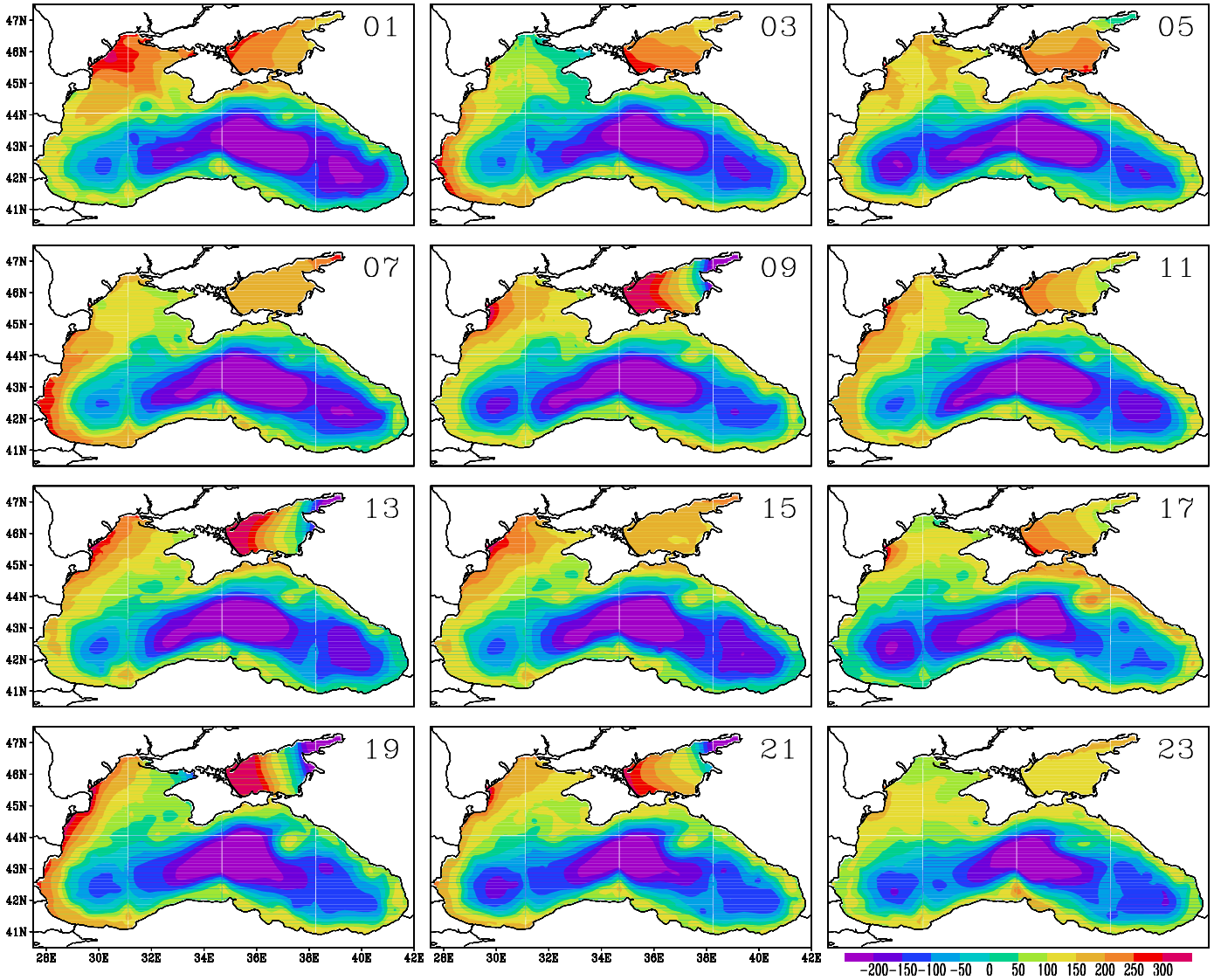

Fig. 8.1. Sea surface elevation maps [mm] for Decembver 1990

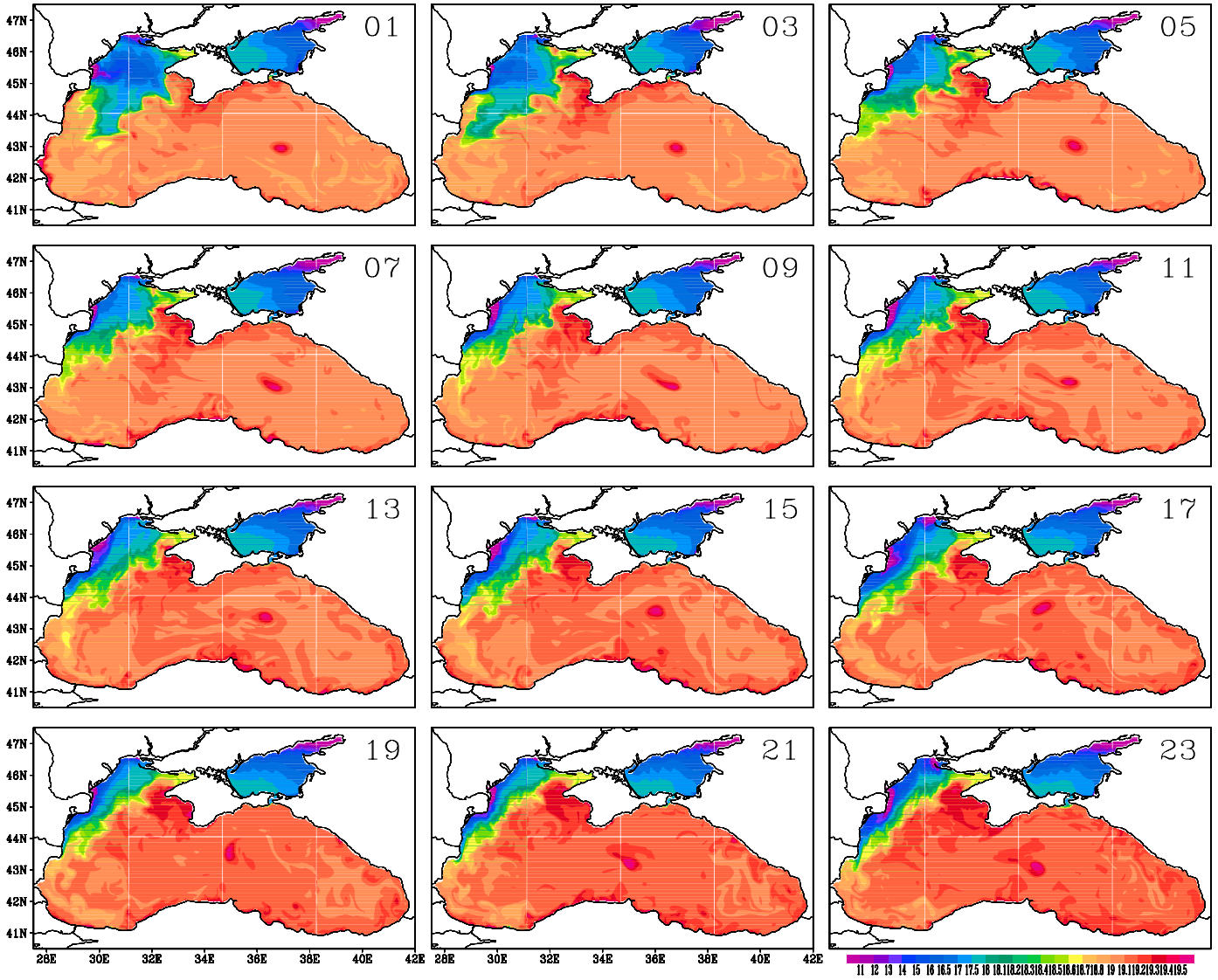

Fig. 8.2. Sea surface salinity maps [PSU] for Decembver 1990

9. Conclusions and “else to be done”.

Climatological and real forcing numerical simulations for the Black Sea are performed and 10 year model integration is completed. The data sets for sea level, temperature, salinity and velocity are available with a resolution of 1 day in time and 5’ in space. During the integration monthly mean fields were calculated and saved. Using these variables the characteristics of the surface and bottom mixed layers (depth, temperature, salinity and velocity) are calculated. One of the advantages of the model results is the inclusion of Azov Sea in the model area. This are the first reported coupled Azov Sea – Black Sea numerical simulations.

Despite that some problems exist in the deeper parts of the open sea, the model data are of overall good quality. Specifically they are suitable to investigate the time and space variability of physical variables in the shelf and coastal areas.

A new, more accurate method to include the water optical characteristics by means of an optical depth estimated from the satellite data is presented. Identical experiments differing only in the light propagation equation are performed and compared to each other. It is concluded that including of a proper optical depth is important for maintaining the sea stratification. However the great amount of model data is still to be investigated in detail before reaching firm statements. Several experiments are still to be done, like the integration with much smaller averaged value for the optical depth (for example 5 m instead of 10 m as it is in the E10 experiment). Very important next step will be the implementation of seasonal varying optical depth as it is in reality.

In this light also including the fresh water flux at the surface will be helpful to maintain the adequate density stratification.

The high space resolution (2’) model set-up is prepared and integrated for 1 year period. A 1’ setup is also ready to be integrated. These are the numerical experiments with the finest resolution for the whole Black Sea reported so far. However, running these models requires substantial computer resources in terms of both processor time and hard disc space. More effort should be invested in order to complete this integration in the near future.

Acknowledgement

Many scientists and institutions contributed to this study by either providing data, discussing problems and results or giving important advice, we would like to thank all of them. Specifically we would like to mention the continuous efforts and support from Karsten Bolding and Hans Burchard in developing and maintaining the GETM code and answering our stupid questions. Mark Dowell calculated the optical attenuation length for the Black Sea and provided us with the data, we are optimistic that his efforts will lead soon to a joint paper. Without the extreme helpful support from the European Centre for Medium Term Weather Forecasting (ECMWF), which provided access to all their meteorological analysis and reanalysis (ERA40) data the good and realistic level of the performed multiannual simulations would have never been reached. This work was done within the institutional project ECOMAR (2121) in framework programme FP6, supported by the JRC programme directorat and DG Environment.

10. References.

Blatov, A. S., N. P. Bulgakov, V. A. Ivanov, A. N. Kosarev and V. S. Tujilkin. 1984. Variability of hydrophysical fields in the Black Sea. Gidrometeoizdat, Leningrad, 240 (In Russian)

Blumberg AF, Mellor GL (1987), A description of a coastal ocean circulation model. In N.~S. Heaps, editor, Three dimensional ocean models, pages 1--16. American Geophysical Union, Washington, D.C.

Bolding K, Burchard H, Pohlmann T, Stips A, (2002), Turbulent mixing in the Northern North Sea: a numerical model study., Cont Shelf Res, 22, 2707--2724

Bryan K., 1969 ,A numerical model for the study of the world ocean. J Computat Phys, 4, 347--376

Bulgakov, S. V., G. K. Korotaev. 1984. Possible mechanism of stationary circulation of the Black Sea. Integrated investigations of the Black Sea, Sevastopol, Marine Hydrophysical Institute, 32-40 (in Russian).

Burchard H., Bolding K., 2002, GETM, a general estuarine transport model. Scientific documentation. Technical report, European Commsission, Ispra

Burchard H., Bolding K., Villarreal M., 1999, GOTM-- a general ocean turbulence model. Theory, applications and test cases. Technical Report EUR 18745 ENean Commission

Cox M.D., 1984, A primitive equation, 3-dimensional model for the ocean. Technical Report~1, Geophysical Fluid Dynamics Laboratory, University of Princeton, Princeton

Ducet, N., P.-Y. Le Traon, and P. Gauzelin, 1999. Response of the Black sea mean level to atmospheric pressure and wind. Journal of Marine Systems, 22, 311-327.

Filippov D. M. 1965. The cold intermediate layer in the Black Sea. Oceanology, 5, 47-52

Fofonoff N.P., Millard R.C., 1983, Algorithms for computation of fundamental properties of sea water. UNESCO Technical Papers in Marine Science, 44 ,1--53

Haidvogel D.B., Beckmann A., 1999, Numerical Ocean Circulation Modelling, volume~2 of Series on Environmental Science and Management. Imperial College Press, London

Jerlov NG (1968), Optical oceanography. Elsevier

Kantha L.H., Clayson C.A., 2000, Numerical models of oceans and oceanic processes, volume~66 of International Geophysics Series. Academic Press

Kolesnikov. 1953. Seasonal course of temperature, stability and vertical turbulent heat exchange in the open part of the Black Sea, Trudi Mor. Gudrol. Inst. USSR AS, 3, 3-13. (in Russian)

Lascaratos, A. 1993. Estimation of deep and intermediate water mass formation rates in the Mediterranean Sea. Deep-Sea Res. II, *40***,** 1327-1332

Oguz, T, S Besiktepe, O. Bastrurk, I. Salihoglu, D. Aubreym A. Balci, E. Demirov, V. Diaconu, L. Dorogan, M. Duman, L. Ivanov, S. Konovalov, A. Stoyanov, S. Turgul, V. Vladimirov and A. Hilmaz. 1993. CoMSBlack '92A Physical and Chemical Intercalibration Workshop. IOC, Workshop Report No. 98. pp86.

Oguz, T., D. Aubrey, V. Latun, E. Demirov, L. Kolesnikov, H. Sur, V. Diaconu, S. Besiktepe, M. Duman, R. Limeburner and V. Eremeev. 1994. Mesoscale circulation and thermohaline structure of the Black Sea during HydroBlack'91, Deep Sea Res., 41, 603-628.

Ovchinnikov, I. M. And Yu. I. Popov. 1987. Evolution of the Cold Intermediate Layer in the Black Sea. Oceanology, 27, 555-560

Paulson CA, Simpson JJ 1977, Irradiance measurements in the upper ocean. J Phys Oceanogr, 7, 952—956

Pedlosky J., 1987, Geophysical fluid mechanics.Springer, New York, 2 edition

Rachev, N. H. and Stanev, E. V. 1997. Eddy processes in semi-enclosed seas. A case study for the Black Sea, J. Phys. Oceanogr., 27, 1581-1601.

Simonov A. I. and E. N. Altman, Editors. 1991. Hydrometeorology and hydrochemistry of the USSR seas. Vol. IV, The Black Sea, Gidrometeoizdat, 430 pp.

Sorkina, A.I. (Editor).1974. Reference book on the Black Sea Climate, Moscow, Gydrometeoizdat, 406 pp.,(in Russian).

Stanev, E. V. 1990. On the mechanisms of the Black sea circulation. Earth-Science Rev., 28, 285-319.

Stanev, E. V., J. V. Staneva, and V. M. Roussenov. 1997. On the Black Sea water mass forma tion. Model sensitivity study to atmospheric forcing and parameterization of some physical processes. J. Mar.Sys., 13, 245-272.

Stanev, E. V., and N. H. Rachev. 1999. Numerical study on the planetary Rossby modes in the Black Sea. J. Mar Sys., 21, 283-306.

Stanev, E. V. and J. V. Staneva, 2000. The impact of the baroclinic eddies and basin oscillations on the transitions between different quasi-stable states of the Black Sea circulation. J. Mar. Sys., 24,1-2,3-26.

Stanev, E, V, and J. V. Staneva, 2001. The sensitivity of the heat exchange at ocean surface to meso and sub-basin scale eddies. Model study for the Black Sea. Dyn. Atmos. and Oceans, 33, 163-189.

Stanev, E.V., Bowman, M.J., Peneva E.L., Staneva, J.V., 2003, Control of Black Sea intermediate water mass formation by dynamics and topography: comparisons of numerical simulations, survey and satellite data., Journal of Marine Research, 41, 59-99

Staneva, J. V., and E. V. Stanev. 1997. Cold intermediate water mass formation in the Black Sea. Analyses on numerical model simulations. E. Özsoy and A. Mikaelyan (eds.): Sensitivity to Change: Black Sea, Baltic Sea and North Sea , NATO Series, Kluwer academic publisher, 375-393.

Stips A, Burchard H, Bolding K, Eifler W (2002), Modelling of convective turbulence with a two-equation k-ε turbulence closure scheme. Ocean Dynamics, 52, 153—168

Stips A, , Bolding K, Pohlman T., Burchard H (2004), Simulating the temporal and spatial dynamics of the North Sea using the new model GETM. Ocean Dynamics, 54, 250-286

Apendix: List of produced files and calculated variables.

1. Variables

1.1 In the monthly mean files:

	Model variable name	Description
1	bathymetry	Model bathymetry
2	swrmean	Short wave radiation
3	ustarmean	Bottom friction velocity
4	ustar2mean	Standart deviation of bottom friction velocity
5	hmean	Mean layer thickness
6	uumean	Mean zonal velocity
7	vvmean	Mean meridional velocity
8	Wmean	Mean vertical velocity
9	tempmean	Mean temperature
10	saltmean	Mean salinity

1.2 In the daily snapshots files:

	Model variable name	Description
1	bathymetry	Model bathymetry
2	hcc	HCC
3	elev	Sea Surface Elevation
4	u	Integrated zonal velocity
5	v	Integrated meridional velocity
6	h	Layer thickness
7	uu	Zonal velocity
8	vv	Meridional velocity
9	w	Vertical velocity
10	salt	Salinity
11	temp	Temperature
12	tke	Turbulent kinetic energy
13	num	Horizontal eddy viscosity
14	nuh	Horizontal eddy diffusivity

2. Monthly mean files names:

The quoted “year”and “mo” denote the year, month during the integrations.

“year” = 1990 1991 1992 1993 1994 1995 1996 1997 1998 1999 2000

“mo” = 01 02 03 04 05 06 07 08 09 10 11 12

The “proc” stays for the number of processor in the parallel run.

“proc”= 000 001 002 003 004 005 006 007

2.1 For J6 experiment.

```
imwcluster:/data/penevel/light_jerlov_t6/bs_jervov6_”year”_”mo”.mean.nc
```

2.2 For KDE experiment

```
imwcluster:/data/penevel/light_kde_hor/bs_kde_”year”_”mo”.mean.nc
```

2.3 For E10 experiment

```
imwcluster:/data/penevel/light_ver6_BSAS/bs_exp10_”year”_”mo”.mean.nc
```

2.4 For 2min experiment

```
imwcluster:/data/penevel/BS_2min/bs_2min_prof_”year”_”mo”.mean.”proc”.nc
```

3. Daily snapshots files names:

3.1 For J6 experiment.

```
imwcluster:/scratch5/penevel/light_jerlov_t6/bs_jervov6_”year”_”mo”.3d.n
c
```

3.2 For KDE experiment

```
imwcluster:/scratch5/penevel/light_kde_hor/bs_kde_hor_”year”_”mo”.3d.nc
```

3.3 For E10 experiment

```
imwcluster:/scratch6/penevel/light_exp10/bs_exp10_”year”_”mo”.3d.nc
```

3.4 For 2min experiment

imwcluster:/scracth4/penevel/BS_2min/bs_2min_prof_”year”_”mo”.3d.”proc”.nc

Mission of the JRC

The mission of the JRC is to provide customer-driven scientific and technical support for the conception, development, implementation and monitoring of EU policies. As a service of the European Commission, the JRC functions as a reference centre of science and technology for the Union. Close to the policy-making process, it serves the common interest of the Member States, while being independent of special interests, whether private or national.

EUROPEAN COMMISSION
DIRECTORATE-GENERAL
Joint Research Centre

Mission of the JRC

The mission of the JRC is to provide customer-driven scientific and technical support for the conception, development, implementation and monitoring of EU policies. As a service of the European Commission, the JRC functions as a reference centre of science and technology for the Union. Close to the policy-making process, it serves the common interest of the Member States, while being independent of special interests, whether private or national.

EUROPEAN COMMISSION
DIRECTORATE-GENERAL
Joint Research Centre